Mathematical modeling of neuro-immune processes in epileptogenesis

Dissertation
zur Erlangung des Doktorgrades
der Naturwissenschaften

vorgelegt beim Fachbereich Informatik und Mathematik
der Johann Wolfgang Goethe Universität
in Frankfurt am Main

von
Danylo Batulin
aus Sewerodonezk, Ukraine

Frankfurt 2022
(D 30)

vom Fachbereich Informatik und Mathematik der
Johann Wolfgang Goethe - Universität als Dissertation angenommen.

Dekan: Prof. Dr. Martin Möller

1. Gutachter: Prof. Dr. Jochen Triesch

2. Gutachter: Prof. Dr. Peter Jedlicka

Datum der Disputation : 13.06.2023

Abstract

This thesis presents a first-of-its-kind phenomenological framework that formally describes the development of acquired epilepsy and the role of the neuro-immune axis in this development. Formulated as a system of nonlinear differential equations, the model describes the interaction of processes such as neuroinflammation, blood-brain barrier disruption, neuronal death, circuit remodeling, and epileptic seizures. The model allows for the simulation of epilepsy development courses caused by a variety of neurological injuries. The simulation results are in agreement with experimental findings from three distinct animal models of epileptogenesis. Simulations capture injury-specific temporal patterns of seizure occurrence, neuroinflammation, blood-brain barrier leakage, and progression of neuronal death. In addition, the model provides insights into phenomena related to epileptogenesis such as the emergence of paradoxically long time scales of disease development after injury, the dose-dependence of epileptogenesis features on injury severity, and the variability of clinical outcomes in subjects exposed to identical injury. Moreover, the developed framework allows for the simulation of therapeutic interventions, which provides insights into the injury-specificity of prominent intervention strategies. Thus, the model can be used as an *in silico* tool for the generation of testable predictions, which may aid pre-clinical research for the development of epilepsy treatments.

Key words: epilepsy, epileptogenesis, model, neuro-immune, neuroinflammation, blood brain barrier, seizure

Summary

Epilepsy is one of the most common neurological diseases affecting around 70 million people worldwide. The disease is recognized as a spectrum of conditions due to its heterogeneity in symptoms, causes, and developmental courses. The two key unifying features of epilepsy are the presence of periods of abnormal neural activity, called spontaneous recurrent seizures, and the modification of neural networks to the state in which seizures are likely to occur. The disease is associated with seizure-related disability, comorbidities, stigma, high healthcare-related costs, and increased mortality, all of which put a heavy burden on affected individuals, their caregivers, and healthcare systems around the globe.

Approximately one-third of epilepsy cases are classified as pharmacoresistant, which means that there is no efficient pharmacological treatment capable of alleviating the seizure burden. Moreover, no known medication is available to prevent the development of the disease, so-called epileptogenesis. Surgical intervention, a primary treatment method in pharmacoresistant epilepsy, has several limitations: it can not be applied to all subtypes of epilepsy, it may have suboptimal efficiency, and it is simply not available for all epilepsy patients, 80% of whom reside in low- and middle-income countries.

One of the reasons for the absence of efficient epilepsy treatments is the fact that the development of the disease remains poorly understood. Intensive research efforts in the last decades have revealed that neuro-immune cross talk plays a central role in epileptogenesis. The list of the key physiological and pathological processes that contribute to disease development is known. However, a mechanistic understanding of their complex *interactions* is still missing.

This doctoral thesis presents a first-of-its-kind theoretical framework that describes the process of epileptogenesis and the role that neuro-immune interactions play in it. Being formulated as a system of nonlinear differential equations, the model allows for the simulation of epilepsy development courses caused by a variety of neurological injury types. Moreover, the system can be utilized as an *in silico* tool for the simulation of disease interventions, generating testable predictions for

the pre-clinical research on novel therapeutic intervention strategies.

The structure of the mathematical model was designed taking into consideration the evidence on the principles of epilepsy development obtained from human and animal model studies. The model describes the interplay of processes such as neuroinflammation, blood-brain barrier disruption, neuronal death, circuit remodeling, and epileptic seizures. Two versions of the mathematical model of epileptogenesis were developed. The first, a stochastic model accounts for the occurrence of discrete seizures in time, which allows for a direct comparison of simulation results to experimental data. In the second version, a simplified rate model, seizure activity is approximated with a smooth seizure rate function, which simplifies the mathematical analysis and visualization of the dynamic changes in the system.

This mathematical model allows for the simulation of epileptogenesis caused by a variety of neurological injuries with a single parameter set. This was tested on the data from three distinct animal models of epileptogenesis: the blood-brain barrier disruption rodent model, Theiler's murine encephalomyelitis virus mice model, and the pilocarpine status epilepticus rodent model. The blood-brain barrier disruption rodent model mimics the condition in which the pathological course of epileptogenesis is triggered by a dysfunction of the blood-brain barrier. The Theiler's murine encephalomyelitis virus mice model recapitulates the development of infection-induced epilepsy. Finally, the pilocarpine status epilepticus rodent model mimics the epilepsy development caused by an extremely long episode of seizure activity, the so-called status epilepticus. The simulation of epilepsy caused by these different types of neurological injuries is carried out by the analysis of the key effects of epileptogenic injuries and their translation into the input signal sequences that mimic injury effects. The simulation results are in agreement with the data obtained from the three aforementioned animal models, capturing injury-specific temporal patterns of seizure occurrence, neuroinflammation, blood-brain barrier leakage, and progression of neuronal death.

In addition to the reproduction of the experimental data from the animal models, our computational modeling results capture and provide an explanation for other features of epileptogenesis such as the variability of epileptogenesis outcomes in subjects exposed to similar injuries and dose-dependence of risk and severity of epilepsy on injury intensity. In addition, the modeling results highlight the multicausality of epileptogenesis, in which several pathological processes may drive the development of the disease in isolation or in combination with other mechanisms. For instance,

according to the data from experimental studies, the extent of neuronal loss is associated with the severity of the seizure burden. At the same time, neuronal loss is not a necessary component for epileptogenesis, as was also shown experimentally. The mathematical model captures these observations. Moreover, it suggests that, despite not being necessary, neuronal loss may itself be sufficient for triggering epileptogenesis.

The mathematical analysis of the developed framework reveals that in the absence of neuronal loss three steady states exist in the dynamical landscape of the system: a 'healthy' steady state, a saddle point, and an 'epileptic' steady state. The saddle point resides on the separatrix, which divides the state-space of the system into the basins of attraction of the two stable steady states. We show that with increasing extent of neuronal loss the basin of attraction of the 'healthy' steady state shrinks. If a critical extent of neuronal loss is reached, a saddle-node bifurcation will occur due to collision of the saddle point with the 'healthy' attractor. Thus, for a supracritical extent of neuronal loss, only one 'epileptic' attractor remains, which means that the progression of epileptogenesis is inevitable. In such cases, however, the disease may still take years or decades to develop. Such long time scales of epileptogenesis are also reported in clinical and animal model data, where seizure manifestation may occur in years or decades after the neurological injury. This decades-long disease progression is somewhat surprising, since in the mathematical model the slowest processes are operating on the time scales of days and weeks. A closer look at the system dynamics reveals that paradoxically slow epileptogenesis takes place when the injury pushes the system state to the vicinity of the saddle point. This mechanism underlying slow epileptogenesis is not specific to the pathology being caused by neuronal loss, but is also observed in the simulations for the blood-brain barrier disruption animal model.

The model also captures the dose-dependence effects of the injury intensity on the epileptogenesis features. As reported in human and animal model studies, the intensity of the neurological injury can modulate the severity of the seizure burden and the disease time course. This is illustrated with the simulations of the blood-brain barrier disruption rodent model, in which the latent period (time between injury onset and seizure manifestation) and seizure frequency were modulated by adjusting the severity of the epileptogenic injury. This adjustment can be obtained by either modulation of the duration of the time window, in which the blood-brain barrier is being affected, or by modulation of the intensity of the disruption effects. Moreover, the simulation results suggest that the severity of the injury can define the

risk of epilepsy development. Depending on the severity of the injury, pathological effects may either push the system state to the basin of attraction of the 'epileptic' steady state or keep it within the basin of attraction of the 'healthy' fixed point, if the injury is too weak. The latter would lead to a gradual increase in inter-seizure intervals over time and eventual recovery.

The clinical outcomes of patients suffering from an epileptogenic injury of the same kind are known to vary considerably. This variability may be partially explained by inter-personal genetic and epigenetic differences. However, experimental studies, in which genetic profiles of animals and other conditions are preserved, also illustrate the high variability of epileptogenesis outcomes. The model not only captures such effects but also suggests that epileptogenesis outcomes may vary even in hypothetically identical subjects exposed to identical injuries. The origin of such variability is the stochastic nature of epileptic seizures. This stochasticity-induced noise in timing and frequency of seizure occurrence may determine to which of the basins of attraction the state of the system converges and at which time. This is illustrated by the heterogeneous outcomes of simulations with a cohort of identical subjects exposed to infectious injury of identical severity.

The mathematical model presented in this thesis can also be used as an *in silico* tool for the generation of testable predictions for research on therapeutic strategies. Mathematical modeling allows to simulate various intervention strategies with various targets and time windows in the animal model of choice. The simulated suppression of the pathological effect of epileptic seizures on blood-brain barrier permeability revealed that transient (limited in time) interventions may be as effective as permanent ones if the time window for intervention is selected correctly. In addition, simulation results highlight that therapeutic interventions should be designed to be injury-specific. In the case of infection-induced epileptogenesis, the intervention time window has to coincide with the injury onset. On the other hand, in the case of epileptogenesis induced by status epilepticus, the transient intervention has to be applied with a certain delay in order to prevent the development of epilepsy. These kinds of predictions can be generated with the model and used as guidance for the experimental design in the research on therapeutic intervention strategies.

The scientific findings presented in this thesis have been published in the Cell Press iScience journal article 'A mathematical model of neuro-immune interactions in epileptogenesis for discovering treatment strategies' under the authorship

of Danylo Batulin, Fereshteh Lagzi, Annamaria Vezzani, Peter Jedlicka, and Jochen Triesch. The author contributions are the following:

- Conceptualization, DB, AV, PJ, JT;
- Methodology, DB, FL, PJ, JT;
- Software, DB, FL;
- Formal Analysis, DB, FL;
- Writing – Original Draft, DB;
- Writing – Review & Editing, DB, FL, AV, PJ, JT;
- Visualization, DB;
- Supervision, AV, PJ, JT;
- Project Administration, DB, PJ, JT;
- Funding Acquisition, PJ, JT.

The full list of publications associated with the doctoral studies period:

- Batulin, D., Lagzi, F., Vezzani, A., Jedlicka, P., Triesch, J. (2022). A mathematical model of neuroimmune interactions in epileptogenesis for discovering treatment strategies. iScience, 25(6), 104343.
- Stöber, T., Batulin, D., Triesch, J., Narayanan, R., Jedlicka, P. (2022). Degeneracy in epilepsy: Multiple routes to hyperexcitable brain circuits and their repair. arXiv preprint arXiv:2206.09621.
- Sommer, P., Batulin, D., Triesch J. A Model of Viral/SARS-CoV-2 Spreading and Grey Matter Loss in the Human Brain (in preparation).

Zusammenfassung

Epilepsie ist eine der häufigsten neurologischen Erkrankungen und betrifft weltweit etwa 70 Millionen Menschen. Die Krankheit wird aufgrund ihrer Heterogenität in Symptomen, Ursachen und Entwicklungskursen als Spektrum von Bedingungen angesehen. Die zwei wichtigsten einheitlichen Merkmale von Epilepsie sind das Auftreten von Zeiträumen abnormaler neuraler Aktivität, genannt spontane rekurrente Anfälle, und die Veränderung von neuralen Netzwerken in einen Zustand, in dem Anfälle mit höherer Wahrscheinlichkeit auftreten. Die Krankheit ist mit anfallsbedingter Behinderung, Begleiterkrankungen, Stigma, hohen Gesundheitskosten und erhöhter Sterblichkeit verbunden. All diese Faktoren stellen nicht nur eine schwere Belastung für die betroffenen Personen dar, sondern auch für deren Angehörige, Betreuer und das weltweite Gesundheitssystem.

Etwa ein Drittel der Epilepsie-Fälle werden als pharmakoresistent eingestuft, was bedeutet, dass es keine effiziente pharmakologische Behandlung gibt, die die Anfallsbelastung lindern kann. Darüber hinaus gibt es keine bekannte Medikation um das Entstehen der Krankheit, die sogenannten Epileptogenese, zu verhindern. Eine primäre Behandlungsmethode pharmakoresistenter Epilepsie ist chirurgische Intervention. Letztere hat vielfältige Einschränkungen: Sie kann nicht auf alle Epilepsie-Subtypen angewendet werden, der Eingriff führt nicht immer zum Behandlungserfolg, und chirurgische Intervention ist für die meisten Epilepsie-Patienten nicht verfügbar, da 80% der Epilepsiepatienten in Ländern mit niedrigen und mittlerem Einkommen leben.

Einer der Gründe für das Fehlen effektiver Epilepsie-Behandlungen ist, dass die Entwicklung der Krankheit immer noch schlecht verstanden ist. Intensive Forschungsbemühungen in den letzten Jahrzehnten haben gezeigt, dass neuro-immune Wechselwirkungen eine zentrale Rolle bei der Epileptogenese spielen. Während die wichtigsten physiologischen und pathologischen Prozesse, die zur Krankheitsentwicklung beitragen, bekannt sind, fehlt noch immer ein mechanistisches Verständnis ihrer komplexen *Interaktionen*.

Diese Dissertation ist der erste theoretische Ansatz zur Beschreibung der Epileptogenese und der Rolle, die neuroimmunologische Wechselbeziehungen in ihr spielen.

Das Modell besteht aus einem System von nichtlinearen Differentialgleichungen und erlaubt die Simulation der Entwicklung von Epilepsie nach einer Vielzahl von neurologischen Verletzungen. Darüber hinaus kann das System als *in-silico*-Werkzeug für die Simulation von Krankheitsinterventionen verwendet werden, um damit testbare Vorhersagen für vorklinische Forschung zu neuartigen therapeutischen Interventionsstrategien zu generieren.

Die Struktur des mathematischen Modells wurde unter Berücksichtigung der Prinzipien der Entwicklung von Epilepsie entworfen, die aus menschlichen und tierischen Modellstudien entnommen wurden. Das Modell beschreibt das Zusammenspiel von Prozessen wie zum Beispiel Entzündungen des Nervensystems, Störungen der Blut-Hirn-Schranke, neuronalem Zelltod, Veränderungen von neuronalen Schaltkreisen, und epileptischen Anfällen. Dabei wurden zwei Versionen des mathematischen Modells der Epileptogenese entwickelt. Die erste Version ist ein stochastisches Modell, das das Vorkommen von diskreten epileptischen Anfällen im Zeitverlauf berücksichtigt, und dadurch einen direkten Vergleich der Simulationsergebnisse mit experimentellen Daten erlaubt. Die zweite Version ist ein 'simplified rate' Modell, in dem Anfallaktivität durch eine 'smooth seizure rate' Funktion angenähert wird, was die mathematische Analyse und Visualisierung der dynamischen Veränderungen im System vereinfacht.

Das mathematische Modell erlaubt die Simulation der Epileptogenese als Folge einer Vielzahl von neurologischen Verletzungen unter Verwendung eines einzelnen Sets an Parametern. Dies wurde an Daten von drei unterschiedlichen Tiermodellen der Epileptogenese getestet: einem Nagetiermodell für den Zusammenbruch der Blut-Hirn-Schranke, einem Mausmodell von Theiler's 'murine encephalomyelitis virus', und einem Nagetiermodell des 'pilocarpine status epilepticus'. Das Maus-Modell für den Zusammenbruch der Blut-Hirn-Schranke imitiert einen pathologischen Verlauf der Epileptogenese als Folge einer Dysfunktion der Blut-Hirn-Schranke. Das Theiler's 'murine encephalomyelitis virus' Modell rekapituliert die Entwicklung von infektionsbedingter Epilepsie. Schliesslich imitiert das 'pilocarpine status epilepticus' Nagetiermodell die Entwicklung von Epilepsie durch extrem lange Episoden von Anfallaktivität, den sogenannten Status Epilepticus. Die Simulation von Epilepsie als Folge dieser unterschiedlichen neurologischen Krankheitsbilder wird erreicht durch die Analyse der Auswirkungen von epileptogenen Trauma und deren Übertragung auf die initialen Signalsequenzen, welche das Trauma imitieren. Die Simulationsergebnisse stimmen überein mit Daten aus den drei oben genannten Tiermodellen, und detektieren verletzungsspezifische zeitliche Muster von Anfallereignissen,

neuronale Entzündungen, Durchbrechungen der Blut-Hirn-Schranke, und fortschreitendem neuronalen Zelltod.

Zusätzlich zur Reproduktion experimenteller Daten der verschiedenen Tiermodelle, erlauben die Resultate unseres Computermodells ein vertiefendes Verständnis andere Eigenschaften der Epileptogenese. Diese sind beispielsweise die Variabilität der Epileptogenese in Patienten trotz ähnlicher Verletzungen, und die Abhängigkeit der Dosis von Risiko und Schwere der Epilepsie von Verletzungsintensität. Zusätzlich zeigen die Resultate unseres Modells die Multikausalität von Epileptogenese auf, also dass mehrere pathologische Prozesse zur Entwicklung der Krankheit entweder in Isolation oder in Kombinationen mit anderen Mechanismen führen können. Zum Beispiel zeigen experimentelle Studien, dass der Verlust von Neuronen mit der Schwere von epileptischen Anfällen zusammenhängt. Gleichzeitig ist der Verlust von Neuronen keine notwendige Komponente für Epileptogenese, wie auch experimentell bestätigt wurde. Das mathematische Modell erfasst diese Beobachtung. Zusätzlich schlägt unser Modell nicht nur vor, dass, obwohl dies keine notwendige Bedingung ist, der Verlust von Neuronen eine ausreichende Bedingung für die Auslösung von Epileptogenese ist.

Die mathematische Analyse des von uns entwickelten dynamischen Systems zeigt, dass, falls kein Verlust von Neuronen vorhanden ist, drei Gleichgewichtszustände existieren: ein ‘gesunder’ Gleichgewichtszustand, ein Sattelpunkt und ein ‘epileptischer’ Gleichgewichtszustand. Der Sattelpunkt liegt an der Separatrix, welche den Zustandsraum des Systems in zwei Attraktionsbecken der beiden stabilen Gleichgewichtszustände trennt. Wir zeigen, dass sich mit Anstieg von neuonalem Zelltod das Attraktionsbecken des ‘gesunden’ Gleichgewichtszustand verkleinert. Falls eine kritische Anzahl an Zelltod eintritt, entsteht eine Sattelpunkt-Bifurkation aufgrund der Kollision des Sattelpunkts mit dem ‘gesunden’ Attraktor. Daher existiert ab einem kritischen Wert von neuronalem Zelltod nur der ‘epileptische’ Attraktor, was zur Folge hat, dass ein voranschreiten der Epileptogenese unaufhaltbar ist. Jedoch kann es immer noch Jahre oder Jahrzehnte dauern, bis sich die Krankheit entwickelt. Solche langen Zeitskalen von Epileptogenese wurden auch in klinischen Studien und Tiermodellen nachgewiesen, in denen epileptische Anfälle sich erst Jahre nach der neurologischen Verletzung manifestieren können. Dieser jahrzehntelange Prozess der Krankheitsmanifestierung mag überraschen, da die langsamsten Prozesse im mathematischen Modell Zeitskalen von Tagen bis Wochen haben. Nähere Analyse des dynamischen Systems zeigt, dass dies paradox-langsame Epileptogenese zustande kommt, wenn die Verletzung den Zustand des Systems in die Nähe

des Sattelpunktes bringt. Der Mechanismus, der hinter der langsamen Epileptogenese steckt ist nicht spezifisch zur Pathologie die von Verlust von Neuronen ausgelöst wird, sondern kann in den Simulationen auch im Falle der im Störung der Blut-Hirn-Schranken im Tiermodell beobachtet werden.

Das Modell erfasst auch die Dosis-abhängigen Effekte von Traumaintensität von Eigenschaften der Epileptogenese. Wie in Studien mit Patienten oder in Tierstudien bereits erwiesen, kann die Intensität der neurologischen Traumata die Stärke der epileptischen Anfälle und den Krankheitsverlauf beeinflussen. Dies illustrieren wir in unseren Simulationen der Störungen der Blut-Hirn-Schranke im Mausmodell, in der die verborgene Zeitperiode (Zeit zwischen Verletzung und Manifestation der epileptischen Anfälle) und die Frequenz der epileptischen Anfälle durch Anpassen der Schwere des epileptogenen Trauma moduliert wird. Diese Anpassung kann entweder durch Modulation des Zeitraums in der die Blut-Hirn-Schranke beeinflusst wird, oder durch Modulation der Intensität der Störung zustande kommen. Zusätzlich zeigen unsere Simulationen, dass die Schwere des Traumas das Risiko der Entwicklung von Epilepsie definieren kann. Abhängig von der Schwere des Traumas, drängen die pathologischen Effekte den Systemzustand in das Attraktionsbecken dass zu dem 'epileptischen' Gleichgewichtszustand führt, oder es bleibt in dem Attraktionsbecken des 'gesunden' Fixpunktes, falls das Trauma schwach genug ist. Letzteres würde zu einem graduellen Anstiegt des Intervalls zwischen zwei Anfällen führen, und damit zu eventueller Genesung.

Es ist bekannt, dass die klinischen Auswirkungen von Patienten, die an einem epileptogenen Trauma derselben Art leiden, sehr unterschiedlich sind. Diese Variabilität lässt sich zum Teil durch genetische und epigenetische Unterschiede zwischen den einzelnen Personen erklären. Allerdings zeigen auch experimentelle Studien, bei denen die genetischen Profile von Tieren und andere Bedingungen konstant gehalten wurden, eine hohe Variabilität der Auswirkungen der Epileptogenese. Das Modell erfasst nicht nur solche Effekte, sondern legt auch nahe, dass die Auswirkungen der Epileptogenese selbst bei hypothetisch identischen Personen, mit identischen Krankheitsbildern, variieren können. Der Grund für diese Variabilität ist die stochastische Natur epileptischer Anfälle. Dieses durch die Stochastik bedingte Rauschen in Bezug auf Zeitpunkt und Häufigkeit des Auftretens von Anfällen kann bestimmen, zu welchem der Anziehungsbereiche der Zustand des Systems konvergiert und zu welchem Zeitpunkt. Dies wird durch die heterogenen Ergebnisse von Simulationen mit einer Kohorte identischer Probanden veranschaulicht, die einem infektiösen Trauma gleichen Schweregrades ausgesetzt waren.

Das in dieser Arbeit vorgestellte mathematische Modell kann auch als *in-silico*-Instrument zur Erstellung überprüfbarer Vorhersagen für die Erforschung therapeutischer Strategien verwendet werden. Die mathematische Modellierung ermöglicht es, verschiedene Interventionsstrategien mit unterschiedlichen Zielen und Zeitfenstern im Tiermodell der Wahl zu simulieren. Die simulierte Unterdrückung der pathologischen Wirkung epileptischer Anfälle auf die Permeabilität der Blut-Hirn-Schranke hat gezeigt, dass transiente (zeitlich begrenzte) Interventionen ebenso wirksam sein können wie permanente, wenn das Zeitfenster für die Intervention richtig gewählt wird. Darüber hinaus machen die Simulationsergebnisse deutlich, dass therapeutische Eingriffe traumaspezifisch gestaltet werden sollten. Im Falle der infektionsbedingten Epileptogenese muss das Zeitfenster für die Intervention mit dem Beginn des Traumas übereinstimmen. Bei der durch einen Status Epilepticus ausgelösten Epileptogenese hingegen muss die transiente Intervention mit einer gewissen Verzögerung erfolgen, um die Entwicklung einer Epilepsie zu verhindern. Solche Vorhersagen können mit dem Modell erstellt und als Anleitung für die Versuchsplanung bei der Erforschung von therapeutischen Interventionsstrategien verwendet werden.

Die in dieser Arbeit vorgestellten wissenschaftlichen Ergebnisse wurden in der Zeitschrift Cell Press iScience in dem Artikel "A mathematical model of neuroimmune interactions in epileptogenesis for discovering treatment strategies" unter der Autorenschaft von Danylo Batulin, Fereshteh Lagzi, Annamaria Vezzani, Peter Jedlicka und Jochen Triesch veröffentlicht. Die Beiträge der Autoren sind die folgenden:

- Konzeptualisierung, DB, AV, PJ, JT;
- Methodik, DB, FL, PJ, JT;
- Software, DB, FL;
- Formale Analyse, DB, FL;
- Schreiben – Originalentwurf, DB;
- Schreiben – Überprüfung und Bearbeitung, DB, FL, AV, PJ, JT;
- Visualisierung, DB;
- Beaufsichtigung, AV, PJ, JT;

- Projektverwaltung, DB, PJ, JT;
- Beschaffung von Finanzmitteln, PJ, JT.

Die vollständige Liste der Veröffentlichungen im Zusammenhang mit dem Promotionsstudium:

- Batulin, D., Lagzi, F., Vezzani, A., Jedlicka, P., Triesch, J. (2022). A mathematical model of neuroimmune interactions in epileptogenesis for discovering treatment strategies. iScience, 25(6), 104343.
- Stöber, T., Batulin, D., Triesch, J., Narayanan, R., Jedlicka, P. (2022). Degeneracy in epilepsy: Multiple routes to hyperexcitable brain circuits and their repair. arXiv preprint arXiv:2206.09621.
- Sommer, P., Batulin, D., Triesch J. A Model of Viral/SARS-CoV-2 Spreading and Grey Matter Loss in the Human Brain (in Vorbereitung).

Contents

List of Figures

List of Tables

List of Abbreviations

AED	Anti-Epileptic Drug
BBB	Blood-Brain Barrier
CNN	Convolutional Neural Network
CNS	Central Nervous System
CT	Computed Tomography
EEG	Electroencephalography
ECM	Extracellular Matrix
iEEG	intracranial Electroencephalogram
IL	Interleukin
ILAE	International League Against Epilepsy
LPS	Lipopolysaccharide
LSTM	Long Short-Term Memory
MEG	Magnetoencephalography
MRI	Magnetic Resonance Imaging
NO	Nitric Oxide
PET	Positron Emission Tomography
PFU	Plaque Forming Units
PNN	Perineuronal Net
ROS	Reactive Oxygen Species
SE	Status Epilepticus
SEM	Standard Error of the Mean
SPECT	Single-Photon Emission Computed Tomography
SUDEP	Suden Unexpected Death in Epilepsy
SVM	Support Vector Machine
TBI	Traumatic Brain Injury
TGF	Transforming Growth Factor
TLE	Temporal Lobe Epilepsy
TLR	Toll-Like Receptor
TMEV	Theiler's Murine Encephalomyelitis Virus
TNF	Tumor Necrosis Factor
WHO	World Health Organization

to Ukrainian resistance forces and foreign volunteers . . .

Chapter 1

Introduction and research goals

This chapter is dedicated to familiarizing the reader with the current state of epilepsy research: the diversity of the disease spectrum, the main causes and mechanisms of its development, available treatment types and their limitations. Further, the role of mathematical modeling and other methods of epilepsy research is discussed. At the end of the chapter, the research objective of this dissertation is formulated.

1.1 Seizures, epilepsy and epileptogenesis

Epilepsy is one of the most common neurological diseases. According to International League Against Epilepsy (ILAE), epilepsy is not one condition but a diverse family of disorders, which have in common an abnormally elevated predisposition to seizures (Fisher et al., 2005). Epilepsy affects approximately 70 million people worldwide with disease incidence ranging from 40 to 100 per 100 000 people per year in different countries (Thijs et al., 2019). Approximately 80% of people suffering from epilepsy live in low- and middle-income countries, and three-quarters of people residing in low-income countries do not get the necessary treatment (World Health Organization, 2022). The disease dramatically lowers the quality of life of patients and their families. The main factors for it are seizure-related disability, comorbidities, stigma, healthcare-related costs, and increased mortality (Fisher et al., 2005; Moshé et al., 2015).

The key symptom of epilepsy is the presence of spontaneous recurrent seizures. They are defined as transient episodes of abnormal excessive or synchronous neural activity in the brain. These episodes have to be unprovoked and recurring to be considered spontaneous recurrent seizures. The misdiagnosis is common due to confusion of epileptic seizures with convulsive syncopes or psychogenic non-epileptic

attacks (Moshé et al., 2015). Reliable diagnosing of epilepsy is based on consideration of medical recordings that are obtained with a range of methods. Among these methods are the evaluation of a patient's clinical history, records on seizure events, electrocardiogram recordings, analyzing electroencephalogram (EEG) for the presence of interictal epileptiform discharges, assessment of structural and functional neuroimaging results (computed tomography (CT), magnetic resonance imaging (MRI), positron emission tomography (PET), etc), blood tests, and other techniques (Pillai and Sperling, 2006; Thijs et al., 2019; Bandopadhyay et al., 2021).

Another important characteristic of epilepsy disorder, in addition to the enduring predisposition of the central nervous system (CNS) to generate spontaneous recurrent seizures, is the development of a neuronal network, in which spontaneous seizures are likely to occur (Duncan et al., 2006). This process is called epileptogenesis, and it is associated with neural circuits gradually becoming more prone to hypersynchronous, excessive, and oscillatory activity. This activity, when sustained, may disrupt other physiological processes in the CNS (Thijs et al., 2019). In other words, epileptogenesis is a process of epilepsy development over time. Until the last decade, epileptogenesis was conceptualized to be complete at the time of a first spontaneous recurrent seizure. However, this concept has been recently challenged by several experimental and clinical observations, and, consecutively, epileptogenesis is now considered to be a continious and gradual process, which persists also after the onset of spontaneous recurrent seizures (Pitkänen et al., 2015).

1.2 Epilepsy as a spectrum disorder

Epilepsy, as a family of disorders, is highly heterogeneous in disease etiology, predisposition factors, symptoms, developmental courses, and other aspects (Fig. 1.1) (Moshé et al., 2015; Thijs et al., 2019; Pennell, 2020). The classification of epilepsy is constantly evolving, with more than 50 epilepsy syndromes described (Berkovic et al., 2006).

1.2.1 Classification in regard to the brain area of seizure onset

Epilepsy can be classified in regard to the brain area of onset of its key symptom — spontaneous recurrent seizures (Scheffer et al., 2017). There are two main types: focal and generalized. In "focal (partial) epilepsy", seizures originate within

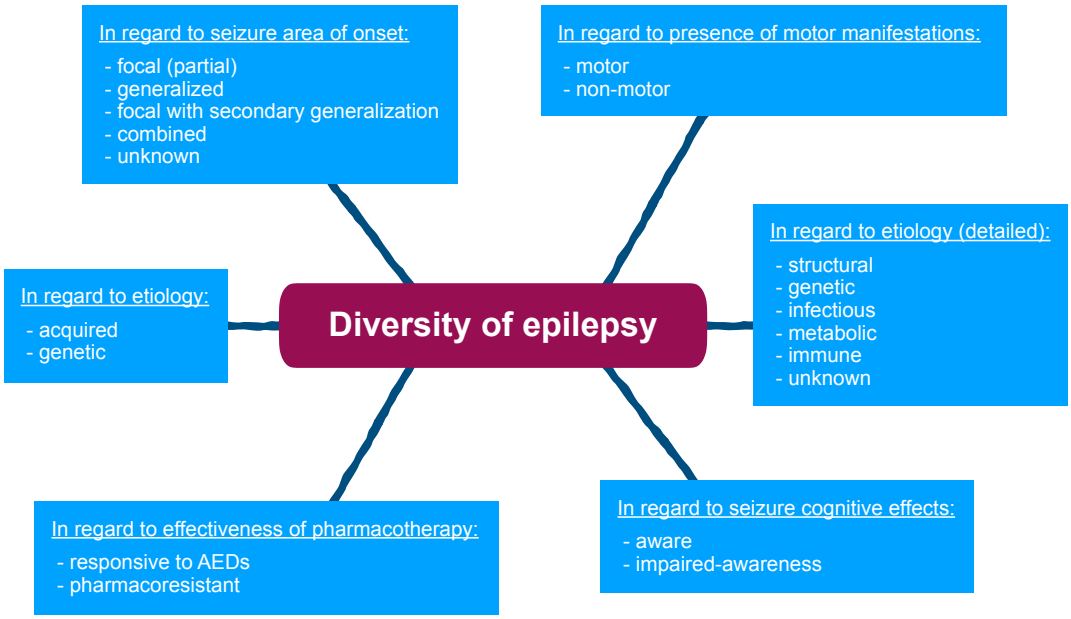

FIGURE 1.1: Diversity of epilepsy in regard to different factors.

circuits limited to only one cerebral hemisphere (Moshé et al., 2015). This type of epilepsy accounts for approximately 60% of known disease cases with its most common subtype — temporal lobe epilepsy (TLE) (Téllez-Zenteno and Hernández-Ronquillo, 2012). If synchronous activity of a focal seizure over time spreads to another hemisphere, such a distinct seizure subtype is called "focal-onset seizures with secondary generalization" (Tomlinson and Venkataraman, 2017). Contrary to focal epilepsy, if both hemispheres are (potentially asymmetrically) activated during the onset of a seizure, such case is classified as a "generalized epilepsy" type (Moshé et al., 2015; Falco-Walter, Scheffer, and Fisher, 2018). In some cases, it is impossible to determine whether a seizure is generalized or focal, so the epilepsy type is marked as "unknown" (Scheffer et al., 2017). Moreover, some epilepsy syndromes, such as Dravet syndrome and Lennox-Gastaut syndrome, are characterized by the presence of both focal and generalized seizures, and such conditions constitute the recently established group of "combined generalized and focal epilepsies" (Falco-Walter, Scheffer, and Fisher, 2018).

1.2.2 Other modalities for classification on seizure characteristics

Classifying the epilepsy types based on the features of epileptic seizures is not limited to consideration of an area of seizure onset. Another common classifying factor is

the presence or absence of motor manifestations during seizures (Fisher et al., 2017). Thus, focal-, generalized-, combined- and unknown-onset epilepsies could be motor or non-motor. One of the most common non-motor cases of epilepsy is generalized absence seizures. This condition is characterized by brief and sudden episodes of the arrest of motor initiation due to a disturbance of premotor–frontal lobe function with common loss of consciousness during the attack (Hughes, 2009). Furthermore, epilepsy can be classified as "aware" or "impaired awareness" depending if a patient is experiencing the decay of awareness during a seizure (Fisher et al., 2017). However, this characteristic is omitted for generalized seizures because awareness is impaired in most generalized epilepsy cases. Further classification of epilepsy types based on features of seizures exists (Falco-Walter, Scheffer, and Fisher, 2018), which highlights the diversity and heterogeneity of the disease spectrum.

1.2.3 Classification in regard to disease etiology

Epilepsy cases are classified not only based on features of epileptic seizures. An important aspect, which is taken into consideration in the choice of treatment strategy, is the etiology of the disease (Goldenberg, 2010). According to the 2017 ILAE classification of epilepsies (Scheffer et al., 2017), six etiologic categories are defined: structural, genetic, infectious, metabolic, immune, and unknown. In the case of a structural etiology, abnormalities detected with structural neuroimaging and electroclinical assessment suggest that they are the likely cause of the patient's seizures. For the genetic etiology category, a specific disease-causing variant of a gene, which is assumed to be pathogenic for epilepsy, should be found. Alternatively, a relevant family history record and typical seizure features without a genetic study may be sufficient for genetic etiology classification (Falco-Walter, Scheffer, and Fisher, 2018). An infectious etiology is classified when a patient develops epilepsy as a result of infection, but not when seizures are occurring during the acute infection (e.g. encephalitis or meningitis) (Scheffer et al., 2017). In the case of metabolic etiology, epilepsy develops as a result of a condition from a variety of metabolic disorders. Immune etiology is conceptualized as a condition where autoimmune-mediated CNS inflammation causes epilepsy development. For the unknown category, no etiology can be reliably classified with existing methods. The etiological categories are not hierarchical, and several (potentially all) may apply to a single patient with epilepsy (Falco-Walter, Scheffer, and Fisher, 2018).

1.2.4 Genetic and acquired epilepsies

Another common epilepsy classification, which has been coined more than half a century ago Lennox and Lennox-Buchthal, 1960, and is still in use today with varying terminology, is dividing epilepsy cases into "genetic" and "acquired" (Shorvon, 2011; Falco-Walter, Scheffer, and Fisher, 2018; Zilberter, Popova, and Zilberter, 2021). In a genetic case, epileptogenesis results from pathological processes associated with de-novo (Epi4K Consortium, 2013) or inherited (Steinlein, 2004) mutations. For example, mutations in genes that code for voltage-gated and ligand-gated ion channels or their subunits (Berkovic et al., 2006; Lerche et al., 2013). In acquired epilepsy case, epileptogenesis is caused by an identifiable and acute brain injury or neurological disease (Zilberter, Popova, and Zilberter, 2021). Etiology of conditions that can cause acquired epilepsy is diverse. Considering the previously described classification of epilepsies according to their etiology, one can subdivide etiologic categories into having acquired or genetic causes. For example, most epilepsies with metabolic etiology are genetic, but some may be acquired (Falco-Walter, Scheffer, and Fisher, 2018). On the other hand, causes of structural etiologies are usually acquired (e.g. stroke, trauma), but may also be genetic (e.g. various malformations of cortical development) (Scheffer et al., 2017).

Importantly, "predisposing" (genetic) and "precipitating" (acquired) factors of epileptogenesis are not mutually exclusive (Lennox and Lennox-Buchthal, 1960). Moreover, it has been hypothesized that genetic component contributes to acquired epilepsy development because among subjects exposed to similar brain insult, only a fraction develops epilepsy. However, there is no conclusive evidence because research on the genetic contribution to acquired epilepsy is in its early phase (Perucca and Scheffer, 2021). Interestingly, epilepsies that are classified as genetic comprise only approximately 30% of all cases (Berkovic et al., 2006). Thus, the remaining 70% of epilepsy cases include an acquired component as a main or contributing cause of epileptogenesis. This brings epileptogenesis caused by a wide range of acute injuries and neurological diseases into the research spotlight.

1.3 Brain insults leading to acquired epilepsy

The list of conditions that are able to cause acquired epilepsy is long and diverse. However, in every case, the neuronal activity becomes characteristically hypersynchronous. This suggests that pathologies affect similar fundamental brain functions associated with the modulation of excitability in neuronal networks (Zilberter, Popova, and Zilberter, 2021). Both chronic, such as cerebrovascular diseases, and acute conditions, such as head trauma, are among the known causes of acquired epilepsy (DeLorenzo, Sun, and Deshpande, 2006). Among conditions causing acquired epileptogenesis, the most extensively documented and studied ones are stroke, traumatic brain injury (TBI), and status epilepticus (SE) (Pitkänen et al., 2015). SE is a neurological emergency in which a patient suffers from a prolonged (usually >5 minutes) or a series of seizures with an incomplete return to consciousness (Betjemann and Lowenstein, 2015). The data suggest that the incidence of acquired epilepsy is the highest during the first 5 years after injury, and also it varies depending on the brain insult type (Pitkänen et al., 2015). For example, the chance of epileptogenesis is higher for the SE survivors than for people having a stroke. Another important aspect is that an intensity of an injury modulates a chance of epilepsy development in a dose-dependent fashion. For example, the risk of epilepsy development is much higher after a severe TBI rather than after a mild one (Annegers et al., 1998). It has also been found that the types of injuries that are the most likely to cause epileptogenesis are age-specific (Sirven, 2015). In children they are birth trauma, infections, and congenital abnormalities; in middle years — head injuries, infections, alcohol and stimulant drugs; in older adults — brain tumors and cerebrovascular diseases.

1.3.1 Chronic conditions

A wide range of chronic conditions, among which are neurological and neurodegenerative diseases, have been identified as causes of acquired epilepsy. For example, the incidence of epilepsy in patients with cerebral palsy reaches up to 50% for some forms of the disease (Guerrini, 2006). Together with acute cerebrovascular conditions, such as stroke, chronic cerebrovascular conditions are also associated with epileptogenesis. For example, vascular malformations may cause epilepsy even in the absence of overt bleeding (Sirven, 2015). Regarding the effects of neoplasms, approximately 10-15% of all adult-onset epilepsy cases are associated with tumors (Lynam et al., 2007). The risk of epilepsy development is lower with malignant brain tumors, such as glioblastoma, and higher with some less-malignant infiltrative

lesions, such as World Health Organization (WHO) grade 2 diffuse gliomas (Sirven, 2015). Interestingly, for 30-50% of people with brain tumors, an epileptic seizure is a presenting clinical sign of the disease (Breemen, Wilms, and Vecht, 2007). Patients suffering from neurodegenerative diseases also have an increased risk of seizure occurrence, particularly in later disease stages. For instance, the risk of epilepsy development in patients suffering from Alzheimer's disease ranges from 0.5% to 64% depending on the severity of the neurodegenerative condition (Horváth et al., 2016).

1.3.2 Brain trauma

Among acute insults, that are associated with acquired epilepsy, TBI accounts for approximately 5% of all epilepsy cases (Pitkänen and Immonen, 2014). In the early stages after trauma, seizures are associated with hypoxia, increased intracranial pressure, ischemia, and other transient changes in the CNS. However, in the later stages, seizures are associated with permanent neuropathological changes and, consecutively, epileptogenesis (Sirven, 2015). The probability of epilepsy development over 30 years after severe, moderate, and mild TBIs are 17%, 4%, and 2% respectively (Annegers et al., 1998). This highlights the evident dose-dependence of epileptogenesis risk on the intensity of an insult. Despite the fact that an increasing number of researchers are focusing on studying the molecular and cellular mechanisms driving post-traumatic epileptogenesis, the identification of TBI-specific mechanisms of disease development remains an unresolved challenge (Pitkänen and Immonen, 2014).

1.3.3 Stroke

Another major cause of epileptogenesis is a stroke. At least 5% of its survivors develop acquired epilepsy with recurrent seizures, as a study based on more than 100 000 patient records suggested (Zou et al., 2015). Seizure manifestation and epilepsy development are more common in the case of hemorrhagic rather than ischemic stroke (Bladin et al., 2000). In regard to epilepsy manifestation, there are two peaks in seizure occurrence: during the first days, and in the period from 6 to 12 months after a stroke (Olsen, 2001). In addition to the primary injury (a stroke itself), there are likely smaller-scale changes in vasculature and white matter that contribute to the epileptogenic effect (Pitkänen, Roivainen, and Lukasiuk, 2016). Similar to the TBI case, the severity of a stroke is a predictive factor for the likelihood of epilepsy development (Alberti et al., 2008), which suggests that dose-dependence is a generalizable feature of acquired epilepsy.

1.3.4 Infections

Infections of the CNS are the major risk factor for the risk of epilepsy development worldwide (Vezzani et al., 2016). In the developing countries, where 80% of people suffering from epilepsy reside (World Health Organization, 2022), brain infections are by far the main cause of seizures and acquired epilepsy (Singhi, 2011). For instance, in sub-Saharan Africa infections were found to be the cause of the disease in up to 26% of patients with epilepsy (Preux and Druet-Cabanac, 2005). The CNS infections capable of causing seizures and epileptogenesis are associated with a wide range of pathogens (Vezzani et al., 2016). Among these infections are viral (e.g. herpes simplex, human herpesvirus-6), bacterial (e.g. bacterial meningitis, tuberculosis), parasitoses (e.g. malaria, cerebral toxoplasmosis), fungal (e.g. candidiasis, aspergillosis), and prion infections. For instance, children with a history of malaria have a 9 to 11-fold increased chance of developing chronic epilepsy (Sirven, 2015). Another example of a brain infection, which is strongly associated with severe seizures and post-infection epilepsy, is herpes simplex encephalitis. The reason is likely the involvement of a highly epileptogenic frontotemporal cortex in the course of encephalitis (Misra, Tan, and Kalita, 2008). Vezzani et al., 2016 have conceptualized the overlap in the pathogenesis of acquired epilepsy caused by infectious and sterile (non-infectious) inflammatory responses. The overlap is characterized by molecular mechanisms and activation pathways that often overlap for sterile inflammation and those induced by infection.

1.4 Epilepsy treatments and their limitations

Epilepsy puts a heavy burden on affected individuals, their caregivers and public health in general. The main factors of this effect are seizure-related disabilities, increased mortality, comorbidities, stigma, and additional medical costs (Moshé et al., 2015). The mortality rate for people with epilepsy is 2 to 5 times higher in high-income countries and may reach up to a 37-fold increase in low-income countries (Moshé et al., 2015). Approximately one-third of all premature deaths are attributable to epilepsy, either directly (e.g. due to SE, sudden unexpected death in epilepsy (SUDEP)), or indirectly (e.g. due to suicide, drowning) (Thijs et al., 2019). Overall, the life expectancy may be reduced by up to 10 years, in particular for symptomatic epilepsy patients (Gaitatzis et al., 2004). In addition to increased mortality rates, people with epilepsy are frequently affected by comorbidities. Each second patient suffers from one or several additional medical problems (Thijs et al.,

2019). Among them are anxiety disorder, depression, autism spectrum disorders, arthritis, type 1 diabetes, and others. Interestingly, some psychiatric diseases are considered to be risk factors for epileptogenesis and vice-versa, which hints toward shared causes and pathological mechanisms (Moshé et al., 2015).

1.4.1 Available medication

Antiseizure medication (pharmacotherapy) is the most commonly offered treatment for patients with epilepsy (Stephen and Brodie, 2011). The objective of anti-epileptic drugs' (AED) use is to suppress seizures as early as possible without causing side effects (Thijs et al., 2019). Choosing an appropriate therapy for a patient usually includes the following steps: deciding on treatment start day, selecting the most appropriate AED, and dosage optimization (Moshé et al., 2015). A selection of AED for a particular patient should take into account, among other individual characteristics, the type of seizures, epilepsy syndrome, tolerability risks, and comorbidities (Thijs et al., 2019). For example, such drugs as ethosuximide may be effective against absence seizures, while phenobarbital and primidone are effective against focal and generalized seizures, but specifically not against absence seizures (Perucca, 2015). The advantages and disadvantages of each drug have to be considered taking into account also individual characteristics and medical history of a patient. For example, if a patient suffers from both focal and absence seizures, one should not choose phenobarbital as an AED. This is due to the fact that phenobarbital has been reported to aggravate the absence seizures in the fraction of exposed patients (Perucca and Tomson, 2011). For patients that are seizure-free for more than 2 years of AED therapy, potential discontinuation of treatment is considered taking into account the presence and severity of AED's side effects, the prognosis of seizure recurrence, age, and other factors (Moshé et al., 2015).

1.4.2 Pharmacoresistance

Despite the availability of over 25 medication types worldwide, current AEDs are effective only in about two-thirds of epilepsy cases (Thijs et al., 2019). Thus, more than 30% of patients with epilepsy exhibit drug resistance to AEDs (Juvale and Che Has, 2021). Such cases are called pharmacoresistant epilepsy, which is formally defined as a failure to achieve seizure freedom after adequate trials of two tolerated and appropriately selected AEDs (Kwan et al., 2010). Up to 60% of patients with focal epilepsy and approximately 20% of patients with generalized epilepsy develop pharmacoresistant epilepsy (Pati and Alexopoulos, 2010). In contrast to other patients, individuals with pharmacoresistant epilepsy continue experiencing seizures, which

frequently leads to further neuropsychological, psychiatric, and social impairments (Alexopoulos, 2013). Pharmacoresistance remains a major challenge in epilepsy research, which, to a large extent, has not been tackled by the AEDs introduced in the past two decades (Moshé et al., 2015).

1.4.3 Surgery as epilepsy treatment

Surgery is considered to be the most effective intervention for achieving long-term seizure freedom in individuals with drug-resistant focal epilepsy (Thijs et al., 2019). Surgical procedures may include resection, destruction, or disconnection of epileptic brain tissue (Moshé et al., 2015). Among patients, who underwent surgery, almost three-quarters have a 50% or larger reduction in seizure frequency and almost half remained free from debilitating seizures five years after surgery (Mohan et al., 2018). Referring patient with epilepsy as a candidate for surgery is based on the assessment of a list of criteria, which may speak against or in favor of a surgery (Fig. 1.2): response to AEDs (present vs absent); seizure type (generalized vs focal); cause (genetic or metabolic vs structural); impact of seizures on cognition and quality of life (not significant vs significant); location of the epileptogenic zone (not localized, multiple vs well localized, single) (Moshé et al., 2015). Various advanced invasive and noninvasive techniques are used in the assessment of epilepsy patients as candidates for surgery. Among them are EEG, MRI, PET, single photon emission computed tomography (SPECT), magnetoencephalography (MEG), subdural grids, and depth electrodes (Najm et al., 2013).

There is a considerable amount of factors that limit the use of surgery in patients with pharmacoresistant epilepsy. For instance, the epileptogenic region can not be identified in a large number of patients, or it is localized within functional brain tissue, which makes the use of surgical methods unreasonable or impossible (Fattorusso et al., 2021). Moreover, epilepsy surgery is associated with complications and risks, that are inherent to neurosurgical interventions (hemorrhage, infections, memory deficits, etc) (Thijs et al., 2019). Despite a common belief that surgical treatment in epilepsy patients remains underutilized (Engel Jr, 2018), the evidence suggests that the outcome of surgical procedures remains suboptimal in a significant number of patients (Najm et al., 2013) and there is only a short list of studies that consider the long-term outcomes of surgery (Mohan et al., 2018). The data suggest that among patients with negative outcomes of epileptic surgery, there are early and late temporal patterns of seizure recurrence (Najm et al., 2013). Early cases of recurrence are evident shortly after surgery, and their driving mechanism is likely

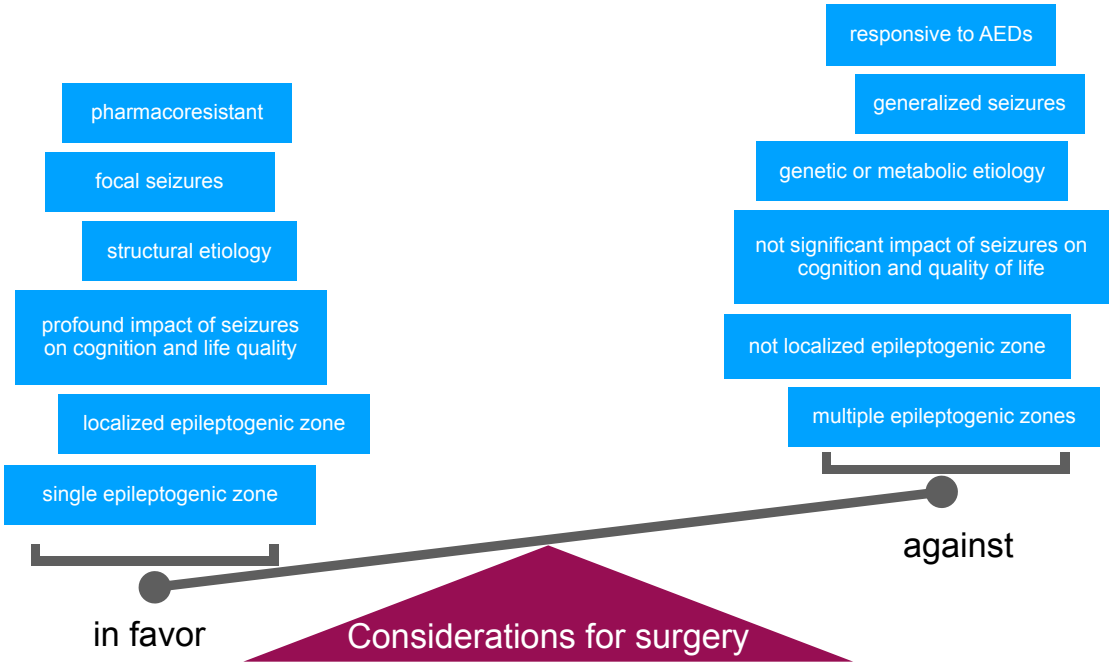

FIGURE 1.2: Criteria speaking in favor and against a surgical intervention.

to be a failure to either define or resect an epileptogenic zone. On the other hand, detection of late recurrences requires long-term follow-up studies. For instance, a study of 284 epilepsy surgery patients showed that 47% of patients remained seizure-free 5 years after surgery and only 38% 10 years after surgery (Mohan et al., 2018). This suggests an approximately 20% drop in surgery efficacy due to late epilepsy recurrence during only extra 5 years follow-up period. Such late epilepsy recurrence is hypothesized to arise from a development or maturation of a new epileptic focus (de novo epileptogenesis) (Najm et al., 2013).

Another important factor in the consideration of surgery as an epilepsy treatment strategy is the availability of neurosurgical services in the first place. Despite a considerable increase in the availability of neurosurgeons over the last decade in all geographic regions, including low- and middle-income countries, the absolute majority of African, South Asian, and Oceanic countries have around or less than 1 neurosurgeon per 1 million people (Mukhopadhyay et al., 2019). This, together with the impossibility or unreasonableness of surgery application in some patients with pharmacoresistant epilepsy, constitutes the necessity for further research on alternative intervention strategies.

1.4.4 Alternative treatment methods

A considerable amount of patients suffering from pharmacoresistant epilepsy are not eligible or do not have access, to surgery. In such patients, neurostimulation is becoming a commonly accepted complementary or alternative treatment technique to pharmaceuticals (Fattorusso et al., 2021). For instance, over the last 15 years, more than 70 000 patients with epilepsy worldwide were treated with vagus nerve stimulation (Moshé et al., 2015). More than half of them experienced a 50% or higher reduction in seizure frequency, but only less than 5% became seizure-free with such treatment. Alternative non-pharmacological treatment techniques such as neurostimulation and diet therapy are considered to be promising, but the long-term efficacy does not appear satisfactory from currently available data (Fattorusso et al., 2021).

1.4.5 Absence of antiepileptogenic treatment

Another conceptual issue with available epilepsy treatments is the absence of techniques for disease prevention. By definition, the AEDs are meant to suppress the occurrence of epileptic seizures, but they happen to fail to alter the disease prognosis (Thijs et al., 2019). The prevention of epilepsy remains an urgent unmet medical need (Löscher, 2020), which requires the development of not only antiseizure but also antiepileptogenic treatment. The evidence of antiepileptogenic effects of already known compounds and interventions is accumulating (Hufthy et al., 2022). Among those with a potential for antiepileptogenic effects are some AEDs, dietary treatments, modulators of glutamatergic transmission, brain cooling, and others (Moshé et al., 2015). For those, a range of neurobiological processes has been considered potential targets for antiepileptogenic and disease-modifying therapies (Thijs et al., 2019). Among them are the accumulation of neurodegenerative proteins, pro-inflammatory processes, neurogenesis, and others. However, it is still to be established if any of these processes are fundamental to epileptogenesis (Thijs et al., 2019). While the pre-clinical (animal model) studies on potential antiepileptogenic agents are in their active phase, no clinically validated antiepileptogenic treatments are available yet (Löscher, 2020).

1.5 Current methods in epilepsy research

1.5.1 Research on human patient data

A wide range of neuroimaging techniques, such as MRI, X-ray CT scanning, PET (Duncan, 2019), and other medical recordings, such as patient-reported seizure diaries (Fisher et al., 2012), EEG, electro-cardiogram (Thijs et al., 2019), are used in the process of epilepsy diagnosing and selection of an appropriate treatment plan. These data, together with data collected in a framework of clinical research trials (e.g. post mortem tissue analysis (Lalwani et al., 2020), neuroimaging recordings (Rüber et al., 2018), etc), are used to generate insights into principles of epilepsy development. A range of hypotheses about epileptogenesis principles and the involvement of other processes in epileptogenesis have been suggested based on clinical data. For example, dysfunction of the blood-brain barrier (BBB) is hypothesized to contribute to epileptogenesis. The quantitative MRI study confirmed the temporal and anatomical association between epileptic seizures and the BBB leakage (Rüber et al., 2018). Another example of insights into epileptogenesis derived from human patient data is finding that epilepsy can arise from the combination of effects of multiple mutations that are not individually deleterious (Kaplan, Isom, and Petrou, 2016). This was illustrated by sequencing 237 ion-channel genes in 152 patients with idiopathic epilepsy (Klassen et al., 2011).

However, the use of clinical data in epilepsy research is associated with a list of limitations, such as scarcity and inconsistent timing of recordings, diversity and evolving nature of epilepsy disorders, and considerable noise effects due to inter-patient differences in the disease history, medication plans, etc. For instance, the design of studies on the involvement of genetic factors in epilepsy development includes a list of issues with epilepsy phenotype definition, data collection, methods of analysis, and the interpretation of results (Greenberg and Subaran, 2011). Another important aspect for use of clinical data in epilepsy research is the existing legislative base and its inter-country variability. This may affect the ease of data transfer, aggregation, processing, and publishing. However, these obstacles are being addressed by evolving global research initiatives, such as European Union's Clinical Trials Regulation (European Medicines Agency, 2022). Such initiatives are aimed at standardizing the procedures for multinational projects with high levels of transparency and safety for clinical trial participants. In summary, despite considerable improvement in clinical trial design, further optimization of trial methodology is needed to comply with ethical concerns and to provide reliable and generalizable

results (Ferlazzo et al., 2017). In addition, modern epilepsy data are collected in the scale of petabytes, and therefore it requires the big data principles for proper handling in order to harness its full research potential (Lhatoo et al., 2020).

1.5.2 Research with animal models of epilepsy

The use of animal models, in comparison to the clinical data, allows for the design of experiments with controlled conditions (e.g. similar genetic profiles of animals, identical exposure factors, etc) with a necessary number of subjects and a well-matched control population. This makes animal model studies crucial for research both on principles of epileptogenesis and pre-clinical studies on treatment techniques. The important distinction in animal models of epilepsy is whether they are models for epileptic seizures (for example, obtained by electric stimulation of an animal's CNS) or epileptogenesis, in which seizures are spontaneous and recurrent (Grone and Baraban, 2015). In recent decades, a range of animal models of epilepsy has been developed mimicking the most known causes of epileptogenesis. Among them are epilepsies caused by genetic factors, stroke, traumatic brain injuries, infections, SE, and others (Pitkänen et al., 2015). While epilepsy animal models were developed for various species (even for invertebrates and non-human primates), the key species for epileptogenesis research are rodents, such as the Norway rat (*Rattus norvegicus*) and the house mouse (*Mus musculus*) (Grone and Baraban, 2015). For instance, the most extensively utilized model of post-traumatic epilepsy, called "fluid percussion injury", is implemented in both rats and mice (Keith and Huang, 2019). On the other hand, Theiler's Murine Encephalomyelitis Virus (TMEV) animal model of infection-caused epilepsy is specific to the C57BL/6J genetic strain of mice (DePaula-Silva et al., 2017). Importantly, no single animal model of epilepsy represents this disease fully, which is expected if we consider the breadth of a spectrum of disorders represented by the term epilepsy (Grone and Baraban, 2015). However, the variability of animal models can be seen as their instrumental advantage, which allows scientists to implement an appropriate setup for a concrete research question.

Similar to clinical data, animal models have a range of disadvantages and limitations. The key question to any hypothesis or observation in the animal model study is whether they translate to the human condition, or whether this finding is specific to a concrete animal model (Klein et al., 2018). Another important aspect of studies with animal models is ethical considerations. As of today, a substantial amount of experimental measurements require invasive procedures or even animal

sacrifice. For example, investigation of neuronal loss signs in the brain of an animal with high spatial resolution requires examination of tissue prepared in the form of brain slices. Thus, for each time point, which the researcher would like to include in the experiment, a separate batch of animals has to be prepared and sacrificed. Such allocation of animals may be justified in an experiment with a hypothesis that is well motivated by prior evidence. On the other hand, an explorative research project, which is especially relevant to such multidimensional issues with lots of unknowns as epileptogenesis, is less likely to be implemented due to ethical considerations. Moreover, experimental studies within and across different animal models and research laboratories do not follow standardized protocols (e.g. timeline of recordings, protocols of saving data), which does not allow for aggregation of available data together for direct comparison of phenomena observed in various studies. However, there are evolving initiatives for standardization of data collection and experimental procedures (Wagenaar et al., 2015; Harte-Hargrove et al., 2017), which have a high potential for the facilitation of collaborative epilepsy research.

1.6 Mathematical modeling as a research tool

In recent decades, mathematical modeling and other computational methods got considerable attention as research tools in life sciences. In the context of research on diseases and pathologies, a variety of mathematical models have been formulated and used for the generation of novel insights. For example, the mechanistic model developed by Adler et al., 2020 describes the myofibroblast-macrophage circuit dynamics and explains how transient and persistent insults lead to either healing or fibrosis. Another modeling example, considering the CNS pathology, is the phenomenological framework of neuron-glia cross talk developed by Nold et al., 2020. This model provides insights into how the compromise between short-term resilience and long-term prevention of tissue damage may lead to the development of neurodegeneration. In addition to fundamental research on principles of physiological processes and pathologies, mathematical models play a critical role in the modern drug-discovery process, complementing and enriching the standard toolset of pharmacological research (Peletier and Gabrielsson, 2018).

In the context of epilepsy, the variety of modeling techniques used in, and the range of scientific questions addressed by mathematical models are as large as the diversity of known epilepsy syndromes. Mathematical models are used in seizure

prediction (Yang et al., 2018; Peng, Song, and Yang, 2021), epileptogenesis detection (Lu et al., 2020), fundamental research on principles of seizure generation (ictogenesis) (Jirsa et al., 2014; Chang et al., 2018) and other applications. By far, the most popular modeling techniques in epilepsy research are dynamical system models and algorithms built on artificial neuronal networks.

1.6.1 Models for epileptogenesis detection

The use of mathematical models in epilepsy research and clinical applications dates as far back as the 1970s. In their pioneering work, Feeney and Walker, 1979 have presented a mathematical model that can be used to estimate the probability of post-traumatic seizures based on the list of risk factors and time since an injury. Interestingly, as of today, the problem of reliably predicting which patients will eventually develop epilepsy after trauma remains partially unresolved (Rubinos, Waters, and Hirsch, 2022). Nevertheless, considerable progress has been achieved both in seizure prediction and the identification of subjects undergoing epileptogenesis. For example, the model developed by Lu et al., 2020 allows not only to identify subjects undergoing epileptogenesis but also to classify early vs late epileptogenesis stages. The model is built on deep neural network technology and receives as input the intracranial electroencephalogram (iEEG) signal. The detection of epileptogenesis in the early stages, even before the manifestation of spontaneous recurrent seizures, provides a valuable therapeutic window, in which early interventions may be applied. Moreover, by analyzing the activity of the trained deep neural network, one can decode which sections of the EEG signal the network has considered to be informative for classification. Thus, the model also provides novel EEG biomarkers for different phases of epileptogenesis (Lu et al., 2020).

1.6.2 Seizure prediction models

The reliable prediction of upcoming epileptic seizures would remove the burden of unpredictability and risk of harm in patients suffering from pharmacoresistant epilepsy. Even though the issue is not yet fully resolved, there is already a number of promising developments in this direction (Kuhlmann et al., 2018). Seizure prediction systems vary in their core technology (e.g. convolutional neural networks (CNNs), support vector machines (SVMs), and others) and ability to work reliably with scalp EEG signals. A wide range of models has been reported as successful in seizure prediction using iEEG data. For example, the two-level sparse multiscale classification model allows for robust classification of interictal (time period between seizures) and preictal (time interval shortly before a seizure) states from

iEEG recordings in animal models and human data (Yu et al., 2021). However, the majority of patients with pharmacoresistant epilepsy need a non-invasive solution for seizure prediction with scalp EEG signals. In the pre-clinical studies, several research groups reported a considerable improvement in the performance of seizure predictors on scalp EEG, which was obtained using machine deep learning methods. For instance, Usman, Khalid, and Bashir, 2021 have designed an ensemble classifier that combines the output of SVM, CNN, and long short-term memory (LSTM) network. This tool reached the sensitivity and specificity of 96.28% and 95.65% with an average seizure anticipation time of 33 minutes. Another detection method, which was designed by Jana and Mukherjee, 2021, is built on CNN technology with an aim of fitting to the requirements of a transportable real-time prediction device. According to the pre-clinical results, with data from as few as 6 recording EEG electrodes, the method predicts seizures with 10 minutes of anticipation time, 97.83% and 92.36% sensitivity and specificity respectively.

1.6.3 Models of ictogenesis and seizure dynamics

A considerably large group of models describe such aspects of epilepsy as a generation, propagation, and termination of seizures. These models are used not only in studying the nature of epileptic seizures but also can be used in clinical applications. For example, dynamical network models are designed for *in silico* exploration of the potential impact of surgical resection in presurgical planning (Junges et al., 2019; Junges et al., 2020). In fundamental research on seizures, various detailed biophysical models and dynamical system tools are used (Depannemaecker et al., 2021). These models span different spatial scales, from a single cell to large-scale networks. They are used, among others, for studying the effects of cell loss on network excitability (Santhakumar, Aradi, and Soltesz, 2005), spatiotemporal patterns of seizure propagation (González-Ramírez et al., 2015), or improvement of classification of epileptic seizure types (Depannemaecker et al., 2021).

Among the most renowned mathematical models in epilepsy research is a generic model called "Epileptor" designed by Jirsa et al., 2014. It is built on only five state variables linked by integral-differential equations. Despite the simplicity, the setup is sufficient to describe the onset, duration, and offset of seizure-like events as well as their recurrence. Originally based on an experimental model system of ictal-like discharges from *in vitro* in mouse hippocampi (Jirsa et al., 2014), the model is being consistently used, further developed, validated, and mathematically analyzed in consecutive studies (Naze, Bernard, and Jirsa, 2015; El Houssaini, Bernard, and Jirsa, 2020). However, since the objective of modeling was to describe the seizure

dynamics and not to account for all possible biophysical details, the variables of the Epileptor model are abstract by design (Jirsa et al., 2014). Thus, the interpretation and translation of findings, regarding the factors that push the system to a state of seizure generation, into a list of biological processes remains a challenge.

1.6.4 Models of epileptogenesis

Despite the fact that understanding the process of epileptogenesis is the focus of epilepsy research, the methodology of mathematical modeling in the context of epileptogenesis remains underutilized. The absolute majority of existing mathematical modeling studies in epilepsy research are neuron-centric, which means that they are built on biophysical or abstract models of neuronal cells. In such models, the processes of the neuro-immune axis, which have been shown to play a crucial role in epileptogenesis (Vezzani, Balosso, and Ravizza, 2019; Vezzani et al., 2022; Altmann et al., 2022), are either oversimplified or completely omitted. However, there is an exception — the model developed by Savin, Triesch, and Meyer-Hermann, 2009, which accounts for the interaction between the immune system and neuronal population. This model is built on a two-dimensional neuron model with an additional component of synaptic scaling by neuron-glia cross talk. This pioneering study has generated a list of insights into possible mechanisms and dynamics of neuro-immune processes' impact on epileptogenesis. However, except for one study (Savin, Triesch, and Meyer-Hermann, 2009), which focused on tumor necrosis factor (TNF) effects on changes in network excitability, no other mathematical model has been designed to describe the process of epileptogenesis and account for the role of neuro-immune processes in it as of writing this thesis.

1.7 Research goals

The goals of this doctoral project are:

1. to conduct a comprehensive literature research to determine the key players of the neuro-immune axis, which have to be included in the framework describing the epileptogenesis;

2. to develop a phenomenological mathematical model that will:

    - account for the roles of neuro-immune processes in epileptogenesis;
    - allow for simulation of acquired epileptogenesis with its injury-specific characteristics;
    - reproduce existing experimental and clinical findings;
    - provide insights into principles of epilepsy development;
    - allow for the generation of testable predictions on intervention strategies.

Chapter 2

Epilepsy and the brain

This chapter is dedicated to familiarizing the reader with the physiological and pathological processes that are involved in epileptogenesis phenomena. Among them are neuroinflammation, BBB disruption, neuronal death, and circuit remodeling. For each of these processes, the key cell types and their functions are described. Further, the interaction of these processes with each other and their role in epileptogenesis are discussed.

2.1 BBB disruption

The BBB is a physical barrier between the periphery of the organism and the CNS. This complex multicellular structure is crucial for the protection of the cells populating the neural tissue from molecules and cells circulating in the blood. These blood-borne factors, in case of penetration into the extracellular space of the brain tissue, can have neuroactive or toxic effects (Smith, 2003). Known since the 19th century, the BBB was believed to be absolutely unpenetrable, which implied the absence of immune system effects in the brain. However, nowadays it is clear that the BBB not only allows certain molecules and cells to infiltrate the brain, but its permeability may be also modulated in response to environmental stimuli (Rubin and Staddon, 1999). This brought the BBB to the focus of research in the context of various neurological diseases, among which is also epilepsy (Van Vliet, Aronica, and Gorter, 2015).

2.1.1 Structure and functions of the BBB

The BBB complex structure is constituted of three major cell types: endothelial cells, pericytes, and astroglia (Fig. 2.1) (Keaney and Campbell, 2015). On the

first layer, the endothelial cells form the walls of blood vessels. The margins of endothelial cells form tight junctions, that consist of four classes of proteins: occludin, tricellulins, claudins, and junctional adhesion molecules (Langen, Ayloo, and Gu, 2019). The tight junctions significantly reduce the permeation of polar solutes from the blood plasma to the brain's extracellular fluid (Abbott et al., 2010). On the second layer, the pericytes partially surround the endothelial cells of the BBB since they are distributed discontinuously along the capillaries. On the third layer, the foot processes of astrocytes (type of glial cells in the CNS) enclose the capillaries. Together this multicellular structure forms a highly selective barrier, which encompasses machinery for the active influx and efflux transport and regulation of the permeability for passive transport across the BBB (Langen, Ayloo, and Gu, 2019).

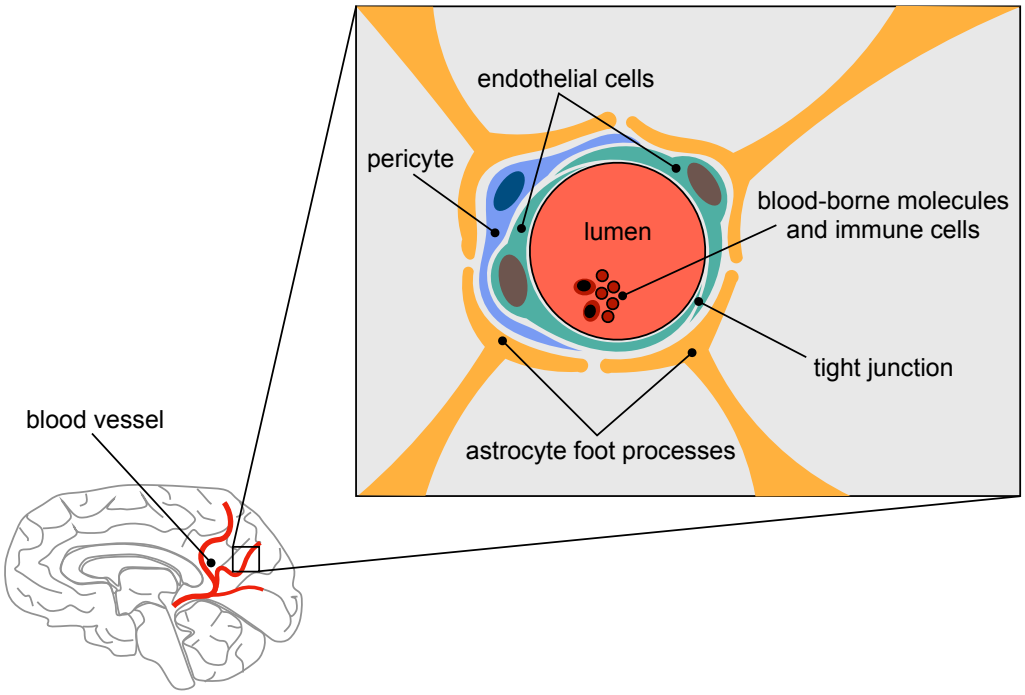

FIGURE 2.1: BBB structure.

The functional BBB is crucial for the maintenance of homeostasis in the CNS. It is playing a central role in the trophic support of the brain, regulating the influx and efflux of nutrients, ions, and oxygen between the brain and the blood (Keaney and Campbell, 2015). The BBB gates the entry of neurotoxins, metals, neuroactive solutes, such as peptide hormones or glutamate, and other factors that may have detrimental effects on the physiological processes of the CNS (Smith, 2003).

Moreover, the BBB is actively removing such factors from the brain by energy-dependent efflux. In the conditions of physiologically functioning BBB, the peripheral leukocytes (immune system cells) infiltration into the brain is highly regulated and the concentration of blood-borne leukocytes in the CNS is significantly lower than in peripheral tissues (Langen, Ayloo, and Gu, 2019). However, in response to danger signals, endothelial cells may become activated and upregulate the cell adhesion molecules, which allows for subsequent transendothelial leukocyte migration. Thus, the process of adaptive immune system cell migration through the BBB (transendothelial leukocyte migration) is currently recognized as a part of normal CNS physiology (Keaney and Campbell, 2015).

2.1.2 Seizures, epileptogenesis and integrity of the BBB

The increase of the BBB permeability has been found not only in the physiological context when it is increased to meet metabolic or immune needs. The dysregulation of the BBB integrity (leakage of the BBB) has been also observed in various neurological diseases and clinical conditions, including multiple sclerosis, hypoxia, Parkinson's, and Alzheimer's diseases (Abbott et al., 2010). In the context of epilepsy, disruption of the BBB is among the risk factors of disease development. The functional and structural alterations of the BBB occur in response to primary brain insults that are associated with epileptogenesis, such as TBI, stroke, infection, and SE (Klein et al., 2018). The BBB disruption and its imitations are used as epileptogenic injuries in several animal models of epilepsy development (Seiffert et al., 2004; Weissberg et al., 2015). In the event of vascular injury or BBB leakage, the albumin-mediated transforming growth factor b (TGF-β) causes local inflammation, which may further lead to acquired epileptogenesis (Bar-Klein et al., 2014).

Interestingly, not only the BBB disruption is able to trigger epileptogenic changes, but seizures themself are causing the leakage of the BBB. A study of both human and rat epileptic brain tissues has revealed a positive correlation of the BBB permeability with the intensity of seizure activity (number of seizures per hour) and a negative correlation of the BBB permeability with the time since the last epileptic seizure (Van Vliet et al., 2007). Moreover, a recent study by Rüber et al., 2018 has illustrated that the BBB disruption is associated with epileptic seizures not only temporally, but also anatomically. This was shown by the region-specific association of seizure activity with markers of the BBB leakage in focal seizure cases and lateralization of leakage markers to the hemisphere of seizure onset for patients with

secondarily generalized epilepsy. Thus, dysregulation of the BBB integrity is at the same time a consequence of epileptic seizures and one of the factors promoting epileptogenesis via secondary neuroinflammatory reaction (Löscher and Friedman, 2020).

2.2 Neuroinflammation

Inflammation is a response of the immune system aimed at the protection and defense of a body (Lyman et al., 2014). Neuroinflammation is a process of inflammation, which is specific in its characteristics to the brain and the spinal cord. This specificity underlies not only in the spatial localization but also in qualitative differences to the peripheral inflammatory process. From a research perspective, neuroinflammation is a non-trivial target since it acts on the intersection of the two complex systems: neural and immune.

Neuroinflammation is an inherent mechanism aimed at the protection and restoration of the structure and function of the CNS in reaction to an insult (More et al., 2013). The insults, that are able to trigger the neuroinflammatory reaction, are tissue damage, autoimmune conditions, infections, stress, or seizures (Vezzani, Balosso, and Ravizza, 2019). Neuroinflammation as a physiological process has been identified as beneficial for the maintenance of an organism through the promotion of tissue repair process, neuroprotection, mediating sickness behavior, and even memory formation (DiSabato, Quan, and Godbout, 2016).

In certain conditions, a neuroinflammatory reaction may be maladaptive. Moreover, it can also constitute a key pathological driver of various neurological and neurodegenerative diseases (Chaney et al., 2021). For instance, neuroinflammation is suspected to induce and accelerate the pathogenesis of such diseases as Parkinson's, Alzheimer's, and Multiple sclerosis. In recent decades, the research community has paid considerable attention to the role of neuroinflammation in epileptogenesis. Nowadays, the neuroinflammatory pathways are considered to be prominent treatment targets and biomarkers for epilepsy (Vezzani, Balosso, and Ravizza, 2019).

2.2.1 Neuroimmunity

For many decades, the CNS was considered to be an immune-privileged site in which the activity of the adaptive immune system and inflammation are highly controlled (Harris et al., 2014). This belief was reinforced, among others, by the fact that in the presence of an intact BBB, the concentration of adaptive immune system agents, such as T and B lymphocytes, is considerably lower in the brain parenchyma than in peripheral tissues (Langen, Ayloo, and Gu, 2019). Nowadays, the CNS is no longer considered to be immune-privileged since accumulating evidence demonstrates the activity of innate and adaptive immune systems in the brain (Fuzzati-Armentero, Cerri, and Blandini, 2019). However, the innate neuro-immune system is structurally and functionally distinct from its peripheral counterpart. The key players of the immune system in the CNS are microglia - the macrophage-like cell type constituting approximately 10% of the brain tissue (DiSabato, Quan, and Godbout, 2016). Being present both in white and grey matter, microglia are constantly surveilling the tissue for danger-associated signals to kick-start a neuroinflammatory reaction. Contrary to the periphery, neuroinflammation does not require the presence of blood-borne cells. Thus, the inflammatory reaction can occur as a result of abnormal changes in the microenvironment (Becher, Spath, and Goverman, 2017). Interestingly, the neuro-immune system is found in close bidirectional communication with the periphery (Kempuraj et al., 2017). This cross talk is even able to modulate the permeability of the BBB that is separating these two systems (Lyman et al., 2014).

2.2.2 Principles of neuroinflammation in detail

In physiological conditions, the resting (quiescent) microglia perform the primary immune surveillance: scanning with their motile processes the tissue for the presence of danger signals (DiSabato, Quan, and Godbout, 2016). Such signals may be represented by danger-associated molecular patterns or a lack of normal signaling from neurons and other glial cells (Jurga, Paleczna, and Kuter, 2020). Once a danger signal is detected, microglia undergo activation (change of phenotype to a pro-inflammatory), which leads to a change of the cell's shape and profile of signaling molecules (Fig. 2.2). Activated microglia secrete cytokines (TNF and interleukins IL-1β, IL-6), chemokines (CCL2, CCL5, CXCL1), reactive oxygen species (ROS), and secondary messengers (nitric oxide (NO) and prostaglandins) (DiSabato, Quan, and Godbout, 2016). These factors, secreted by an activated microglial cell, may be sensed by and lead to phenotypic changes in other brain-resident cells, such as

neurons, astrocytes, endothelial cells, and pericytes. For example, astrocytes and microglia express a range of toll-like receptors (TLRs) that are sensitive to pro-inflammatory factors (e.g. activation of TLR-4 by TNF and IL-1β) and can activate these cells, initiating a neuroinflammatory reaction (Lyman et al., 2014).

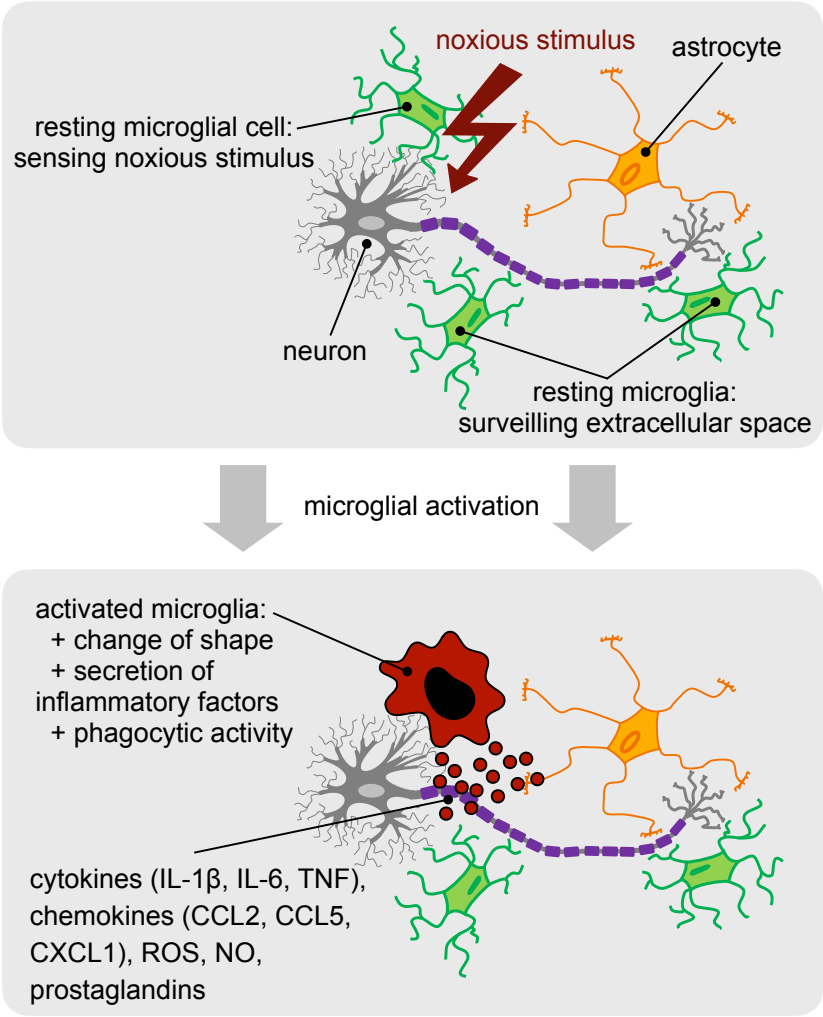

FIGURE 2.2: Microglial activation process.

The intensity and duration of a neuroinflammatory reaction depend on the context: duration and the course of the primary injury or insult (DiSabato, Quan, and Godbout, 2016). After a resolution of an insult, microglial cells continue with phagocytosis of debris in the extracellular space and shift towards anti-inflammatory cell phenotype with protective functions: secretion of anti-inflammatory cytokines, silencing local inflammation, production of mediators of myelin repair, etc (Jurga, Paleczna, and Kuter, 2020). If a noxious stimulus can not be eliminated over an

extensive period of time, a neuroinflammation can become chronic. Contrary to physiological transient activation, excessive and prolonged neuroinflammation is associated with a list of pathological effects, such as synaptic dysfunction, inhibition of neurogenesis, and even induction of cell loss (Lyman et al., 2014). In addition, microglial cells appear to have a low turnover rate, which makes them susceptible to accumulated effects of injuries and aging (DiSabato, Quan, and Godbout, 2016). Microglia show an amplified response to a consecutive insult compared to the first activation, and this phenomenon is called microglial priming (Li et al., 2018). Such an amplified response involves changes in proliferation abilities, morphology, and biochemical markers. Thus, an excessive or prolonged neuroinflammatory reaction may appear not only in a situation when a primary injury is extended in time or can not be resolved but also when the injury was preceded by the priming of microglia.

It is important to mention that in literature the spectrum of microglial phenotypes is frequently described along the 'M1/M2' axis, which corresponds to pro-inflammatory / anti-inflammatory states at the extremes. In this work, such an intuitive description with its well-defined markers was omitted, since it is considered to be an oversimplification. The transcriptome-based network analysis of macrophages exposed to 29 various stimuli revealed that each stimulus triggered an expression of a distinct transcription profile, which can not be aligned on a spectrum with a unidimensional axis (Dubbelaar et al., 2018). Thus, the multidimensional concept of microglial phenotypes has to be considered in the future.

2.2.3 Neuroinflammation and leakage of the BBB

Neuroinflammation can modulate the permeability of the BBB, for instance, in order to recruit peripheral immune cells (DiSabato, Quan, and Godbout, 2016). In the case of peripheral immune reaction, inflammatory factors (e.g. TNF and ILs) can be delivered to the brain by the active BBB transport, and cause a neuroinflammatory reaction in the CNS (Lyman et al., 2014). The inflammatory cytokines, prostaglandins, and other mediators released by activated glia affect the tight junctions and transport mechanisms in endothelial cells, which leads to increased permeability of the BBB (Vezzani, Balosso, and Ravizza, 2019). On the other hand, an increase of the BBB permeability may lead to infiltration of blood-derived proteins, such as albumin, into the extracellular space of the brain tissue (Vezzani, Balosso, and Ravizza, 2019). This leads to the activation of astrocytes and consecutive neuroinflammatory reaction (Löscher and Friedman, 2020). Thus, the BBB disruption

and neuroinflammation form a positive feedback loop, which may be, in addition, reinforced by the leakage-inducing effects of epileptic seizures (Van Vliet et al., 2007).

2.2.4 Neuroinflammation and seizure susceptibility

When the inflammatory milieu exceeds the homeostatic thresholds, the release of inflammatory mediators can lead to an increase in neuronal excitability and, consecutively, lower the seizure threshold (Klein et al., 2018). For example, the IL-1R/TLR4 signaling pathway, which is activated by HMGB1 protein and IL-1β in the course of neuroinflammation, contributes to the hyperexcitability of neuronal population and leads to seizures both in animal models and human patients (Vezzani, Balosso, and Ravizza, 2019). Another cytokine of pro-inflammatory profile — TNF has been identified to cause increased synaptic transmission, hyperexcitability, and elevated susceptibility to seizures (Patel et al., 2017). The genetic suppression of TNF or TNF receptor type 1 (TNFR1) leads to the robust decrease in seizure incidence and severity. On the other hand, suppression of TNF receptor type 2 (TNFR2) exacerbated the pathology, which suggests the antagonistic roles of TNFR1 and TNFR2 as ictogenic and anti-ictogenic respectively (Patel et al., 2017). The overview of pathways, by which neuroinflammation modulates neuronal excitability and seizure threshold, is summarized in the table in Devinsky et al., 2013.

A recent study by Badimon et al., 2020 revealed the ability of microglial cells to suppress neuronal excitability in the activity-dependent and region-specific fashion. Moreover, microglia have been found to be critical for the regulation of network excitability via constraining the excessive neuronal activation that can not be suppressed by inhibitory neurons. Studied the effect of microglial depletion in several animal models, researchers found that microglia-deficient animals become hyperresponsive to sub-threshold ictal stimuli, and their likelihood of seizure development significantly increases (Badimon et al., 2020). Thus, it is tempting to speculate that, in conditions of neuroinflammation, the downregulation of microglial inhibitory effects may be an alternative mediator-independent mechanism for lowering the seizure threshold.

2.3 Neuronal death

For decades, the selective neuronal loss has been known to take place in the hippocampus and other brain areas as a result of epileptic activity (Dam, 1980; Meldrum, 1993). Nevertheless, up until now, it remains unclear whether neuronal death is a cause, consequence, or both in the context of epileptogenesis. For instance, the most common type of pathology associated with TLE is hippocampal sclerosis. However, not all patients with hippocampal sclerosis have TLE, and a significant fraction of people with TLE have no apparent signs of neuronal damage in the hippocampus (Henshall and Meldrum, 2012). Currently, it is under the debate whether isolated brief seizures kill neurons, while repetitive and severe seizures clearly lead to neuronal death (Dingledine, Varvel, and Dudek, 2014).

2.3.1 Diversity of neuronal death mechanisms

In recent decades, the research on cell death became a fast-growing field. Novel mechanisms driving cell loss continue to be discovered, so the classification of types of cell death is frequently updated (Galluzzi et al., 2018). In the context of neuronal cell death in the CNS, four additional mechanisms of cell death have to be taken into account together with the well-known necrosis and apoptosis: necroptosis, phagoptosis, autophagy, and pyroptosis (Dingledine, Varvel, and Dudek, 2014). There is a list of functional differences among these cell death mechanisms. For example, cell death processes can be divided into inflammatory (necrosis, pyroptosis, and necroptosis) and non-inflammatory (apoptosis, autophagy, and phagoptosis) (Dingledine, Varvel, and Dudek, 2014). Inflammatory mechanisms of cell death are accompanied by inflammatory lysis. Lysis underlies the breakdown of a cell membrane with a release of cytosol content into the extracellular space, which can trigger the neuroinflammatory reaction (Scaffidi, Misteli, and Bianchi, 2002). However, not only the mechanisms of cell death, which lead to secondary neuroinflammation, are tightly connected with microglial functions. For instance, microglia may engulf a viable neuronal cell, which constitutes the phagoptosis mechanism (Brown and Neher, 2012). In fact, all cell death types are functionally related to microglia since microglial cells are the macrophage-like cells responsible for the phagocytosis of cell debris in the brain tissue (Perry and Teeling, 2013).

2.3.2 Neuronal death and neuroinflammation

Neuroinflammation, if not adequately controlled, causes damage to neural tissue and leads to induced neuronal death (Vezzani, Balosso, and Ravizza, 2019). In conditions of chronic or excessive neuroinflammation, overactivation of microglia is associated with the degradation of proteins, dysfunction of mitochondria, defects of axonal transport, and dysregulation of mechanisms of neuronal death (Sochocka, Diniz, and Leszek, 2017). This has been illustrated in the experimental setting by the administration of lipopolysaccharide (LPS), which leads to TLR4-mediated activation of microglial cells, but has no direct effects on neuronal cells (Fuzzati-Armentero, Cerri, and Blandini, 2019). Activated microglia induce the apoptosis of neuronal cells, leading to their cell death (Hornik, Vilalta, and Brown, 2016). Moreover, in presence of overactivated microglia, the neurotoxicity is induced by the excessive release of pro-inflammatory cytokines and enzymes, such as TNF, IL-1β, NO, and ROS (Sochocka, Diniz, and Leszek, 2017), which also contribute to the activation of neuronal death pathways (Salucci et al., 2021). In addition, activated astrocytes, which are characteristic of neuroinflammatory tissue, express insufficient glutamate transporters, which promotes excitotoxic neuronal death (Patel et al., 2019). Overall, glutamate-mediated excitotoxicity, necrosis, and apoptosis are considered to be the central mechanisms contributing to neuronal death in epilepsy (Henshall, 2007).

2.4 Circuit remodeling

In the course of reaction to the CNS insult, remodeling of connectivity in the brain can take place on various scales: from synaptic (Kim et al., 2016) to network levels (Jo et al., 2019). Such circuitry remodeling may be caused by a loss in the neuronal population (Isacson and Sofroniew, 1992) or a maladaptive neuro-immune reaction (Fig. 2.3) (Löscher and Friedman, 2020). In the context of epilepsy, circuit remodeling is associated with increased excitability of neuronal circuits and lowering of the seizure threshold (Hunt, Boychuk, and Smith, 2013). For instance, in human TLE cases, the aberrant circuit rewiring in the dentate gyrus is associated with the formation of epileptic foci (Gupta and Schnell, 2019). This rewiring includes alteration of granule cell migration, axonal arborization, and dendritic morphology. On the network level, TLE patients have a pronounced enhancement of connectivity between the sclerotic hippocampus and the ipsilateral thalamus compared to healthy control participants (Dinkelacker et al., 2015). Interestingly, circuit remodeling is suggested to not only be a cause of epileptic seizures, but also its consequence. It was hypothesized that recurrent seizures cause continuous circuit reorganization and

thus contribute to the progression of disease severity (Pitkänen and Sutula, 2002). The growing body of evidence for seizure effects on the BBB permeability and subsequent neuro-immune reaction (Van Vliet et al., 2007; Weissberg et al., 2015; Van Vliet, Aronica, and Gorter, 2015) supports this hypothesis and provides a mechanistic explanation for how seizures may continuously contribute to maladaptive reorganization in the brain.

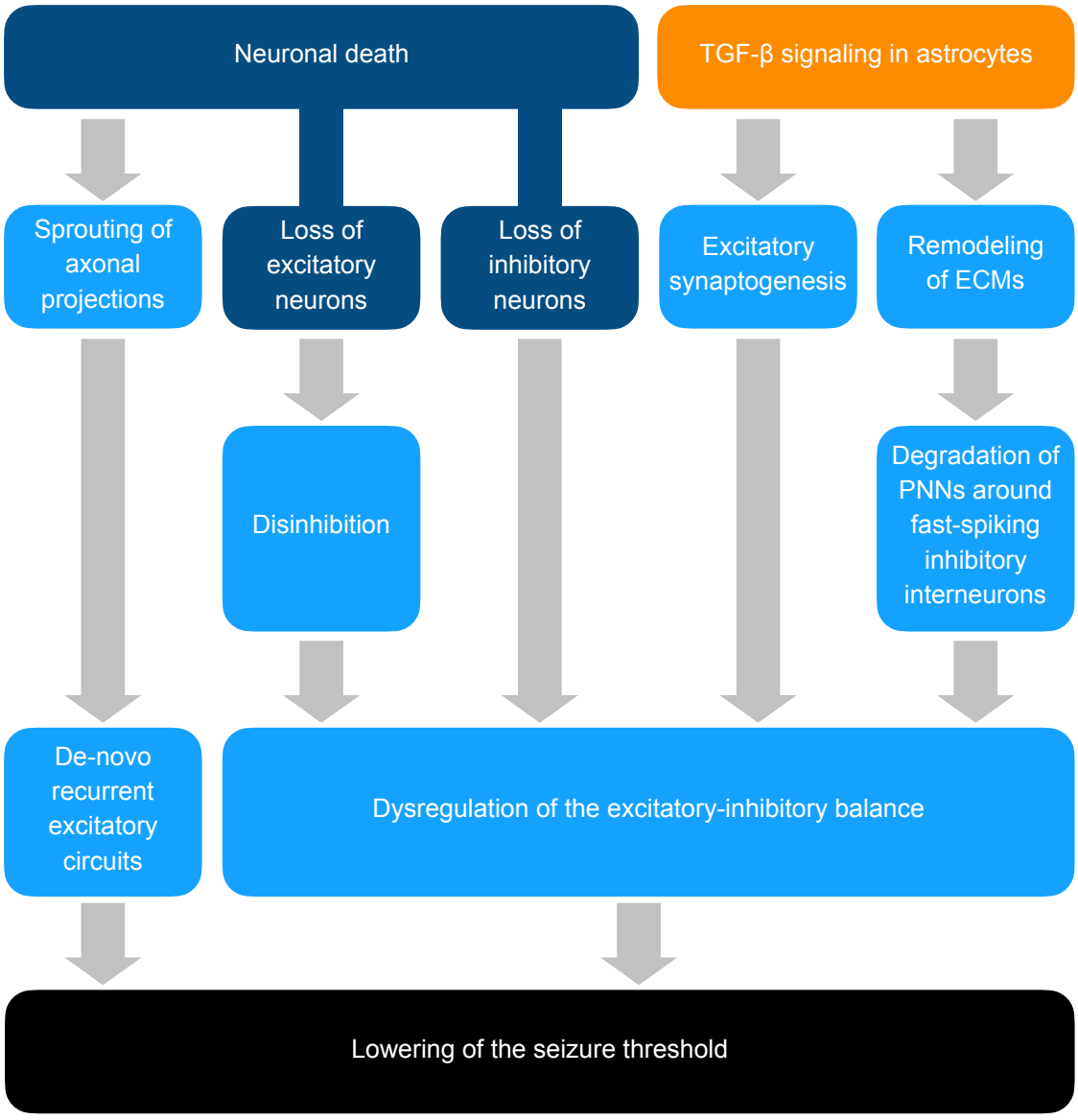

FIGURE 2.3: Mechanisms of circuit remodeling in epilepsy.

2.4.1 Neuronal loss and circuit remodeling

Circuit remodeling associated with neuronal death may be caused by the loss of both excitatory and inhibitory neurons (Fig. 2.3) (Sloviter, 1987; Knopp et al., 2008). The loss of excitatory cells can also contribute to hyperexcitability through disinhibition, which creates an imbalance between excitation and inhibition in the circuit. For example, the loss of a hippocampal basket cell-activating system, rather than a loss of inhibitory basket cells themselves, may lead to disinhibition and thereby play a role in epileptogenesis (Sloviter, 1987). The most well-studied alternation of circuitry associated with neuronal loss is the remodeling of the hippocampus of TLE patients (Tauck and Nadler, 1985; Hendricks, Westbrook, and Schnell, 2019). In the hippocampus circuit, the projections of mossy cells (mossy fibers) are present in healthy brains as axons of granule cells that form synapses with inhibitory interneurons and increase inhibition (Juvale and Che Has, 2021). In pathological conditions of injury, the recurrent excitatory network can be formed by the sprouting of mossy fiber axons onto granule cell dendrites (Hendricks, Westbrook, and Schnell, 2019). A computational model of hippocampal circuitry suggests that even a low level of mossy fiber spouting would be sufficient to cause dentate gyrus hyperexcitability (Santhakumar, Aradi, and Soltesz, 2005). However, blocking the development of mossy fiber sprouting does not consistently reduce seizure frequency in pilocarpine-treated mice (Buckmaster, 2014). This suggests that circuit remodeling associated with neuronal loss is a multifaceted pathological mechanism driving hyperexcitability, lowering seizure threshold, and allowing epileptogenesis.

2.4.2 Non-neuronal causes of circuit remodeling

The neuronal death is not necessary for the network reorganization towards a hyperexcitable profile. The increase of the BBB permeability and subsequent activation of the astrocytes have been shown to disrupt the excitation-inhibition balance in neural circuits and contribute to epileptogenesis (Fig. 2.3) (Weissberg et al., 2015; Kim et al., 2016). As of now, the two mechanisms of astrocyte-associated circuit remodeling have been described in detail. First, the activation of the TGF-β pathway in astrocytes has been shown to cause excessive excitatory synaptogenesis (Weissberg et al., 2015). This long-lasting effect is underlying the occurrence of delayed spontaneous recurrent seizures in subjects with the BBB breakdown. Second, astrocytes are responsible for the maintenance of the extracellular matrices (ECM) - molecular complexes providing structural and biochemical support to surrounding cells (Theocharis et al., 2016). Activation of astrocytes leads to the remodeling of ECMs and persistent degradation of protective ECM structures called perineuronal

nets (PNNs) around fast-spiking inhibitory interneurons (Kim et al., 2017b). The functional deficits in interneurons lead to dysregulation of excitation-inhibition balance and subsequent development and progression of epileptogenesis (Kim et al., 2016). Thus, the TGF-β signaling in the course of astrocytic activation is involved in a range of pathological processes, which favor the pathological hyperexcitability that underlies seizure generation and recurrence (Vezzani, Balosso, and Ravizza, 2019).

Chapter 3

Mathematical model of epilepsy development after injury

This chapter is dedicated to familiarizing the reader with the details of model design, its mathematical description, and its analysis. Further, the simulation paradigms for various types of injuries are explained with 3 animal model examples. The data from these animal models are used for parameter tuning and testing of the performance of the model.

3.1 Mathematical model design

3.1.1 Structure

The structure of the model has been designed in consideration of available evidence on the epileptogenesis process that was discussed in detail in Chapter 2. The model describes interactions between BBB disruption (B), neuronal loss (D), neuroinflammation (I), circuit remodeling (R) and spontaneous recurrent seizures (S) upon neurological injury (Fig. 3.1).

Two seizure-promoting factors are assumed to determine the probability of occurrence of spontaneous recurrent seizures: the level of neuroinflammation and the degree of pathological circuit remodeling (Fig. 3.1, arrows $I \rightarrow S$ and $R \rightarrow S$). The facilitation of neuroinflammatory reaction modulates neuronal excitability, lowers seizure threshold, and, consecutively, also increases the chance of spontaneous recurrent seizure occurrence (Chapter 2.2.4, Fig. 3.1, arrow $I \rightarrow S$). The remodeling component can be constituted by abnormal excitatory synaptogenesis, increase of recurrency in neural circuits due to axonal sprouting, loss of inhibitory neurons, or disinhibition due to loss of excitatory neurons (Chapter 2.4, Figure 2.3). Such remodeling causes an increase of excitability in neuronal circuits and raises the chance

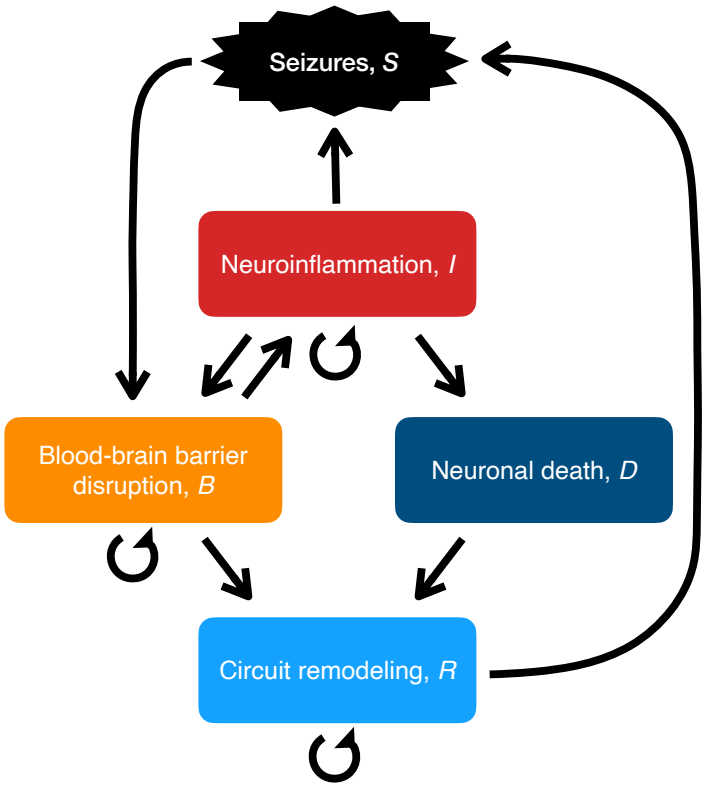

FIGURE 3.1: Structure of the mathematical model summarizing the interactions between variables. The figure was imported from Batulin et al., 2022.

of spontaneous recurrent seizure occurrence (Fig. 3.1, arrow $R \rightarrow S$).

Epileptic seizures induce disruption of the BBB (Chapter 2.1.2, Fig. 3.1, arrow $S \rightarrow B$). This also leads to secondary neuroinflammation due to exposure of the neural tissue to blood-borne cells and molecules that infiltrate into the CNS through the leaky BBB (Chapter 2.2.3, Fig. 3.1, arrow $B \rightarrow I$). Neuroinflammation itself is able to cause dysregulation of the BBB via activation of cells of the neurovascular unit (Chapter 2.2.3), which results in a positive feedback loop in the model (Fig. 3.1, arrow $I \rightarrow B$).

The overactivation of microglia in a course of neuroinflammation may lead to neurotoxicity and induction of neuronal loss (Chapter 2.3.2, Fig. 3.1, arrow $I \rightarrow D$). The neural death, in turn, can lead to remodeling in neural circuits (Chapter 2.4.1, Fig. 3.1, arrow $D \rightarrow R$). In addition to circuit remodeling caused by neuronal loss, the downstream effects of BBB dysregulation and consecutive circuit remodeling are also included in the model (Chapter 2.4.2, Fig. 3.1, arrow $B \rightarrow R$).

3.1.2 Mathematical description

The interactions between the processes involved in epileptogenesis (Fig. 3.1) are modeled with a system of stochastic nonlinear ordinary differential equations:

$$\begin{cases} \tau_I \dot{I} = -I + \kappa_{B\to I} B \\ \tau_B \dot{B} = -B + \kappa_{I\to B} I + S(I,R) \\ \tau_D \dot{D} = \kappa_{I\to D}(1 - \frac{D}{D_{\max}})\max\{0, I - \Theta\} \\ \tau_R \dot{R} = -R + \kappa_{B\to R} B + \kappa_{D\to R} D, \end{cases} \tag{3.1}$$

where $I(t)$ is neuroinflammation intensity; $B(t)$ is the extent of BBB disruption; $D(t)$ is the extent of neuronal death; $R(t)$ is the degree of circuit remodeling.

Except for neural death $D(t)$, all variables are assumed to be reversible. Exception for $D(t)$ is motivated by the fact that the recovery of dead neurons is not possible in the mature CNS. Despite the degree of circuit remodeling $R(t)$ being a reversible variable, the presence of a neuronal death ($D > 0$) causes the irreversible circuit remodeling. This can be seen considering the steady state of Eq. 3.1:

$$\dot{R} = 0. \tag{3.2}$$

Therefore:

$$R = \kappa_{B\to R} B + \kappa_{D\to R} D. \tag{3.3}$$

If $D > 0$, then consecutively:

$$R > 0. \tag{3.4}$$

$\kappa_{B\to I}$, $\kappa_{I\to B}$, $\kappa_{I\to D}$, $\kappa_{B\to R}$, $\kappa_{D\to R}$ are the parameters for coupling strengths of the respective effects between the variables. The processes are assumed to operate on 3 distinct time scales: fast (seconds-minutes) for spontaneous recurrent seizures; intermediate (hours-days) for neuroinflammatory reaction (τ_I); and slow (days-weeks) for recovery of permeability of the BBB (τ_B), neuronal death (τ_D) and circuit remodeling (τ_R).

Mild neuroinflammation is assumed to have no neurotoxic effect since it is a physiological process aimed at maintaining tissue homeostasis. Thus, only highly activated microglia in conditions of neuroinflammation of profound intensity ($I(t) > \Theta$) are assumed to have neurotoxic effects and induce neuronal death. Θ is a neurotoxicity threshold and $D_{\max}$ is the maximum possible extent of neuronal loss.

3.1.3 Stochastic model

Two versions of the model were developed: stochastic, which allows simulation of stochastically occurring seizures, and the rate model, in which seizure activity is approximated by a smooth function. In the stochastic model, the term $S(I, R)$ describes the effect of stochastically occurring seizures on the permeability of the BBB:

$$S = \begin{cases} \kappa_{S\to B}, \text{ during seizure} \\ 0, \text{ beyond seizure,} \end{cases} \tag{3.5}$$

where $\kappa_{S\to B} = \frac{K_{S\to B}}{\lambda_{\max} T_{\text{seizure}}}$ describes the effect of a single spontaneous recurrent seizure on the permeability of the BBB; $\lambda_{\max}$ is a maximum possible number of seizures per day; $K_{S\to B}$ is a scaling parameter defining the maximum possible daily burden of seizure activity on the BBB permeability; T_{seizure} is the parameter corresponding to the seizure duration.

The occurrence of spontaneous recurrent seizures in time is modeled with a Poisson process. This approach is the simplest way to account for stochasticity in the process of occurrence of spontaneous recurrent seizures. The seizure rate (the probability of a seizure occurring per unit time) is assumed to be monotonically increasing with the extent of circuit remodeling $R(t)$ and the intensity of neuroinflammation $I(t)$ according to:

$$\lambda_{\text{s}}(I, R) = \lambda_{\max} \frac{e^{\kappa_{I\to S} I^2 + \kappa_{R\to S} R} - 1}{e^{\kappa_{I\to S} I^2 + \kappa_{R\to S} R} + 1}, \tag{3.6}$$

where $\kappa_{I\to S}$ and $\kappa_{R\to S}$ are parameters scaling the seizure-promoting effects of neuroinflammation (Chapter 2.2.4) and circuit remodeling (Chapter 2.4) respectively. The sigmoid shape of the function (Fig. 3.2) reflects the saturation effect of the maximum possible seizure burden that the nervous system can be exposed to within a finite time interval due to metabolic constraints. The assumption of a quadratic dependence of the seizure rate on the intensity of neuroinflammation minimizes the seizure-promoting effects of mild neuroinflammation $I(t) \gtrsim 0$, which

per se is a physiological reaction to noxious stimuli.

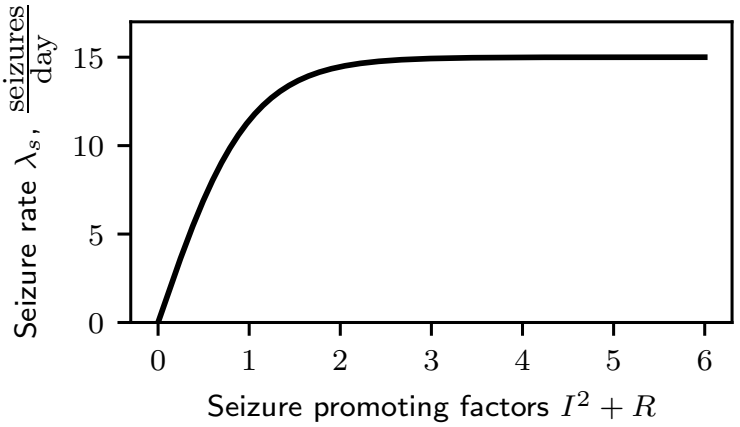

FIGURE 3.2: Seizure rate dependence on seizure promoting factors (neuroinflammation I and circuit remodeling R). The figure was imported from Batulin et al., 2022.

3.1.4 Rate model

In the rate model, the stochastic component of the Poisson process is approximated with a smooth seizure burden function in analogy to the seizure rate function (Eq. 3.6). Thus, the term $S(I, R)$, which describes the effect of stochastically occurring seizures on the permeability of the BBB, becomes:

$$S(I, R) = K_{S \to B} \frac{e^{\kappa_{I \to S} I^2 + \kappa_{R \to S} R} - 1}{e^{\kappa_{I \to S} I^2 + \kappa_{R \to S} R} + 1}. \tag{3.7}$$

The rate version of the model does not allow for tracking in time the occurrence of individual spontaneous seizures. On the other hand, it provides the means for a more intuitive explanation of the dynamics of the system with mathematical analysis methods. For example, we can reduce the dimensionality of the rate model by performing the time scale separation procedure for the equation describing neuroinflammation.

3.2 Mathematical analysis of the model

3.2.1 Time scale separation

Due to the fact that microglia can change their phenotype as fast as in minutes, the time scale of the variable describing neuroinflammation is assumed to be smaller than the time scales of the other processes ($\tau_I < \tau_B,\ \tau_D,\ \tau_R$). Thus, the time scale separation procedure can be performed and Eq. 3.1 becomes:

$$\begin{cases} I = \kappa_{B\to I} B \\ \tau_B \dot{B} = -B + \kappa_{I\to B} I + S(I,R) \\ \tau_D \dot{D} = \kappa_{I\to D}(1 - \frac{D}{D_{\max}})\max\{0, I - \Theta\} \\ \tau_R \dot{R} = -R + \kappa_{B\to R} B + \kappa_{D\to R} D. \end{cases} \tag{3.8}$$

From Eq. 3.8, we can obtain the system of equations for fixed values of neuronal loss extent $D = D_{\text{const}}$, where $0 \leq D_{\text{const}} \leq D_{\max}$. The following system of equations describes the system in the dynamical regime in the absence of neurotoxicity neurotoxicity ($I \approx \kappa_{B\to I} B < \Theta$):

$$\begin{cases} I = \kappa_{B\to I} B \\ \tau_B \dot{B} = -B + \kappa_{I\to B} I + S(I,R) \\ D = D_{\text{const}} \\ \tau_R \dot{R} = -R + \kappa_{B\to R} B + \kappa_{D\to R} D_{\text{const}}. \end{cases} \tag{3.9}$$

Substituting $I = \kappa_{B\to I} B$ in the equation for the extent of BBB disruption, we obtain the system described in $B - R$ dimensions. This system can be used for visualization and analysis of dynamics with state-space plots for variables B and R:

$$\begin{cases} \tau_B \dot{B} = -B + \kappa_{I\to B}\kappa_{B\to I} B + S(\kappa_{B\to I} B, R) \\ \tau_R \dot{R} = -R + \kappa_{B\to R} B + \kappa_{D\to R} D_{\text{const}}, \end{cases} \tag{3.10}$$

where $D = D_{\text{const}}$ and $I = \kappa_{B\to I} B < \Theta$.

For instance, using the system described in Eq. 3.10, we can obtain the state-space representations of the model in the $B - R$ domain (Fig. 3.3) for given values of the neuronal loss variable D (Chapter 3.1.2).

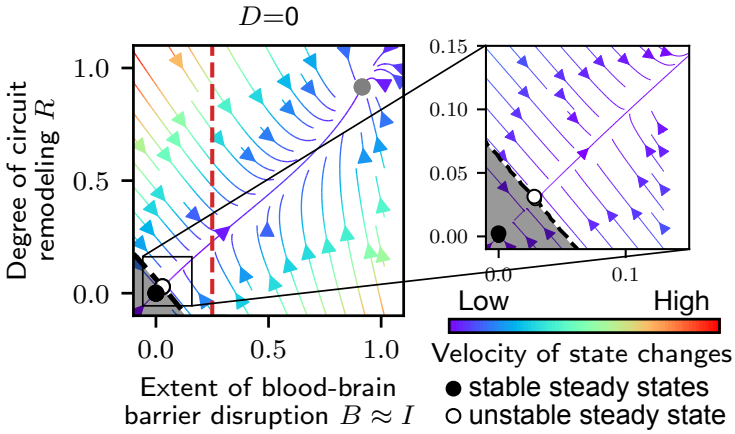

FIGURE 3.3: State-space plot of the rate model. The stability analysis (Chapter 3.2.2) reveals existence of 3 steady states: a 'healthy' stable steady state (black), an unstable fixed point (white), and an 'epileptic' stable steady state corresponding to state of progressed epileptogenesis (gray). The plot illustrates the dynamical landscape of the system, which consists of two attracting points (stable steady states). The basins of attraction of the 'healthy' steady state (shaded area) and of the 'epileptic' steady state are separated by a separatrix (the dashed black line going through the unstable fixed point). The color of arrows indicates the velocity of the state changes in corresponding areas of the state-space. The glial neurotoxicity threshold Θ is illustrated with the red dashed line. The model parameters, for which the state-space was generated, are specified in Chapter 4, Table 4.1. $B \approx I$ according to the Eq. 3.8, where $\kappa_{B\to I} = 1$. The figure was imported from Batulin et al., 2022.

3.2.2 Stability analysis

Considering the steady state ($\dot{B} = 0$, $\dot{R} = 0$), from Eq. 3.10 follows:

$$\begin{cases} -B + \kappa_{I\to B}\kappa_{B\to I}B + S(\kappa_{B\to I}B, R) = 0 \\ -R + \kappa_{B\to R}B + \kappa_{D\to R}D_{\text{const}} = 0 \end{cases} \tag{3.11}$$

Substituting the $S(I, R)$ from Eq. 3.7, we obtain:

$$\begin{cases} -B + \kappa_{I\to B}\kappa_{B\to I}B + K_{S\to B}\frac{e^{\kappa_{I\to S}(\kappa_{B\to I}B)^2+\kappa_{R\to S}R}-1}{e^{\kappa_{I\to S}(\kappa_{B\to I}B)^2+\kappa_{R\to S}R}+1} = 0 \\ -R + \kappa_{B\to R}B + \kappa_{D\to R}D_{\text{const}} = 0 \end{cases} \tag{3.12}$$

The pairs of values $[B^*, R^*]$ that satisfy the Eq. 3.12 correspond to the steady states (fixed points).

The Jacobian of the system around each fixed point is:

$$\mathbb{J} = \begin{bmatrix} \frac{\partial \dot{B}}{\partial B} & \frac{\partial \dot{B}}{\partial R} \\ \frac{\partial \dot{R}}{\partial B} & \frac{\partial \dot{R}}{\partial R} \end{bmatrix}, \tag{3.13}$$

where

$$\frac{\partial \dot{B}}{\partial B} = \frac{1}{\tau_B}(-1 + \kappa_{I\to B}\kappa_{B\to I} + 4K_{S\to B}\kappa_{I\to S}\kappa_{B\to I}B\frac{e^{\kappa_{I\to S}(\kappa_{B\to I}B)^2+\kappa_{R\to S}R}}{(e^{\kappa_{I\to S}(\kappa_{B\to I}B)^2+\kappa_{R\to S}R}+1)^2}), \tag{3.14}$$

$$\frac{\partial \dot{B}}{\partial R} = \frac{1}{\tau_B}2K_{S\to B}\kappa_{R\to S}\frac{e^{\kappa_{I\to S}(\kappa_{B\to I}B)^2+\kappa_{R\to S}R}}{(e^{\kappa_{I\to S}(\kappa_{B\to I}B)^2+\kappa_{R\to S}R}+1)^2}, \tag{3.15}$$

$$\frac{\partial \dot{R}}{\partial B} = \frac{\kappa_{B\to I}}{\tau_R}, \tag{3.16}$$

$$\frac{\partial \dot{R}}{\partial R} = -\frac{1}{\tau_R}. \tag{3.17}$$

The eigenvalues for each fixed point $[B^*, R^*]$ are the eigenvalues of the Jacobian evaluated at $[B^*, R^*]$. Inserting parameter values from Chapter 4 (Table 4.1), we can analyze the fixed point positions and corresponding eigenvalues. We can further describe the state-space of the system:

1.) if $0 \leq D_{\text{const}} < D_{\text{critical}}$, the system has three steady states (Fig. 3.4): a stable steady state (two negative eigenvalues) around the origin; a saddle point (one negative eigenvalue and one positive); a stable steady state (two negative eigenvalues) distanced from the origin in the first quadrant;

2.) if $D_{\text{const}} = D_{\text{critical}}$, a 'healthy' stable fixed point collides with a saddle point, so the system undergoes the saddle node bifurcation (Fig. 3.4). Only two fixed points remain: a stable steady state (negative eigenvalues) distanced from the origin in the first quadrant, and a semistable point (one eigenvalue equal to 0) in the position of collision of two fixed points;

3.) if $D_{\text{critical}} < D_{\text{const}} \leq D_{\text{max}}$, the system has one fixed point - a stable steady state (negative eigenvalues) distanced from the origin in the first quadrant (Fig.

3.4).

D_{critical} is a critical extent of neuronal loss at which the system undergoes the saddle node bifurcation. For analysis of bifurcation and estimation of D_{critical} value, see Chapter 3.2.3. The code for the numerical calculation of the position of the fixed points [B^*, R^*], the eigenvalues, and the critical extent of neuronal loss, which were used in the stability analysis, can be found in GitHub repository of the publication Batulin et al., 2022.

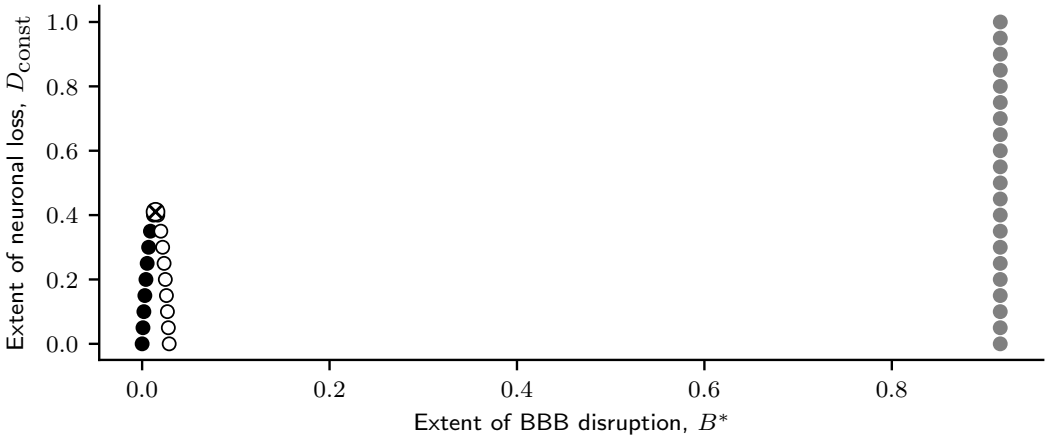

FIGURE 3.4: Saddle node bifurcation illustrated with collision (crossed circle) of stable (black circles) and unstable (white circles) fixed points at the critical value of the extent of neuronal loss ($D_{\text{const}} = D_{\text{critical}} \approx 0.41$). The third fixed point (gray circles) shows low sensitivity to change in neuronal loss due to a low value of $\kappa_{D\to R}$. For values $D_{\text{const}} > D_{\text{critical}}$, only one stable steady state (gray circles) exist. The model parameters are specified in Chapter 4, Table 4.1. The figure was imported from Batulin et al., 2022.

3.2.3 Estimation of the critical extent of neuronal loss

From 3.12, we can express:

$$B = \frac{K_{S\to B}}{1-\kappa_{I\to B}\kappa_{B\to I}} \frac{e^{\kappa_{I\to S}(\kappa_{B\to I}B)^2+\kappa_{R\to S}R}-1}{e^{\kappa_{I\to S}(\kappa_{B\to I}B)^2+\kappa_{R\to S}R}+1}. \tag{3.18}$$

Defining $f = e^{\kappa_{I\to S}(\kappa_{B\to I}B)^2+\kappa_{R\to S}R}$ and $\alpha = \frac{K_{S\to B}}{1-\kappa_{I\to B}\kappa_{B\to I}}$:

$$B = \alpha\frac{f-1}{f+1}. \tag{3.19}$$

From Eq. 3.19, we can derive:

$$f = \frac{\alpha + B}{\alpha - B}. \tag{3.20}$$

Replacing f back with $e^{\kappa_{I\to S}(\kappa_{B\to I}B)^2+\kappa_{R\to S}R}$, we obtain:

$$e^{\kappa_{I\to S}(\kappa_{B\to I}B)^2+\kappa_{R\to S}R} = \frac{\alpha + B}{\alpha - B}. \tag{3.21}$$

Taking logarithm on both sides:

$$\kappa_{I\to S}(\kappa_{B\to I}B)^2 + \kappa_{R\to S}R = \ln\frac{\alpha + B}{\alpha - B}. \tag{3.22}$$

From Eq. 3.22, we can obtain R:

$$R = -\frac{\kappa_{I\to S}(\kappa_{B\to I}B)^2}{\kappa_{R\to S}} + \frac{1}{\kappa_{R\to S}}\ln\frac{\alpha + B}{\alpha - B}. \tag{3.23}$$

Defining $\beta = \frac{\kappa_{I\to S}\kappa_{B\to I}^2}{\kappa_{R\to S}}$, we derive the *nonlinear* R equation:

$$R = -\beta B^2 + \frac{1}{\kappa_{R\to S}}\ln\frac{\alpha + B}{\alpha - B}. \tag{3.24}$$

From Eq. 3.12, we derive the *linear* R equation:

$$R = \kappa_{B\to R}B + \kappa_{D\to R}D_{\text{const}}. \tag{3.25}$$

The intersections between *linear* R and *nonlinear* R correspond to the fixed points of the system.

Given the parameters defined in Chapter 4 (Table 4.1), the system of equations has at least one fixed point (Chapter 3.2.2). In addition to this fixed point, a saddle node bifurcation can emerge when two additional fixed points are generated as a result of a change of parameters in the equations.

Assuming that D_{const} could play the role of a bifurcation parameter, we need to find its value D_{critical}, with which *linear R* becomes tangential to *nonlinear R*. We need to find the first derivative of *nonlinear R* with respect to B, and equate it with the slope of *linear R* to obtain all B^* satisfying the equation.

The derivative of of *nonlinear R* from Eq. 3.24 with respect to B is:

$$\frac{\partial R}{\partial B} = -2\beta B + \frac{2\alpha}{\kappa_{R\to S}(\alpha + B)(\alpha - B)}. \tag{3.26}$$

The slope of the *linear R* from Eq. 3.25:

$$\frac{\partial R}{\partial B} = \kappa_{B\to R}. \tag{3.27}$$

Equating Eq. 3.26 with Eq. 3.27, we obtain the polynomial:

$$2\beta B^3 + \kappa_{B\to R}B^2 - 2\alpha^2\beta B + \frac{2\alpha}{\kappa_{R\to S}} - \alpha^2\kappa_{B\to R} = 0. \tag{3.28}$$

Inserting parameter values (Table 4.1) and solving the polynomial numerically (code available at GitHub, see key resources table of publication Batulin et al., 2022), we obtain the following root values for B^*= [-1.259; 0.7448; 0.01439]. Since the variable describing the extent of BBB disruption can not take negative values, the solution [-1.259] should be discarded. Using the equation for *nonlinear R* (Eq. 3.24), we can calculate the corresponding R^* variable values for B^*= [0.7448; 0.0143]: R^*=[0.4560; 0.0146].

We derive the equation for D_{const} from the *linear R* equation: (Eq. 3.25):

$$D_{\text{const}} = \frac{R + \kappa_{B\to R}B}{\kappa_{D\to R}}. \tag{3.29}$$

For the remaining values of B^* and R^*, we can calculate D^*_{const}=[-577.5155; 0.4103]. Since the extent of neuronal loss also can not take negative values, we discard one of the solutions [-577.5155]. Thus, we have found the only critical extent value of neuronal loss $D_{\text{critical}} = 0.4103 \approx 0.41$ at which the saddle node bifurcation emerges (Fig. 3.4).

3.3 Simulation paradigms for various injury types

The developed mathematical model allows the simulation of various types of neurological injuries and subsequent epileptogenesis. Different insults are simulated as a combination of external inputs to the corresponding model equation:

$$\begin{cases} \tau_I \dot{I} = -I + \kappa_{B\to I} B + I_E \\ \tau_B \dot{B} = -B + \kappa_{I\to B} I + S(I,R) + B_E \\ \tau_D \dot{D} = \kappa_{I\to D}(1 - \frac{D}{D_{\max}})\max\{0, I - \Theta\} + D_E \\ \tau_R \dot{R} = -R + \kappa_{B\to R} B + \kappa_{D\to R} D + R_E, \end{cases} \tag{3.30}$$

where I_E, B_E, D_E, R_E are external neuroinflammatory, BBB disruption, neurotoxic and circuit remodeling inputs respectively.

In this doctoral thesis, the simulation of three of the commonly used animal models of epileptogenesis is presented. These animal models are the BBB leakage rodent model, TMEV mouse model, and pilocarpine rodent model.

3.3.1 BBB disruption rodent model

The BBB disruption rodent model is based on the induction of the BBB leakage. This can be achieved by exposure of the neural tissue to an artificial cerebrospinal fluid containing bile salts, which increases BBB permeability (Seiffert et al., 2004). Alternatively, the extravasation of the serum albumin in the brain parenchyma can be mimicked by the administration of artificial cerebrospinal fluid containing albumin itself or TGF-β (Weissberg et al., 2015).

In the mathematical model framework, the BBB disruption animal model is simulated by the induction of B_E signal (Fig. 3.5), which elevates the value of the variable corresponding to the extent of the BBB disruption B. The duration of the signal T_{off} corresponds to the period of time during which bile salts are administered or albumin/TGF-β is pumped into the brain of an animal in the animal model setup (Fig. 3.5).

The following data from the BBB disruption rodent model (Weissberg et al., 2015) were used in this study:

- duration of the albumin/TGF-β induction equal to 7 days;

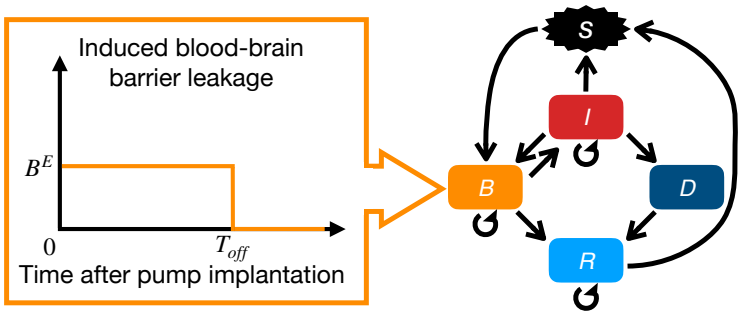

FIGURE 3.5: Simulation schematics for the BBB disruption rodent model. The figure was imported from Batulin et al., 2022.

- latent period (time period between injury and arrival of a first spontaneous seizure) duration of 4.9 ± 1.3 days (mean ± standard error of the mean (SEM)), N=10;
- spontaneous seizures frequency of 1.16 ± 0.16 seizures per day (mean ± SEM), N=10.

3.3.2 TMEV mouse model

The TMEV mouse model is based on the intracerebral infection of C57BL/6J mice with TMEV. This model is widely used in epilepsy research for modeling infection-induced epilepsy in humans (Libbey et al., 2008; Stewart et al., 2010). During the first week post infection, mice develop a profound neuroinflammatory response together with acute symptomatic seizures. This reaction is followed by a distinct latent period, in which no seizures are observed (Stewart et al., 2010).

In the mathematical model framework, the TMEV mouse model is simulated by the induction of the I_E signal (Fig. 3.6), which elevates the value of the variable corresponding to the extent of neuroinflammation I. The time course of the signal is characterized by T_{on} and T_{off}, which mimics the onset and the offset of the inflammatory reaction within the first week after TMEV infection (Fig. 3.6).

The following data from the TMEV mouse model were used in this study: Patel et al., 2017:

- number of seizures per day for N=11 mice extracted from Figure 2. The average seizure frequency per mice was calculated for 3 time intervals: day 1 post infection, days 2-7 post infection and days 8-15 post infection;

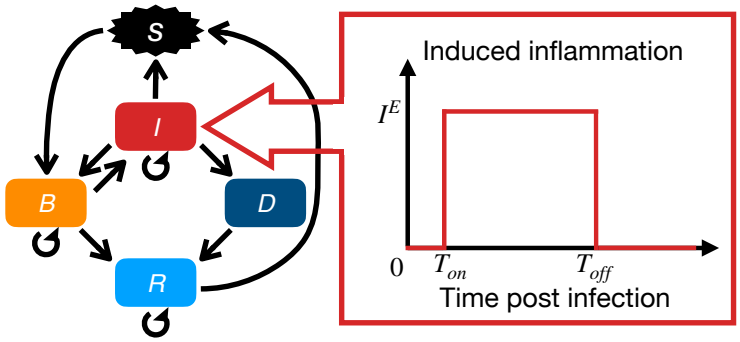

FIGURE 3.6: Simulation schematics for the TMEV mouse model. The figure was imported from Batulin et al., 2022.

- TNF protein concentration fold change (relative to control mice injected with phosphate-buffered saline) on day 1 post infection (N=8): 6.9 ± 0.6, day 5 post infection (N=6): 206.2 ± 14.9, day 14 post infection (N=5): 34.8 ± 7.1. Data are presented in mean ± SEM.

Kirkman et al., 2010:

- neuronal cell loss score for 2 hippocampi (mean ± SEM) on days 1-35 post infection from Figure 2, N=4-13 per time point group.

3.3.3 Chemically-induced (pilocarpine) SE rodent model

The pilocarpine SE rodent model is based on the induction of SE by injection of pilocarpine with later pharmacological termination of SE (Polascheck, Bankstahl, and Löscher, 2010). SE induces neuroinflammation, neuronal death, and profound leakage of the BBB.

In the mathematical model framework, the pilocarpine SE rodent model is simulated by the induction of combined B_E and D_E signals (Fig. 3.7), which elevates the values of the variables corresponding to the extent of BBB disruption B and neuronal death D. The inflammatory perturbation I_E is not defined explicitly since it is indirectly induced by BBB disruption. The duration of the signal T_{off} (Fig. 3.7) corresponds to the period of time, in which SE-associated neuronal loss and BBB leakage are induced (Bankstahl et al., 2018).

The following data from the chemically-induced (pilocarpine) SE rodent model were used in this study:
Brackhan et al., 2016:

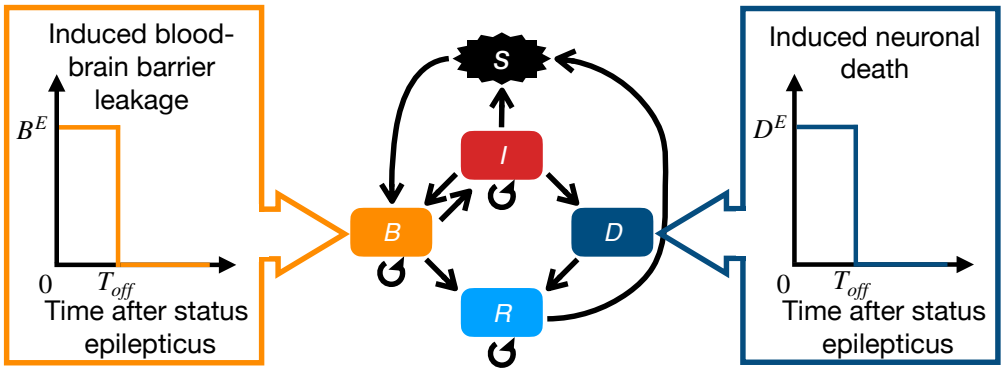

FIGURE 3.7: Simulation schematics for the pilocarpine SE rodent model. The figure was imported from Batulin et al., 2022.

- microglial activation score for the hippocampus (mean ± SEM) on days 0, 2, 5, 14 post SE from Figure 4, N=3-5 per time point group;
- neuronal cell loss score for the hippocampus (mean ± SEM) on days 0, 2, 5, 14 post SE from Figure 4, N=3-5 per time point group.

Zhang et al., 2015:

- NeuN-immunoreactive cells count per mm^2 in the hippocampus of pilocarpine treated animals from Figure 5. Fraction of cells missing (in %) was computed for days 7 and 60 after pilocarpine injection relatively to values for untreated animals.

Chapter 4

Reproduction of injury-specific epileptogenesis characteristics

This chapter is dedicated to familiarizing the reader with the procedure of parameter choice and modeling results that are in agreement with data from three experimental animal models of epileptogenesis.

The mathematical model allows for the simulation of epileptogenesis progression caused by various types of neurological injuries using a single set of parameters (Table 4.1). The parameter values are, whenever possible, directly inferred from the experimental data. For instance, the $\lambda_{\max}$ parameter, corresponding to the maximum daily seizure frequency, was directly inferred from the available experimental data (Libbey et al., 2008; Stewart et al., 2010; Polascheck, Bankstahl, and Löscher, 2010; Bar-Klein et al., 2014; Weissberg et al., 2015; Loewen et al., 2016; Kim et al., 2017a; Patel et al., 2017). The rest of the parameter values are equated to unity and manually adjusted to obtain simulation results that are in agreement with available data from three animal models (Chapter 4.1-4.3). In the process of parameter adjustment, the state space composition (Fig. 3.3), temporal profiles of neuroinflammatory reaction, BBB disruption, neuronal loss, and seizure occurrence are taken into account. The rationale behind the parameter choice, the effect of changing the parameter values, and the specificity of results to chosen parameter set are described in detail in Chapter 4.4.

The modeling of different types of neural injuries is performed by application of the input signals mimicking pathological effects of the respective injury (Chapter 3.3). All experiments presented in this thesis are performed as simulations of the mathematical model. Group allocation and details of simulations are described in Appendix A. No data are excluded as outliers. For stochastic model simulations, the sample size of N=30 was chosen as a twice greater number than the average

Parameter	Description	Value	Units
τ_I	Time scale of neuroinflammatory reaction	1	day
τ_B	Time scale of BBB recovery	10	days
τ_D	Time scale of neuronal death process	10	days
τ_R	Time scale of circuit remodeling	10	days
$\kappa_{I\to B}$	Scaling parameter for effect of neuroinflammation on BBB permeability	0.1	-
$\kappa_{B\to I}$	Scaling parameter for proinflammatory effect of BBB leakage	1	-
$\kappa_{I\to D}$	Scaling parameter for neurotoxic effect of overactivated glia	8	-
$\kappa_{B\to R}$	Scaling parameter for effect of BBB leakage on circuit remodeling	1	-
$\kappa_{D\to R}$	Scaling parameter for effect of neuronal loss on circuit remodeling	0.0005	-
$D_{\max}$	Maximum possible extent of neuronal loss	1	-
Θ	Neurotoxicity threshold of overactivated glia	0.25	-
$\kappa_{I\to S}$	Scaling parameter for strength of seizure-promoting effects of neuroinflammation	2	-
$\kappa_{R\to S}$	Scaling parameter for strength of seizure-promoting effects of circuit remodeling	2	-
$K_{S\to B}$	Scaling parameter for seizure burden on BBB integrity	0.875	-
T_{seiz}	Seizure duration	5	minutes
$\lambda_{\max}$	Homeostatic upper bound of daily seizure number	15	$\frac{\text{seizures}}{\text{day}}$
$\kappa_{S\to B}$	Burden of single seizure on BBB integrity	16.8	-

TABLE 4.1: Model parameter descriptions and values.

sample size in the animal model experiments (Kirkman et al., 2010; Brackhan et al., 2016; Zhang et al., 2015; Weissberg et al., 2015; Patel et al., 2017).

4.1 BBB disruption rodent model

The results of the simulation of the BBB disruption rodent model are illustrated with the time sequences of seizure occurrence (Fig. 4.1). In the simulation, the average duration of the latent period (time period between injury and arrival of first seizure, Fig. 4.2A) and seizure burden (Fig. 4.2B) are in agreement with data reported in the animal model study (Weissberg et al., 2015).

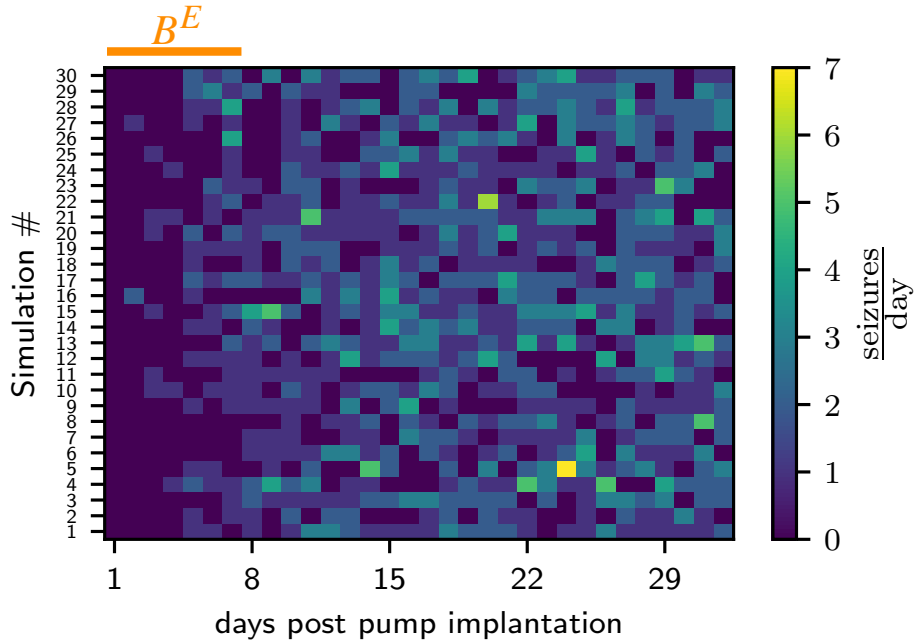

FIGURE 4.1: Time sequences of seizure occurrence in BBB disruption animal model simulation (N=30). The orange bar corresponds to the time window of injury induction. The figure was imported from Batulin et al., 2022.

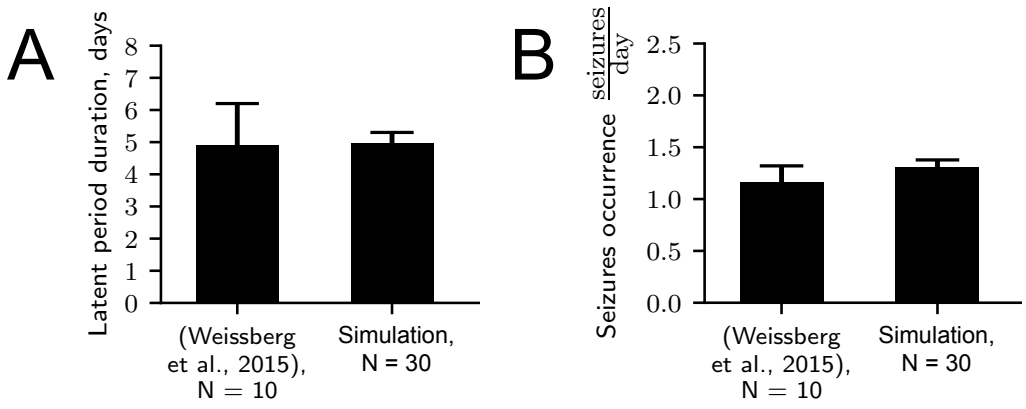

FIGURE 4.2: Comparison of the latent period duration (A) and seizure burden during the first month after injury onset (B) in the BBB disruption animal model data from Weissberg et al., 2015 and simulations with the matched intensity of the injury. Data are represented as mean ± SEM. The figure was imported from Batulin et al., 2022.

Similarly to animal model data, in the simulation, the seizure manifestation is observed either during the infusion of albumin/TGF-β (7 days after pump implantation), or after albumin pump removal (e.g. simulations #6, #7, #8 in Fig. 4.1). Identically to the animal model study, no neuronal death is observed within the

observation period because the neuroinflammation intensity did not reach the neurotoxicity threshold level (Fig. 4.3).

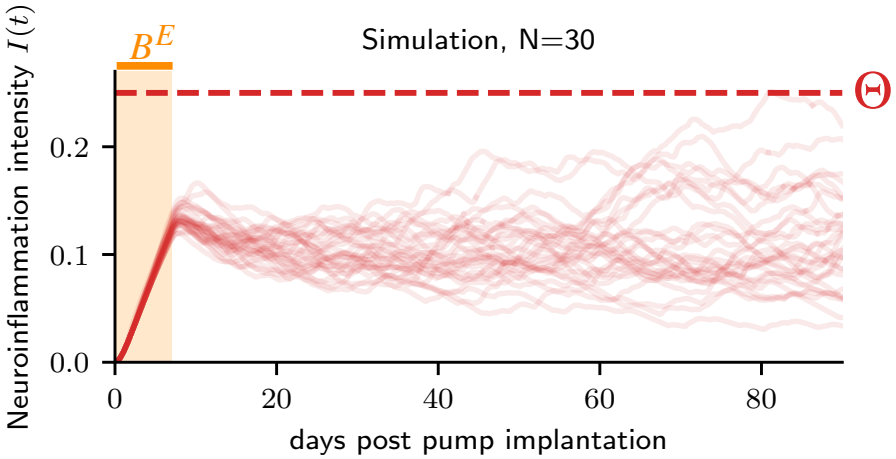

FIGURE 4.3: Time course of neuroinflammation in individual simulations of BBB animal model (N=30). The red dashed line corresponds to the neurotoxicity threshold Θ. The light orange area corresponds to the time window of injury induction. The figure was imported from Batulin et al., 2022.

4.2 TMEV mouse model

The simulation results of the TMEV mouse model capture the profile of seizure occurrence after viral injection, which is characteristic for this animal model (Fig. 4.4). The occurrence of the first seizures can take place already on the second day after the viral injection, while the average latent period duration is 2.83 ± 0.13 days. The early onset seizures are then followed by a period of profound attenuation of seizure activity starting in the 2nd week post-infection (Fig. 4.4).

The mathematical model reproduces not only the characteristic temporal pattern of seizure occurrence (Fig. 4.5A), but also the characteristic time courses of neuroinflammation (Fig. 4.5B) and the neuronal death progression (Fig. 4.5C). Similarly to simulation results, the occurrence of macroscopically measurable neuronal death is reported in the animal model data Kirkman et al., 2010 on day 4 post-infection, which is followed by its progression and saturation from the second week post-infection (Fig. 4.5C).

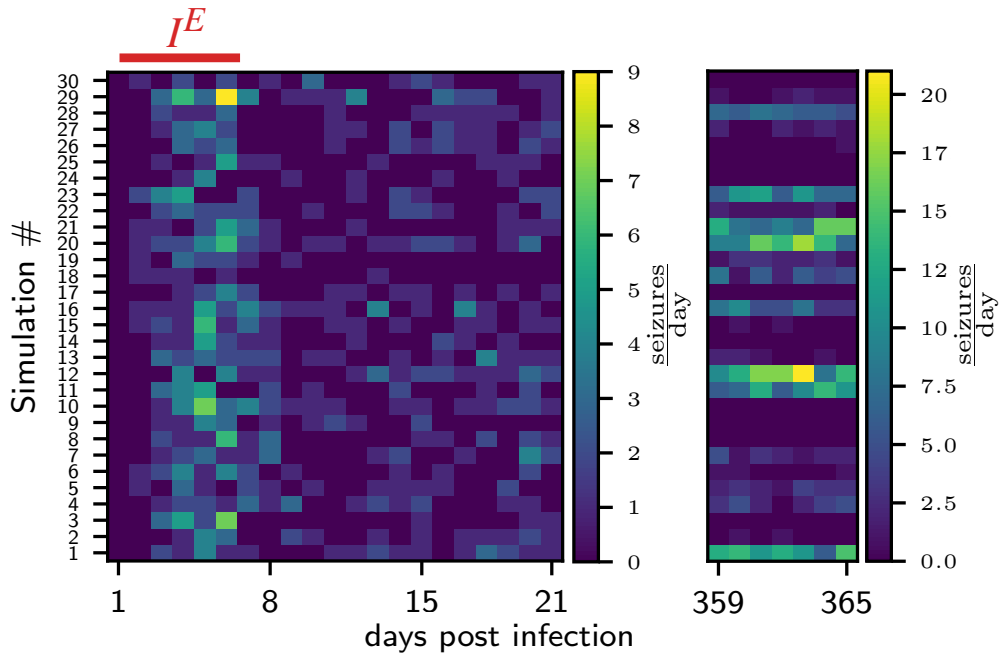

FIGURE 4.4: Time sequences of seizure occurrence in TMEV animal model simulation simulation (N=30). The red bar corresponds to the time window of injury induction. The figure was imported from Batulin et al., 2022.

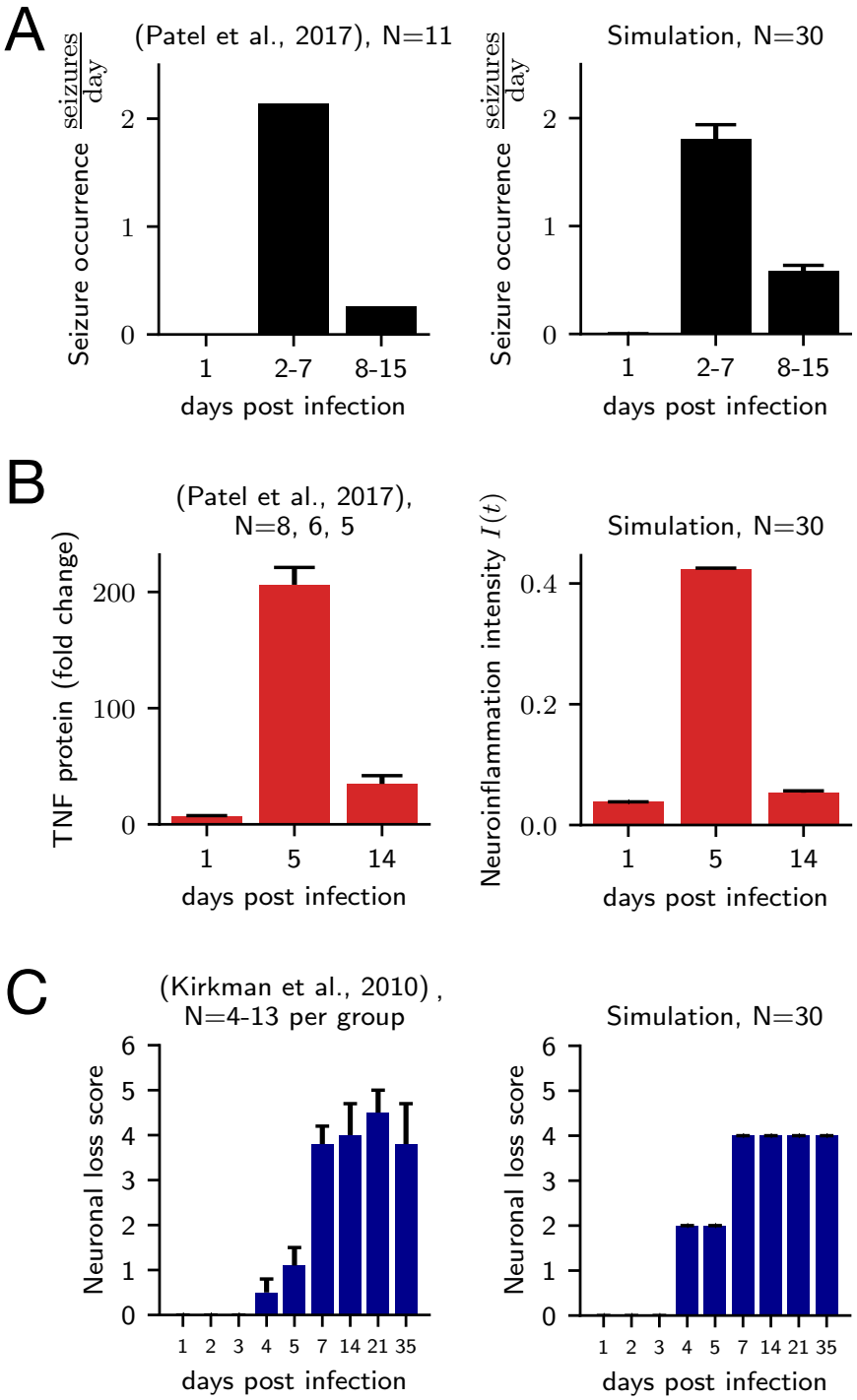

FIGURE 4.5: Comparison of characteristic seizure occurrence pattern (A), neuroinflammation time course (B) and neuronal loss progression (C) from TMEV animal model data (left) and simulation (right). A.) Patel et al., 2017 reported only the total number of seizures per day aggregated over N=11 animals together. C.) The neuronal loss score for the simulation is computed using the masking procedure from (Kirkman et al., 2010). Masking procedure and its effect of 'masking out' variability in the simulation results are explained in Appendix B. Data are represented as mean ± SEM. The figure was imported from Batulin et al., 2022.

The simulation results suggest that the characteristic plateau of neuronal loss originates from the attenuation of the neuroinflammation during the second week after viral injection (Fig. 4.6).

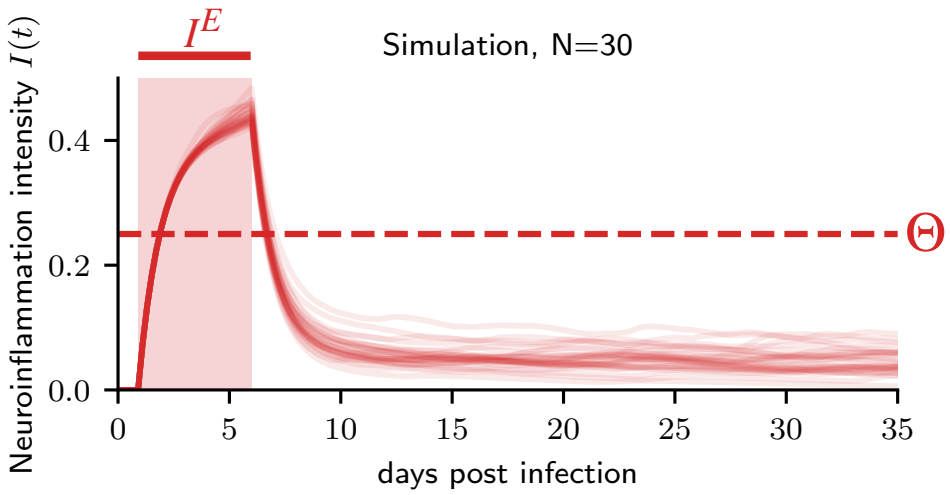

FIGURE 4.6: Time course of neuroinflammation in individual simulations of TMEV animal model (N=30). The red dashed line corresponds to the neurotoxicity threshold Θ. The light red area corresponds to the time window of injury induction. The figure was imported from Batulin et al., 2022.

Also, the animal model data suggest that neuronal death is significantly more abundant in animals that developed seizures versus those that did not (Kirkman et al., 2010). Consistent with this observation, the extent of neuronal death is positively correlated with the severity of seizure burden during the acute post-infection stage in the simulations (Fig. 4.7).

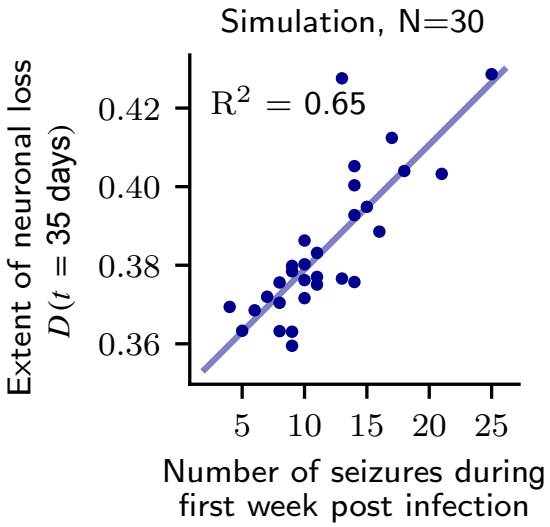

FIGURE 4.7: Neuronal loss one month post infection (day 35) is correlated with severity of seizure burden in the acute phase (week 1 post infection). The blue dots correspond to the individual simulations. The blue line corresponds to linear regression fit with coefficient of determination $R^2 = 0.65$. The figure was imported from Batulin et al., 2022.

4.3 Pilocarpine SE rodent model

The results of the pilocarpine animal model simulation capture the complex temporal profile of the pathology, which is characteristic for this animal model. Neuroinflammation and neuronal death are progressing rapidly during the first week after SE induction, and reach the plateau in the 2nd week after injury (Figs. 4.8A, B). This characteristic slowing down of pathological changes (see the comparison of day 5 and day 14 post-SE) are present also in the simulation results. Moreover, further progression of neuronal loss, which is evident on longer time scales, is also captured by the mathematical model simulation (Fig. 4.8C).

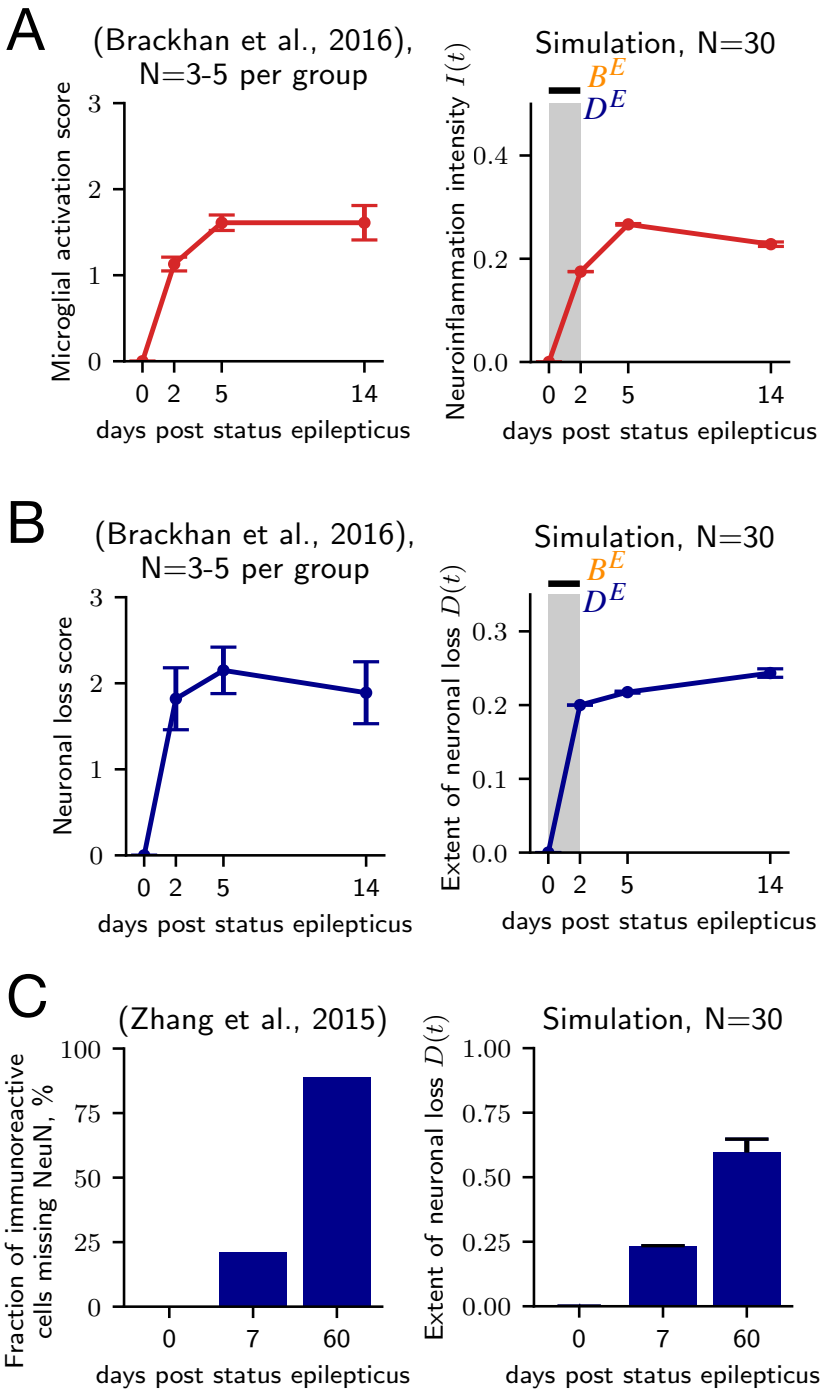

FIGURE 4.8: Comparison of neuroinflammation time courses (A) and neuronal loss progression (B,C) from pilocarpinee animal model data (left) and simulation (right). The gray areas correspond to the time window of injury induction. Data are shown with mean values and SEM error bars. The figure was imported from Batulin et al., 2022.

Despite the relative recovery of the neuroinflammatory intensity and BBB permeability after injury offset, the seizure burden continues to grow due to the gradual increase in the degree of circuit remodeling (Fig. 4.9). The remaining BBB permeability and ensuing neuronal damage cause further circuit remodeling that is driving the course of the pathology. Thus, the attenuation of neuronal death in the 2nd week post-SE (Fig. 4.8B) and further progression in later stages (Fig. 4.8C) are explained by the leveling-off of the neuroinflammation associated with initial injury and subsequent growth of neurotoxicity caused by accumulating seizure burden (Fig. 4.10).

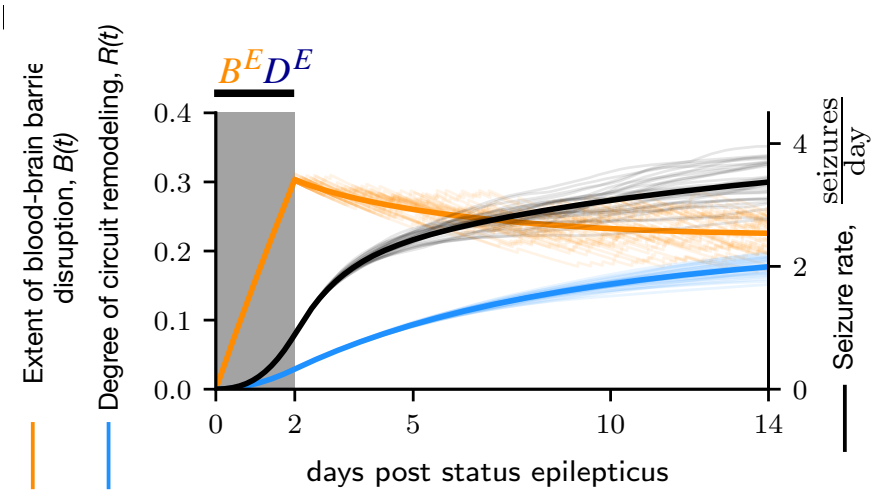

FIGURE 4.9: Processes underlying the rise of seizure rate after injury in pilocarpine animal model simulation. The orange, light blue and black thin lines correspond respectively to extent of BBB disruption, degree of circuit remodeling and seizure rate in individual simulations (N=30). Solid lines correspond to prediction from the rate model. The gray area corresponds to the time window of injury induction. The figure was imported from Batulin et al., 2022.

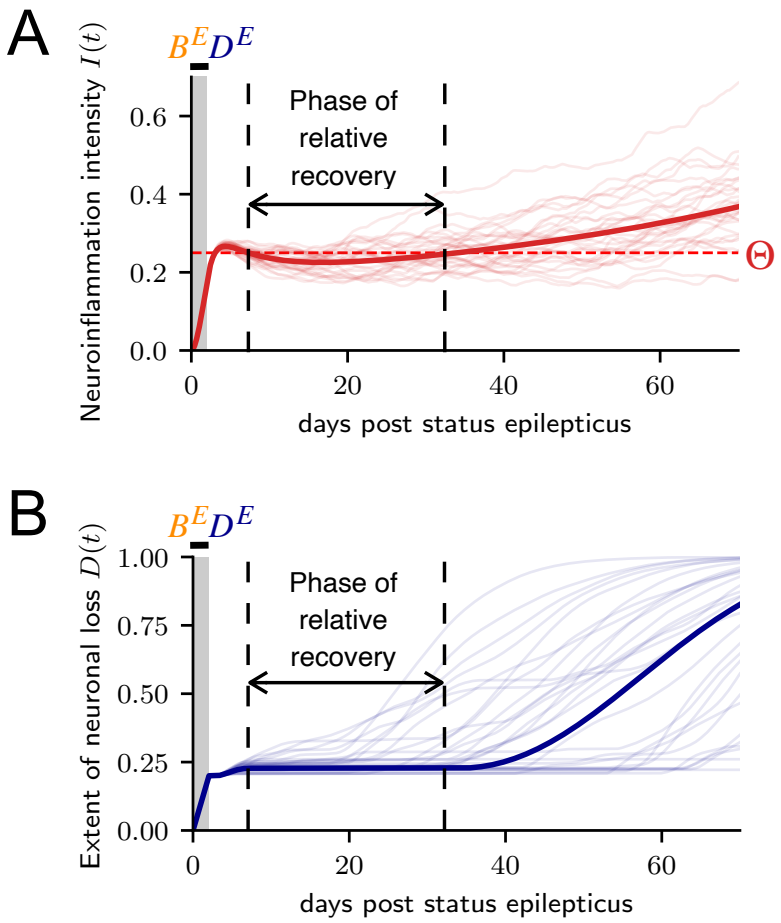

FIGURE 4.10: Development of neuroinflammation (A) and extent of neuronal loss (B) in time with indication of presumed phase of relative recovery characterized by the absence of neurotoxicity in the rate model prediction. The thin lines correspond to individual simulations (N=30). The solid lines correspond to prediction from the rate model. The red dashed line corresponds to the neurotoxicity threshold Θ. The gray area corresponds to the time window of injury induction. The figure was imported from Batulin et al., 2022.

4.4 Specificity of the results to the chosen parameter set

The parameters of the model (Table 4.1) are, whenever possible, directly extracted from the experimental data. The parameters that are not directly measurable are equated to unity and, when needed, manually adjusted with the use of stability analysis to reproduce the available experimental data (Chapter 4.1-4.3). In this section, the effects of parameter alternation and the specificity of the results to chosen parameters are discussed.

As mentioned above, all the unknown parameters are set equal to unity. However, the presence of the positive feedback loop between neuroinflammation $I(t)$ and BBB disruption $B(t)$ variables (Fig. 3.1) imposes the constraint on the $\kappa_{I\to B}$ and $\kappa_{B\to I}$ parameters. This can be observed considering the subsystem of Eq. 3.1, and neglecting the pathological effects of epileptic seizures:

$$\begin{cases} \tau_I \dot{I} = -I + \kappa_{B\to I} B \\ \tau_B \dot{B} = -B + \kappa_{I\to B} I. \end{cases} \tag{4.1}$$

Carrying out the stability analysis, we obtain the rule for the existence of a stable steady state in the form of an inequality: $\kappa_{I\to B}\ \kappa_{B\to I} \leq 1$. Keeping the $\kappa_{B\to I}$ equal to unity, the $\kappa_{I\to B}$ is set to the value 0.1 to satisfy the stability rule. Then, the value of the parameter scaling the seizure burden on BBB integrity $K_{S\to B}$ is manually adjusted to allow (i) for the existence of 3 steady states in the system (Figs. 4.11A-C) and (ii) for the reproduction of animal model data in the simulation (Fig. 4.11D). The partial redundancy in the parameter space (several combinations of parameter values leading to the emergence of identical stability landscapes) is identified when alternative values of $\kappa_{I\to B}$ are considered and $K_{S\to B}$ is adjusted accordingly (Fig. 4.12).

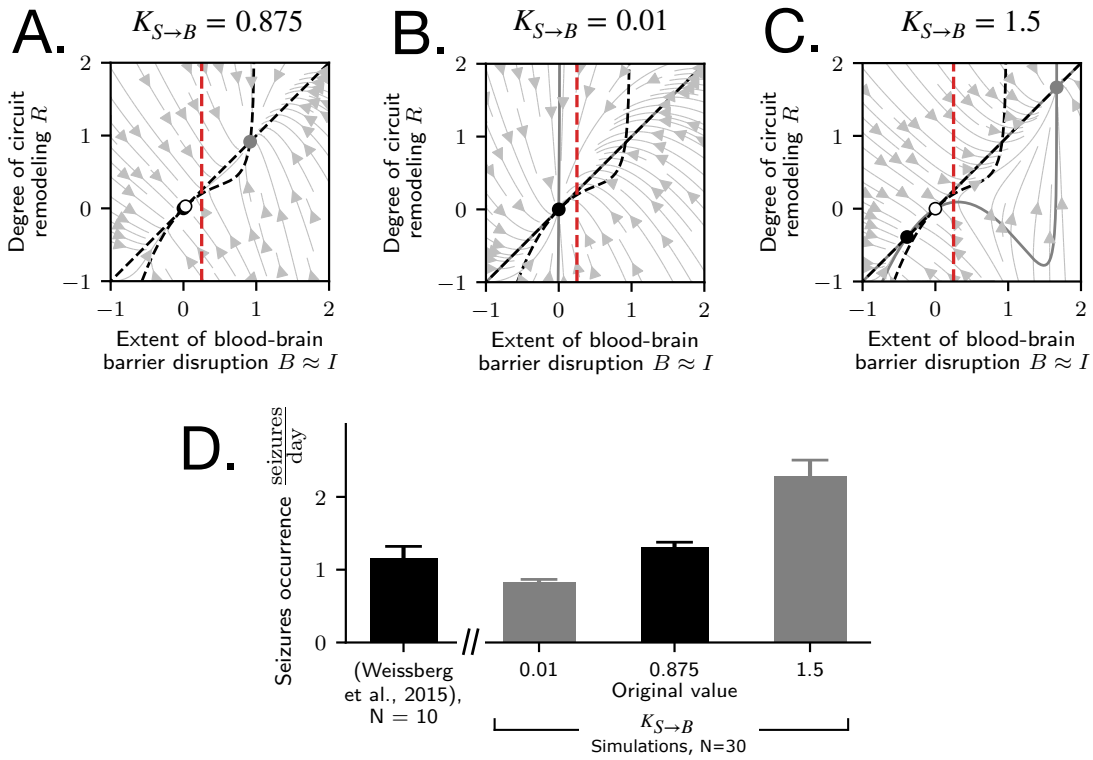

FIGURE 4.11: Consideration of the alternative values of the parameter scaling the seizure burden on BBB integrity. A.) The state-space composition for the intermediate value of the $K_{S\to B}$ contains three steady states in the first quadrant. The circles correspond to the steady states. The black dashed lines correspond to $\dot{B} = 0$ and $\dot{R} = 0$ nullclines. The red dashed line indicates the neurotoxicity threshold. B.) The state-space composition for the low value of the $K_{S\to B}$ contains only a single atractor point in the origin. The gray solid lines correspond to the nullclines. The black dashed lines correspond to the nullclines of the system with the original parameter values used as reference for comparison. C.) The state-space composition for the high value of the $K_{S\to B}$ contains three steady states, but the saddle point migrates to origin and one of the atractors to the third quadrant. D.) Comparison of the simulation results to the BBB disruption animal model data for the originally chosen value of $K_{S\to B} = 0.875$ (black bar) and two alternative values (gray bars). Data are represented as mean ± SEM. The figure was imported from Batulin et al., 2022.

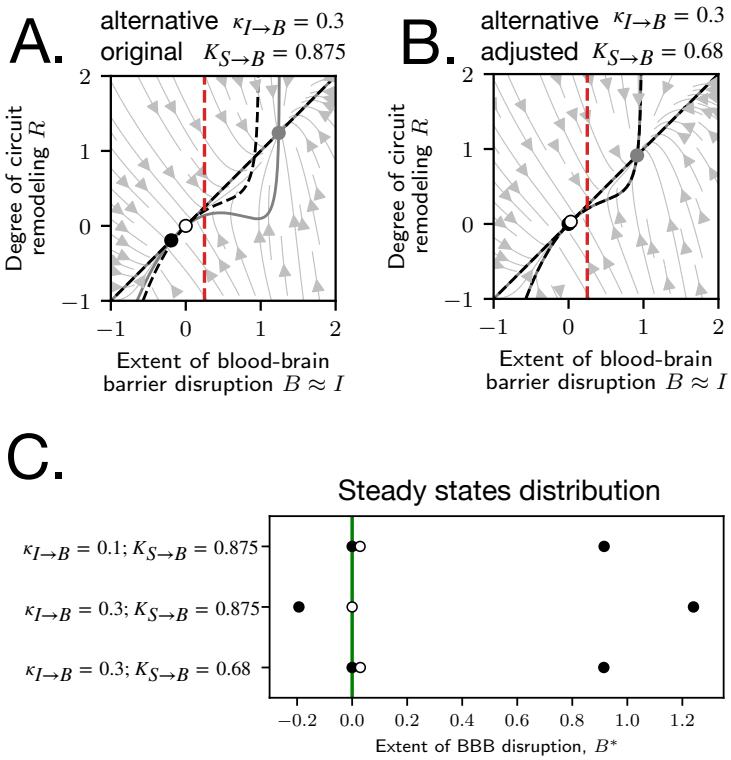

FIGURE 4.12: Illustration of the partial redundancy in the parameter space. A.) The state-space composition for the alternative value of $\kappa_{I\to B} = 0.3$ preserving original value of $K_{S\to B} = 0.875$. The circles correspond to the steady states. The gray solid lines correspond to the nullclines. The black dashed lines correspond to the nullclines of the system with the original parameter values used as reference for comparison. The red dashed line indicates the neurotoxicity threshold. B.) The state-space composition for the alternative value of $\kappa_{I\to B} = 0.3$ and $K_{S\to B} = 0.68$ adjusted to reproduce the stability landscape of the original parameter set. Annotation identical to caption in A. C.) The steady states distribution for the extent of BBB disruption B^* illustrated for the original parameter set (top); alternative parameter set with changed $\kappa_{I\to B}$ (middle); and alternative parameter set with changed $\kappa_{I\to B}$ and adjusted $K_{S\to B}$ (bottom). Vertical green line illustrates the edge of the positive domain for the extent of the BBB disruption ($B^* = 0$). The figure was imported from Batulin et al., 2022.

$K_{S\to B}$ is a parameter of the rate version of the model. In the stochastic model, it corresponds to the group of parameters describing the seizure activity. Among them, the maximum daily seizure frequency $\lambda_{\max}$ is directly inferred from experimental and clinical studies (introduction to Chapter 4) and the average duration of an epileptic seizure is assumed to be equal 5 minutes. Having fixed $K_{S\to B}$ and two other parameters of seizure activity in the stochastic model, we can calculate the effect on BBB disruption evoked by a single seizure $\kappa_{S\to B} = \frac{K_{S\to B}}{\lambda_{\max} T_{\text{seizure}}}$.

The maximum possible extent of neuronal loss $D_{\max}$, a parameter constraining the parameter space, is kept equal to unity (or 100%) for convenience. The neurotoxicity threshold of overactivated glia Θ is adjusted to allow for the reproduction of experimental data. The comparison of simulation results with chosen and alternative parameter values is illustrated in Fig. 4.13.

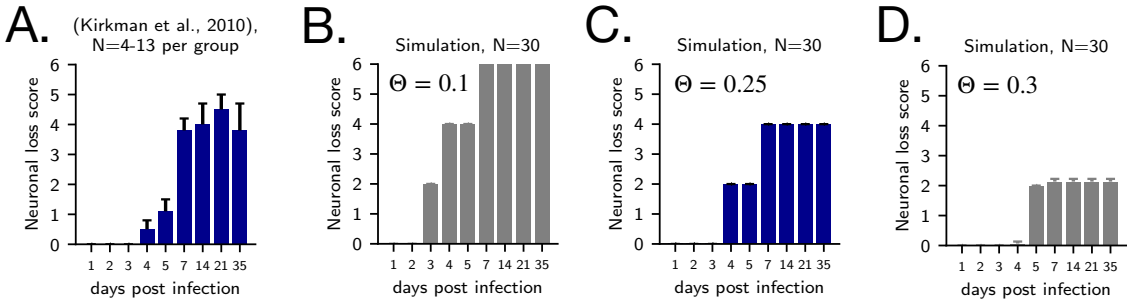

FIGURE 4.13: Consideration of the alternative values of the neurotoxicity threshold parameter: comparison of the animal model data (A) to the model fit with low (B), intermediate (C), and high (D) values of Θ. Data are represented as mean ± SEM. The blue color indicates the bar plots of the animal model data and simulations with chosen parameter set. The figure was imported from Batulin et al., 2022.

The scaling parameter of the neurotoxic effect of overactivated glia $\kappa_{I\to D}$ is adjusted to capture the temporal pattern of neuronal loss progression for the selected neurotoxicity threshold value (Fig. 4.14).

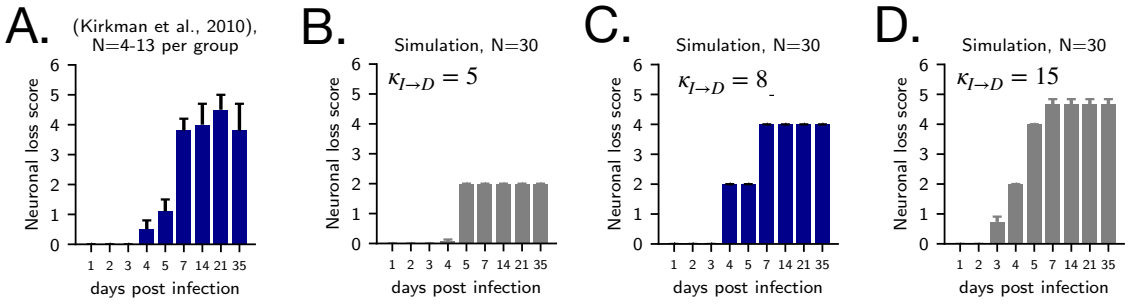

FIGURE 4.14: Consideration of the alternative values of the parameter scaling the neurotoxic effect of overactivated glia: comparison of the animal model data (A) to the model fit with low (B), intermediate (C), and high (D) values of $\kappa_{I\to D}$. Data are represented as mean ± SEM. The blue color indicates the bar plots of the animal model data and simulations with chosen parameter set. The figure is imported from Batulin et al., 2022.

Another attribute of the neuronal-death-related subsystem (right side of Fig. 3.1) is the scaling parameter for the effect of neuronal loss on circuit remodeling $\kappa_{D\to R}$. It is adjusted to (i) allow for the existence of a 'healthy' steady state in conditions of nonzero neuronal loss and (ii) keep the system sensitive to the extent of neuronal loss (Fig. 4.15).

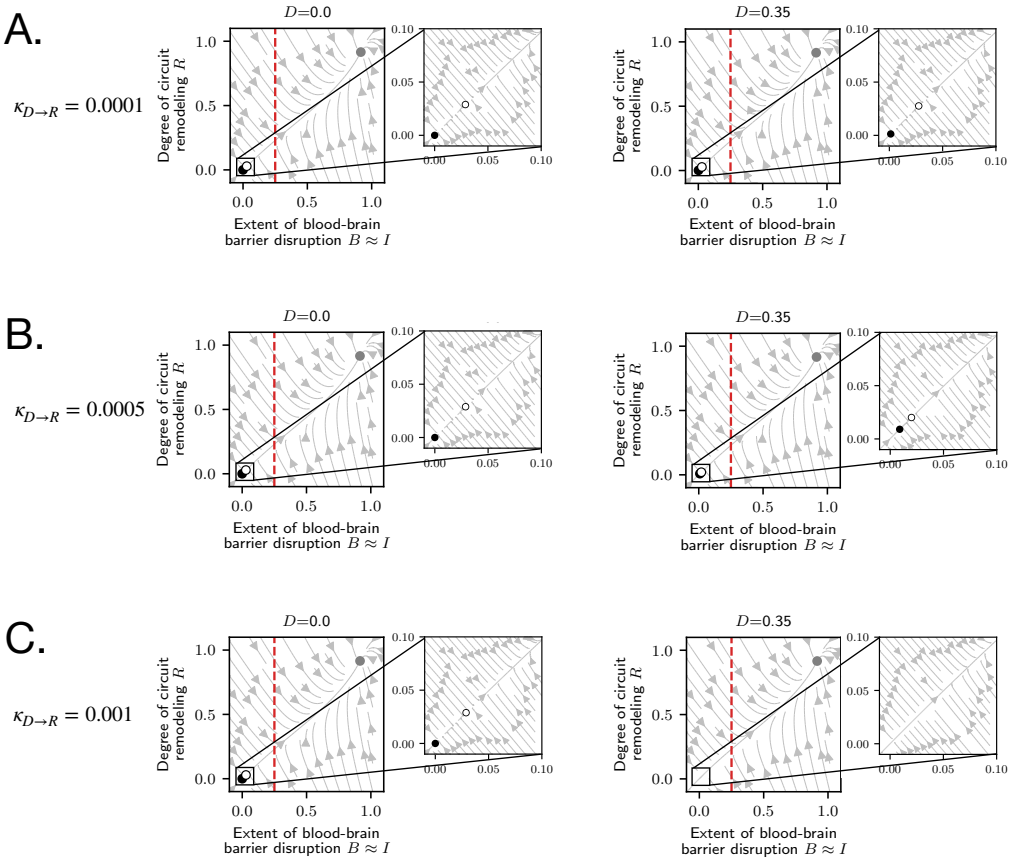

FIGURE 4.15: Consideration of the alternative values of the parameter scaling the effect of neuronal loss on circuit remodeling: the state-space compositions corresponding to the absent (left) and present (right) neuronal death. A.) The state-space composition for the low value of the $\kappa_{D\to R}$ contains three steady states in the first quadrant, but does not show sensitivity to the neuronal loss (right). The circles correspond to the steady states. The red dashed lines correspond to glial neurotoxicity threshold. B.) The state-space composition for the intermediate value of the $\kappa_{D\to R}$ contains three steady states in the first quadrant, and shows sensitivity to the neuronal loss (right). The sensitivity is illustrated by the change of the fixed point locations in response to the presence of neuronal loss. C.) The state-space composition for the high value of the $\kappa_{D\to R}$ contains three steady states in the first quadrant in the absence of neuronal death. However, the system shows hypersensitivity to the neuronal loss, which is illustrated by disappearance of two steady states (right). The figure was imported from Batulin et al., 2022.

The time scale parameters $\tau_I, \tau_B, \tau_D, \tau_R$ do not affect the location of the fixed points (Eq. 3.1) but may determine their stability and velocity of the dynamic changes (Fig. 3.3). The neuroinflammatory reaction is carried out primarily by microglia and assumed to be faster than the rest of the processes (vasculature recovery, neuronal loss and debris removal, circuit remodeling). The 1:10 ratio of the time scales is chosen ($\tau_I = 1$ day, $\tau_B = \tau_D = \tau_R = 10$ days). The τ_B, τ_D, τ_R are set equal because currently available experimental data do not provide additional constraints. In order to confirm the quality of the model fit to the animal model data, the control simulations with alternative ratios of time scales are carried out (Fig. 4.16).

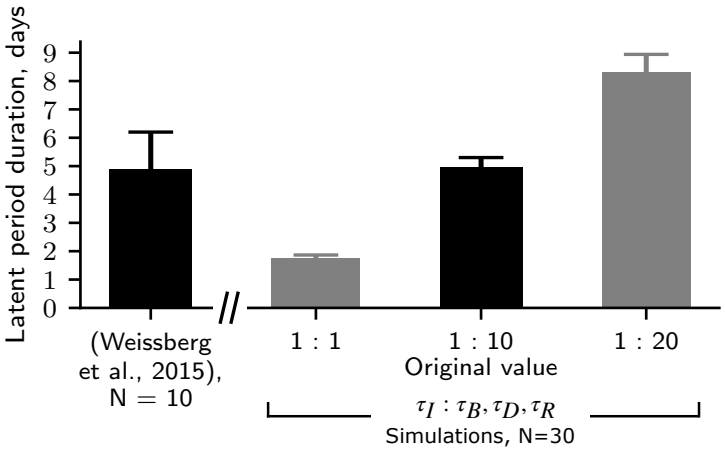

FIGURE 4.16: Comparison of the simulation results to the animal model data for the originally chosen ratio of time scales (black bar) and two alternative values (gray bars). Data are represented as mean ± SEM. The figure was imported from Batulin et al., 2022.

The parameters for the strength of seizure-promoting effects of neuroinflammation ($\kappa_{I\to S}$) and circuit remodeling ($\kappa_{R\to S}$) modulate the seizure rate for a given value of neuroinflammation intensity and extent of circuit remodeling (Fig. 4.17), and, consequently, the composition of the dynamical landscape (Figs. 4.18A, B). The parameter values of $\kappa_{I\to S}$ and $\kappa_{R\to S}$ are adjusted to allow a) for the existence of 3 steady states in the system (Fig. 4.11A) and b) reproduction of animal model data in the simulation (Fig. 4.18C).

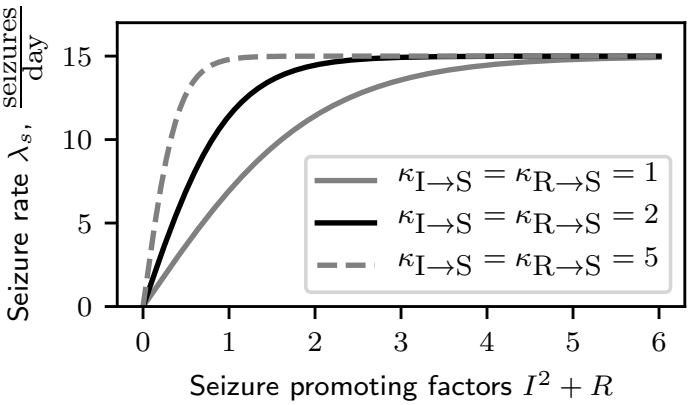

FIGURE 4.17: Changing the parameters for the strength of seizure-promoting effects of neuroinflammation and circuit remodeling leads to scaling of the sigmoid function of seizure rate along the 'x' axis. The figure was imported from Batulin et al., 2022.

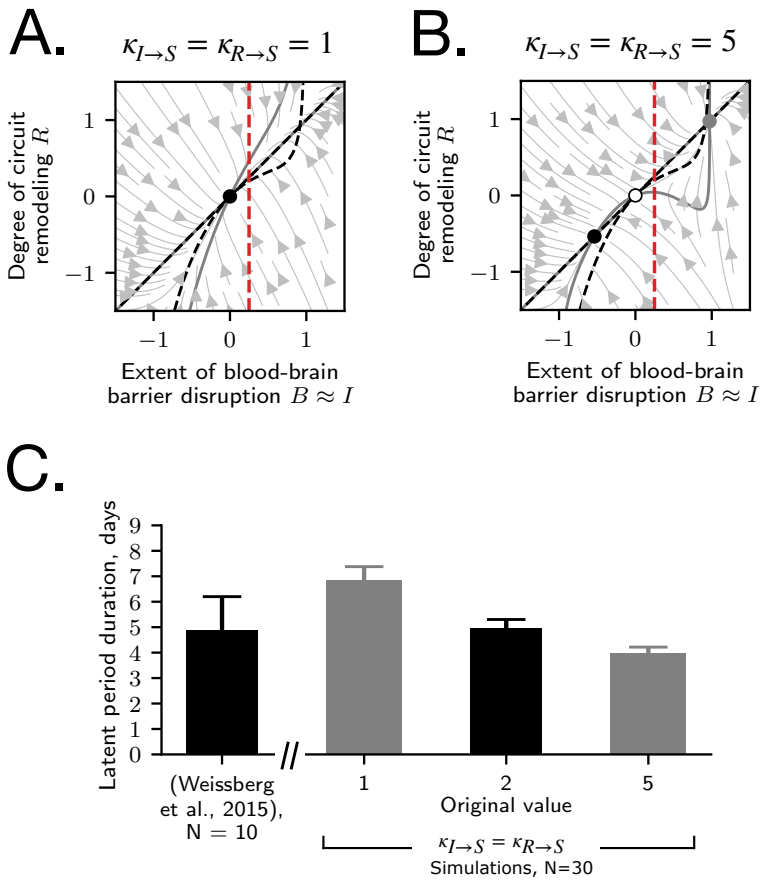

FIGURE 4.18: Consideration of the alternative values of parameters scaling the strength of seizure-promoting effects. The state-space composition for the lower (A) and higher (B) values of $\kappa_{I\to S}$ and $\kappa_{R\to S}$, in regard to the original (intermediate) value $\kappa_{I\to S} = \kappa_{R\to S} = 2$. The circles correspond to the steady states. The gray solid lines correspond to the nullclines. The black dashed lines correspond to the nullclines of the system with the original parameter values used as reference for comparison. The red dashed lines indicate the glial neurotoxicity threshold. C.) The comparison of the simulation results to the animal model data for the originally chosen $\kappa_{I\to S} = \kappa_{R\to S}$ parameters (black bar) and two alternative values (gray bars). Data are represented as mean ± SEM. The figure was imported from Batulin et al., 2022.

Chapter 5

Insights into epileptogenesis and intervention strategies

This chapter is dedicated to familiarizing the reader with the model-generated insights into the phenomena of epileptogenesis: dose-dependence of epilepsy development on injury intensity, the emergence of long time scales of epileptogenesis after transient injury, variability of epileptogenesis outcomes in subjects exposed to identical injury, and multicausality of epileptogenesis. At the end of the chapter, the utility of the mathematical model for the *in silico* research on injury-specific intervention strategies is discussed.

5.1 Dose-dependence of epileptogenesis on injury intensity

The severity of the seizure burden and the risk of epilepsy development depend on the intensity of neurological injury. This was shown in human cases of acquired epilepsy. For instance, human survivors of severe TBI have up to 16.7% chance of developing epilepsy over a time period of 30 years, while in mild TBI cases, the chance of epilepsy development drops to only 2.1% (Annegers et al., 1998).

Dose-dependence can be reproduced in various animals models of epileptogenesis, extending beyond TBI. For example, in the SE model of acquired epileptogenesis, the duration of SE determines the incidence of epilepsy, which can be modulated by pro- and anti-convulsant drugs. In the mouse model of infection-induced epilepsy, increasing the viral dose from 3×10^3 plaque forming units (PFU) to 3×10^6 PFU leads to modulation of epileptogenesis incidence from 25% to 80% respectively (Libbey et al., 2011).

The mathematical model captures the spectrum of the dose-dependence effects of the intensity of neurological injury on the course and severity of the developed pathology. This is illustrated both for cases of increase and decrease in injury severity (Fig. 5.1). In the BBB disruption animal model simulation, the severity of the epileptogenic injury can be modulated with two conceptually different approaches: via modulation of injury intensity (concentration of the albumin/TGF-β in the infused artificial cerebrospinal fluid), or via modulation of the duration of the time window, in which albumin/TGF-β is being administered.

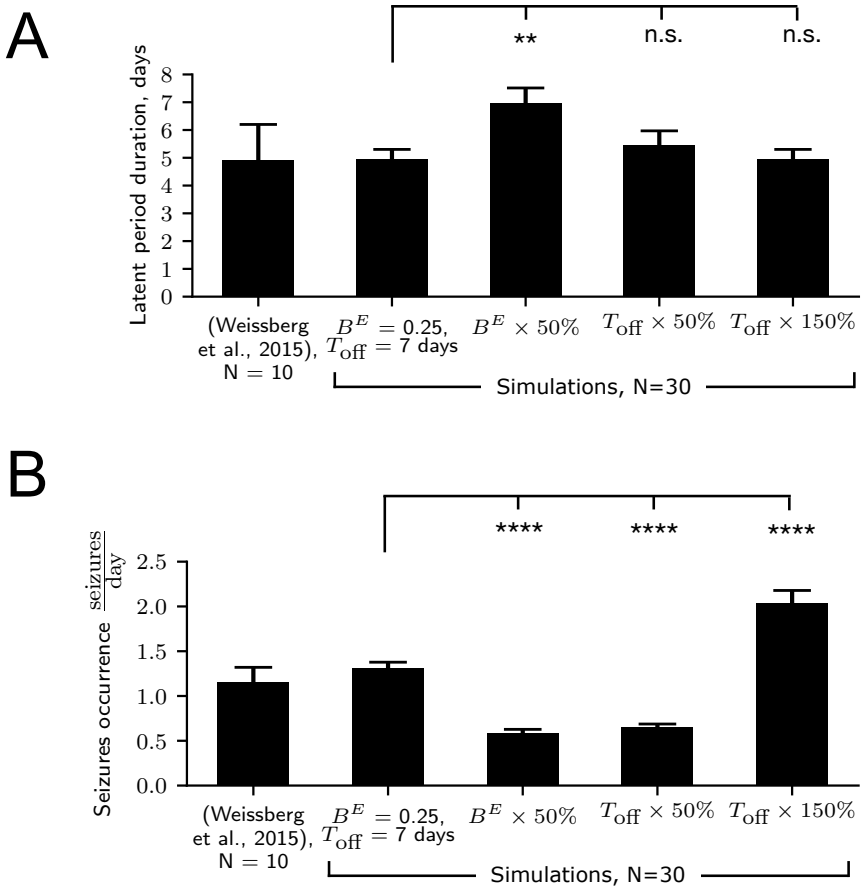

FIGURE 5.1: Dose-dependence of the latent period duration (A) and seizure burden (B) on the severity of neurological injury in BBB disruption rodent model simulation. From left to right: animal model data (Weissberg et al., 2015); simulations with the severity of the injury matched to Weissberg et al., 2015 ($B^E = 0.25$, $T_{\text{off}} = 7$ days); simulations with the severity of the injury decreased via lowering albumin/TGF-β concentration ($B^E \times 50\%$); simulations with the severity of the injury decreased via shortening the time window of albumin/TGF-β infusion ($T_{\text{off}} \times 50\%$); simulations with the severity of the injury increased via prolongation of the time window of albumin/TGF-β infusion ($T_{\text{off}} \times 150\%$). Data are represented as mean $\pm$ SEM. The figure was imported from Batulin et al., 2022.

The shortening of the time window duration by 50% leads to a significant drop in the seizure burden (1.24 ± 0.07 $\frac{\text{seizures}}{\text{day}}$ vs 0.58 ± 0.03 $\frac{\text{seizures}}{\text{day}}$, Fig. 5.1B), but does not have a significant effect on the latent period duration (Fig. 5.1A). On the other hand, the increase in severity of the injury simulated by 50% prolongation of the infusion time window leads to a significant rise in seizure burden (1.24 ± 0.07 $\frac{\text{seizures}}{\text{day}}$ vs 2.13 ± 0.17 $\frac{\text{seizures}}{\text{day}}$, Fig. 5.1B), and no significant effect on the latent period duration is observed (Fig. 5.1B). Contrary to the modulation of injury severity with manipulation of the time window duration, the 50% decrease in the injury intensity leads to both a significant drop in seizure burden (1.24 ± 0.07 $\frac{\text{seizures}}{\text{day}}$ vs 0.62 ± 0.04 $\frac{\text{seizures}}{\text{day}}$, Fig. 5.1B) and the prolongation of the latent period (5.57 ± 0.34 days vs 7.23 ± 0.47 days, Fig. 5.1A).

In addition to the modulation of the seizure burden severity, simulations reveal also the dose-dependence effects of injury severity on the risk of epilepsy development itself (Fig. 5.2). This is illustrated considering the modulation of the injury severity in regard to the reference simulations that match the experimental data from Weissberg et al., 2015 ($T_{\text{off}} = 7$ days). The injury of lowered severity ($T_{\text{off}} \times 50\%$) still leads to epileptogenesis, which, however, develops slower (Fig. 5.2). When the severity of the injury is set even lower ($T_{\text{off}} \times 25\%$), the progressive epileptogenesis does not happen at all and the healthy steady state is restored (Fig. 5.2). From a mathematical perspective, the dose-dependence of epileptogenesis chance originates from the fact that injury of low intensity ($T_{\text{off}} \times 25\%$) fails to push the system state across the separatrix into the basin of attraction of the 'epileptic' steady-state (Fig. 5.3). From the clinical perspective, it would correspond either to recovery of the subject from the neurological injury without seizure manifestation, or to a gradual decrease of the seizure burden over time and the increase of interseizure intervals. In contrast to injuries of lowered severity, the prolonged presence of the epileptogenic trigger ($T_{\text{off}} \times 150\%$) facilitates the process of epilepsy development (Fig. 5.2).

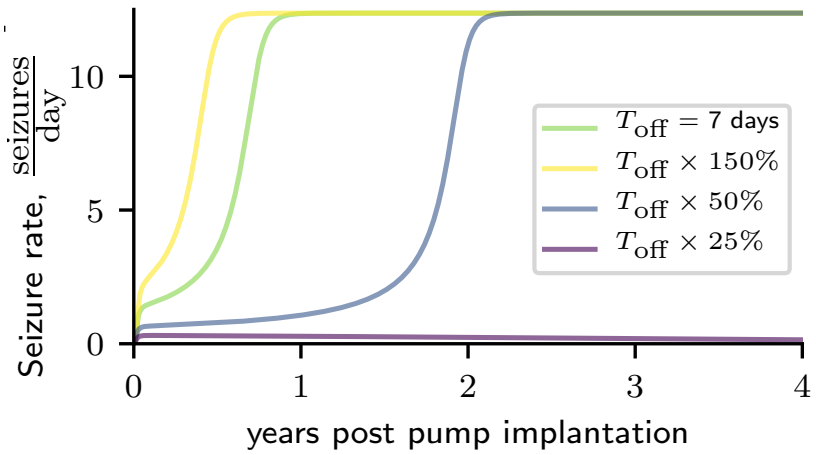

FIGURE 5.2: Epileptogenesis course in response to BBB disruption injuries of 4 different intensities illustrated with seizure rate development over time. Simulations are performed with the rate model. The manipulation of injury severity is implemented by modification of the duration of the time window of albumin/TGF-β infusion (T_{off}). The figure was imported from Batulin et al., 2022.

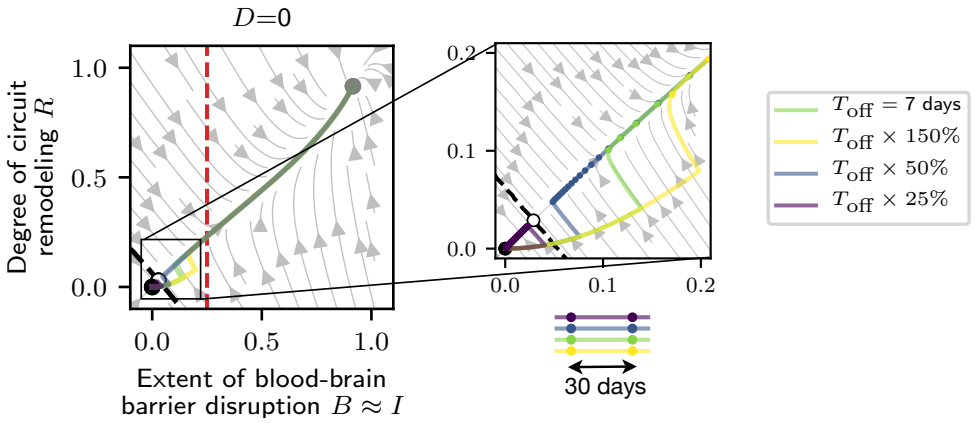

FIGURE 5.3: Dynamics of epileptogenesis in response to BBB disruption injuries of 4 different intensities illustrated over a state-space plot. Simulations are performed with the rate model. Manipulation of injury severity is implemented by modifying the duration of albumin/TGF-β infusion (T_{off}). The dynamical landscape of the system consists of 3 steady states: 'healthy' (black), unstable (white), and 'epileptic' (gray). The dashed black line (separatrix) separates the basins of attraction of the two stable steady states. The red dashed line corresponds to the neurotoxicity threshold Θ. The distance between circles on invidiual traces corresponds to the time intervals of 30 days. The state of the system is being pushed away from the origin by the effect of the injury. The exact trajectory of the state changes depends on the particular point, from which it takes off after the injury offset. The take-off point may be located in either of two basins of attraction, which would determine the progression or recovery after the neurological injury. The figure was imported from Batulin et al., 2022.

5.2 Emergence of long time scales of epileptogenesis

Despite the 'slowest' variables in the model operating on relatively fast time scale of 10 days (Table 4.1), remarkably long time scales of epileptogenesis emerge in the mathematical model (Fig. 5.2). These long time scales are in agreement with clinical observations. For instance, in TBI cases mentioned in the previous section, epileptic seizures can manifest years and decades after the injury (Annegers et al., 1998). The simulation results indicate that for the BBB disruption with 50% intensity relative to the duration used in the experimental study (Weissberg et al., 2015), epileptogenesis progression evolves over 2 years after injury (Fig. 5.2). From the mathematical point of view, the slowing down of the dynamics originates from the fact that the state of the model passes the proximity of the saddle point (Fig. 5.3), where the velocity of state changes is the lowest (Fig. 3.3). Thus, when an epileptogenic injury pushes the state of the system to cross the separatrix in the vicinity of a saddle point,

the epileptogenesis can evolve on time scales of years and decades, even though the transient injury was present only shortly.

5.3 Variability of epileptogenesis risk and pathology severity

The risk and severity of acquired epilepsy in patients suffering from similar epileptogenic injuries are characterized by a high level of variability. For instance, 7% of stroke survivors develop epilepsy, while others remain seizure-free (Zou et al., 2015). It is hypothesized that the risk of epileptogenesis depends on the genetic profile of the subject, list of comorbidities, characteristics of the injury (e.g. severity and localization of the injury in the CNS), and other factors (Pitkänen, Roivainen, and Lukasiuk, 2016). However, evidence from experimental studies suggests that the variability of epileptogenesis outcomes is present also in animal models of the disease, which allow for the preservation of standardized conditions: similar genetic profiles of animals and identical characteristics of applied injuries. For example, in 12 rats treated with an identical dose of pilocarpine, 10 animals developed epilepsy with seizure frequency ranged from 1 to 72 $\frac{\text{seizures}}{\text{week}}$, while 2 others remained seizure-free (Polascheck, Bankstahl, and Löscher, 2010). Up until now, the mechanisms underlying the origin of such variability in epileptogenesis outcomes have not been understood.

The mathematical model captures the phenomena of the variability of epileptogenesis outcomes in identical subjects exposed to identical injury. The identical characteristics of simulated subjects and epileptogenic injury are modeled by the preservation of the parameters of the model (Table 4.1) and parameters of simulated injury (Appendix A). The results of the TMEV animal model simulation on the follow-up period of 1 year after injury (Fig. 5.4) illustrate the variability of the clinical outcome in regard to the presence of epileptogenesis and the severity of seizure burden (Fig. 5.4A). Out of 30 simulations of infection injury, 13 result in full recovery (seizure probability equal 0 $\frac{\text{seizures}}{\text{day}}$), while the remaining simulations exhibit seizure burdens of various severity. Figures 5.4B, C illustrate the examples of 3 simulations with different outcomes 1 year after injury onset: (i) full recovery after seizures on early post-injury time window (simulation #14), (ii) simulation with intermediate severity of spontaneous seizures (simulation #19), and (iii) progressed epileptogenesis reaching the maximum daily seizure frequency (simulation #20).

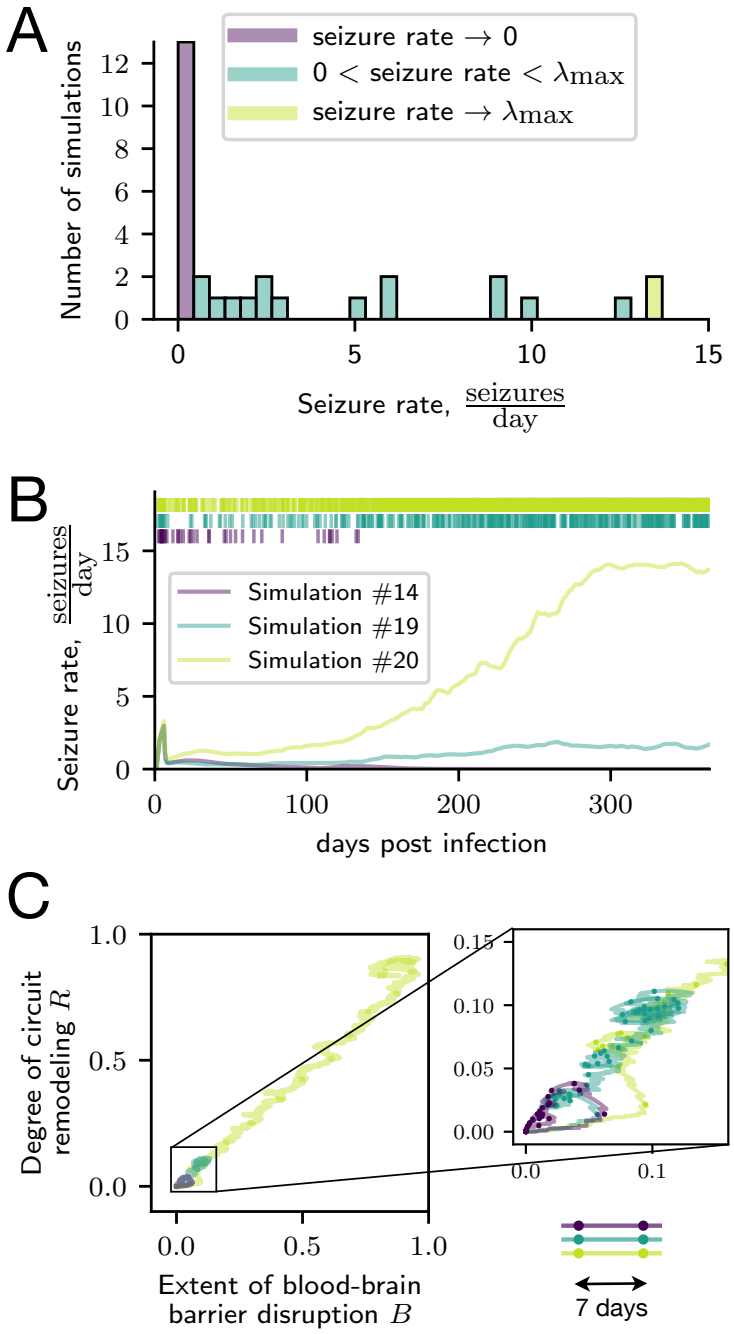

FIGURE 5.4: The variability of epileptogenesis outcomes in identical simulated animals exposed to identical injury. A.) The distribution of the seizure rate one year after infection for 30 TMEV simulations. B.) The examples of the seizure rate development in time for 3 simulations with different seizure burden outcomes. The line color code is consistent in all subfigures. The raster plot on top illustrates the occurrence of seizures in time for corresponding simulations. C.) Epileptogenesis course for 3 simulations with different seizure burden outcomes illustrated in the B-R domain. The distance between circles on trajectories corresponds to the time intervals of 7 days. The overall visualization period is 1 year after infection. The figure was imported from Batulin et al., 2022.

From the mathematical point of view, the variability of the epileptogenesis outcome and severity of the seizure burden originates from the stochastic nature of seizure generation (Fig. 5.4C). This induces noise effects, which may bring the system state either to the basin of attraction of the 'healthy' or the 'epileptic' steady state. Thus, even for the hypothetically identical subjects exposed to identical injury, the epileptogenesis outcome can vary. This would be even more pronounced in the experimental and clinical setups where genetic and epigenetic backrounds vary across subjects.

5.4 Multicausality and degeneracy in epileptogenesis

Epilepsy results from a complex interplay of various pathological processes following neurological injury (Chapter 2). However, the individual pathological trajectories appear to be injury-specific. For example, a profound neuronal loss in the hippocampus, known as hippocampal sclerosis, is associated with TLE and other epilepsy syndromes (Thom, 2014). Moreover, the severity of seizure burden has been shown to positively correlate with the extent of neuronal loss (Lopim et al., 2016). However, the role of neuronal death in epilepsy development is still extensively debated and whether the neuronal loss is a primary cause of epileptogenesis, its consequence, or both remains an open question (Kapur, 2003; Sendrowski and Sobaniec, 2013). For example, the data from the BBB disruption rodent model suggests that epileptogenesis can develop without evident neuronal death (Weissberg et al., 2015). The mathematical model of epileptogenesis, allowing simulation of epilepsy development without neuronal death (Chapter 4.1), suggests that the neuronal loss is not necessary for epileptogenesis, but may itself be sufficient for causing it.

Simulations with induced neuronal loss show that this single perturbation to the model is sufficient to trigger progressive epileptogenesis (Fig. 5.5). Neuronal loss increases seizure rate via induction of remodeling of neural circuits (Fig. 3.1). From a mathematical perspective, the presence of neuronal death leads to a reordering of the stability landscape in the model: the 'healthy' steady-state and the saddle point move towards each other, resulting in a non-zero seizure rate even when the system is resting in the 'healthy' steady state (Figs. 5.6A, B). Further increase of neuronal loss extent leads to the collision of the 'healthy' steady state with the saddle point at a certain value of extent of neuronal cell loss $D_{\text{critical}} \approx 0.41$ (Fig. 5.6C). Thus, for the neuronal cell loss extent greater or equal to D_{critical}, the development

of progressive epileptogenesis towards the 'epileptic' steady-state is inevitable (Figs. 5.5, 5.6C, D). From a clinical perspective, the subcritical extent of neuronal loss elevates the chance of seizure occurrence but does not necessarily trigger epileptogenesis onset. However, even a subcritical extent of neuronal loss may be sufficient for epileptogenesis driven by the pathological effects of spontaneous recurrent seizures (Fig. 5.5).

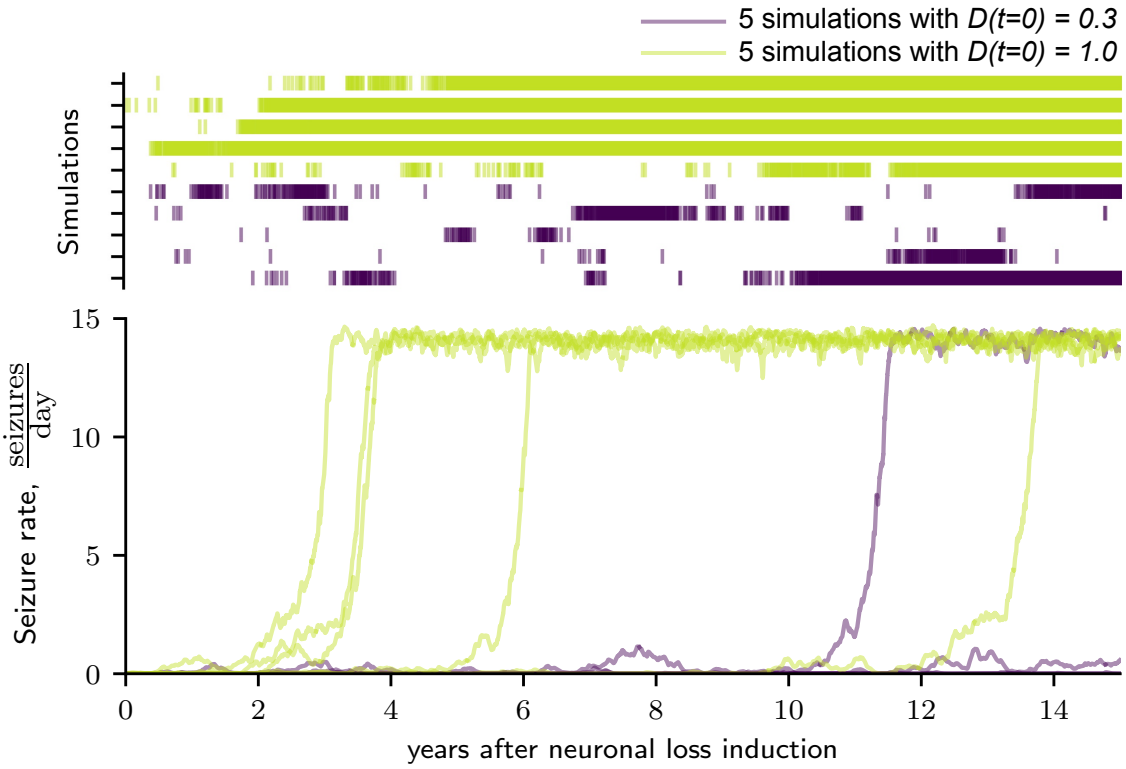

FIGURE 5.5: Epileptogenesis progression in 5 simulations with supracritical ($D = 1.0 > D_{\text{critical}} \approx 0.41$) and subcritical ($D = 0.3 < D_{\text{critical}} \approx 0.41$) extents of neuronal loss. The raster plots above seizure rate traces indicate seizure times of each simulation. The figure was imported from Batulin et al., 2022.

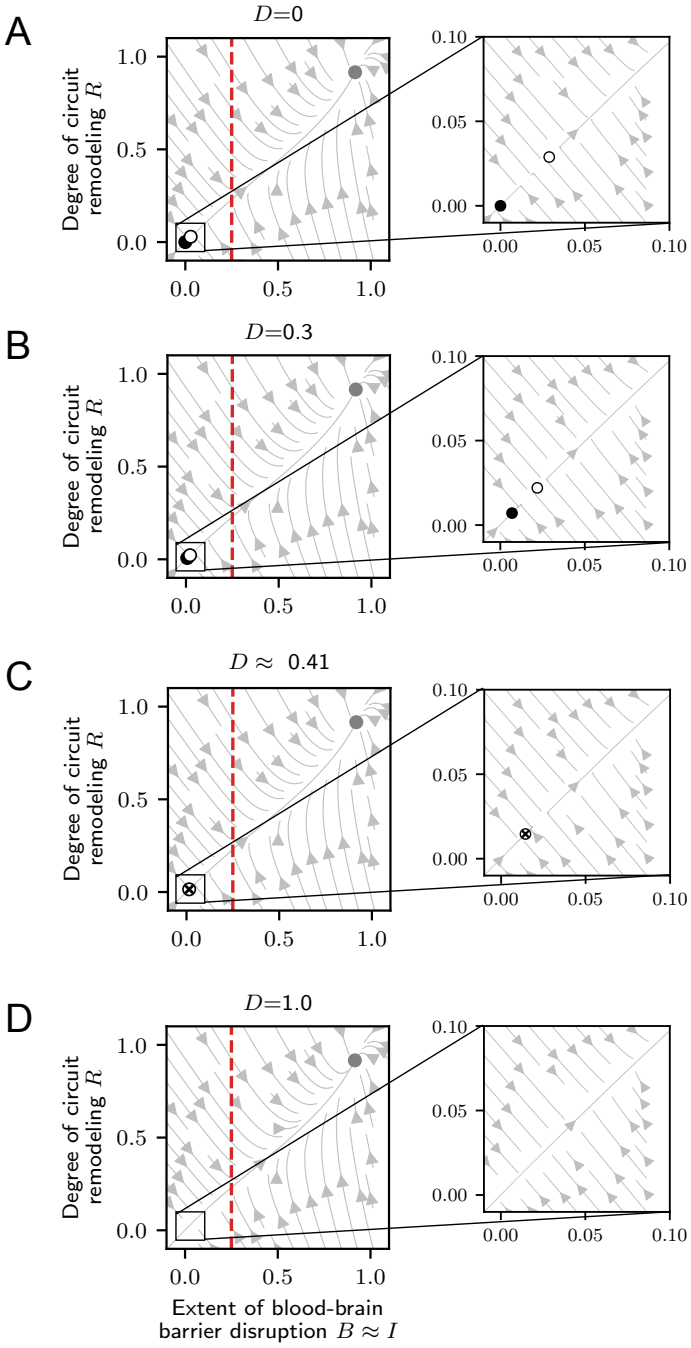

FIGURE 5.6: The effect of neuronal loss on the system stability is illustrated with the state-space plots for absent neuronal loss (A), the subcritical extent of neuronal loss (B), the critical extent of neuronal loss (C), and the supracritical extent of neuronal loss (D). The filled circles correspond to the 'healthy' (black) and the 'epileptic' (gray) steady states. The empty circles correspond to the unstable fixed (saddle) points. The red dashed lines correspond to the neurotoxicity threshold Θ. The figure was imported from Batulin et al., 2022.

In line with experimental findings, the extent of neuronal loss in the mathematical model is correlated with the severity of the seizure burden (Fig. 4.7). Moreover, it also determines the average time until the development of progressive epileptogenesis (Fig. 5.7). Interestingly, the average time of epileptogenesis caused solely by neuronal death is estimated in decades (Fig. 5.7). These time scales are not in the scope of animal model studies, which again highlights the prominent role of mathematical modeling in research on epileptogenesis.

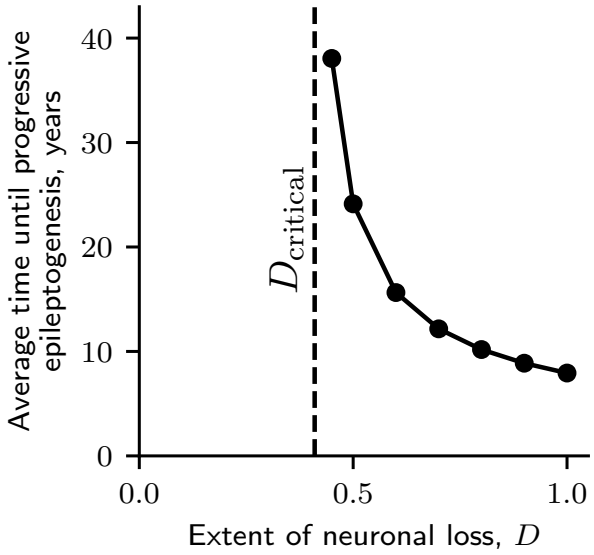

FIGURE 5.7: The dependence of average time until progressive epileptogenesis on the extent of induced neuronal loss. The time of progressive epileptogenesis was heuristically calculated as the time from the start of the simulation to the time point of the neuroinflammation $I(t)$ reaching 90% of the value corresponding to the 'epileptic' steady state. The black dashed line corresponds to the critical extent of neuronal loss $D_{\text{critical}} \approx 0.41$. The figure was imported from Batulin et al., 2022.

The simulation results show that neuronal loss is sufficient for epileptogenesis initiation and progression. At the same time, neurodegeneration is not a necessary criterion for epilepsy development, which is illustrated by simulations of other injury types (Chapter 4.1). Taken together, these findings highlight the multicausal nature of the epileptogenesis phenomena, where distinct processes may drive the process in isolation or in a convergent fashion.

5.5 Mathematical model as a tool for pre-clinical research

The research on therapeutic interventions in epilepsy consists of several stages. Before the clinical trials, a potential medical treatment is tested in animal models of epilepsy. The neuro-immune interactions are considered to be prominent targets in the search for efficient treatments for acquired epilepsy. However, the timing and duration of a potential intervention seem to matter in addition to the selection of a target itself (Vliet et al., 2012; Sliwa et al., 2012). For instance, BBB leakage is among such therapeutic targets. The drug called rapamycin is suspected to have an antiepileptogenic effect, which is obtained via the recovery of BBB integrity. In the model of SE-induced epileptogenesis, the administration of rapamycin over the period of 6 weeks was shown to reduce the seizure frequency, the extent of neuronal loss, and the fraction of animals developing seizures (Vliet et al., 2012). In contrast, the treatment during only 2 weeks had no positive effect (Sliwa et al., 2012).

The mathematical model allows for *in silico* simulation of therapeutic interventions (Fig. 5.8), which may be used in the pre-clinical research. In the simulation setup, one can test various strategies in regard to time windows of drug application, intervention targets, and their combinations. Moreover, one can study the injury-specificity of the efficiency of a particular intervention by simulating various strategies in different animal models.

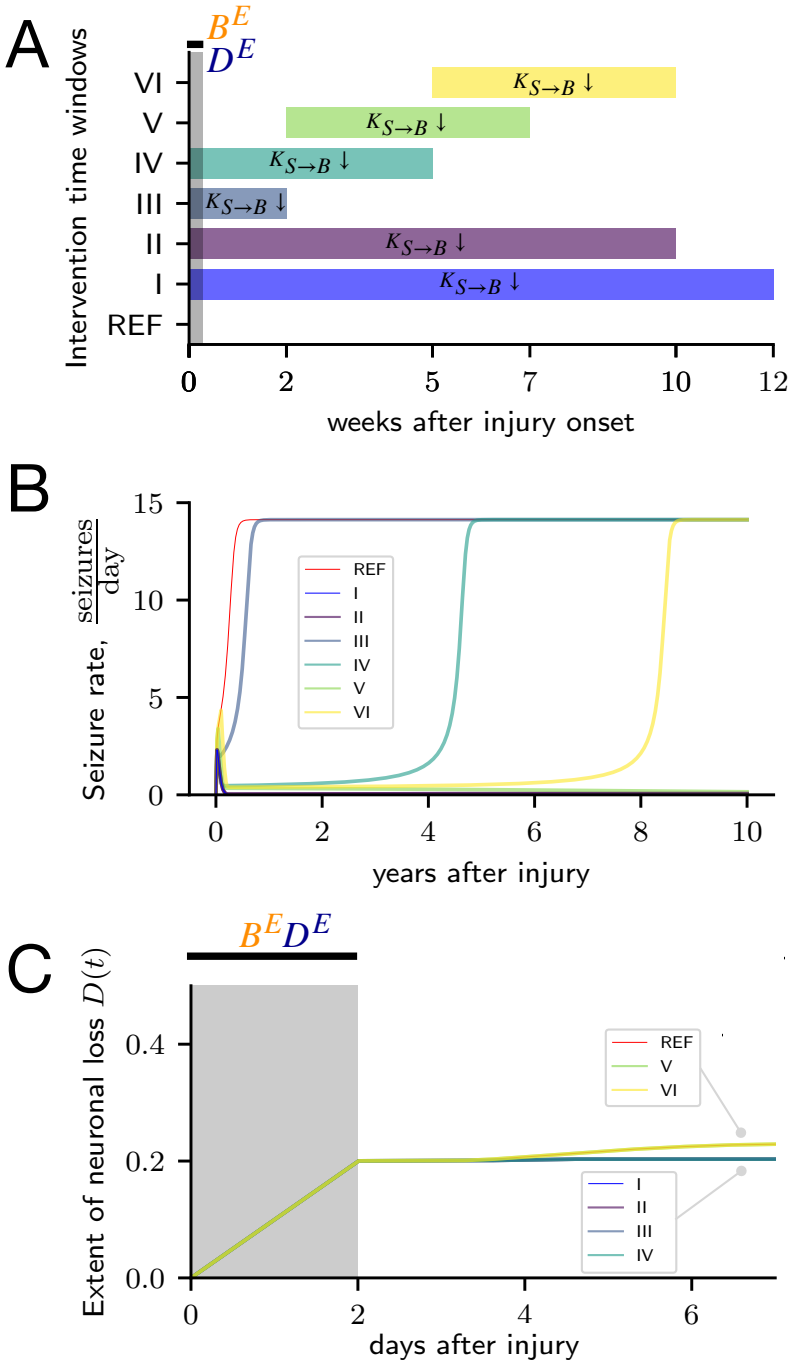

FIGURE 5.8: Simulation of the therapeutic intervention with suppression of the seizure effect on BBB integrity in the pilocarpine rodent model of epileptogenesis. A.) The time windows for 6 different interventions (I-VI) and a reference simulation without intervention (REF). The suppression of seizure effect on BBB integrity is simulated with a 100-fold decrease of respective model variable $K_{S\to B}\downarrow$. Simulations are performed using the rate model. B.) The seizure rate development in simulated animals exposed to various types of intervention. C.) The neuronal loss progression in simulated animals exposed to various types of intervention. The gray areas correspond to the time window of injury induction. The figure was imported from Batulin et al., 2022.

The simulation of SE-induced epileptogenesis and suppression of BBB disruption is aimed to mimic the effect of rapamycin from the animal model study. The permanent suppression of the effect of seizures on BBB integrity (intervention I in Fig. 5.8A) prevents epileptogenesis (Fig. 5.8B). Interestingly, the course of neurodegeneration does not differ between simulation with treatment and reference simulation in the first half of the week after injury onset (Fig. 5.8C). However, despite the identical extent of neuronal loss, the dynamical landscapes are conceptually different due to the effect of suppression of BBB disruption (Fig. 5.9). In the case of the untreated simulation, 3 steady states exist in the state space (Fig. 5.9A), while in the treated case, only a single 'healthy' attractor remains (Fig. 5.9B). This explains why despite the injury and its pathological sequelae, the system gradually and inevitably recovers without epileptogenesis (Fig. 5.9).

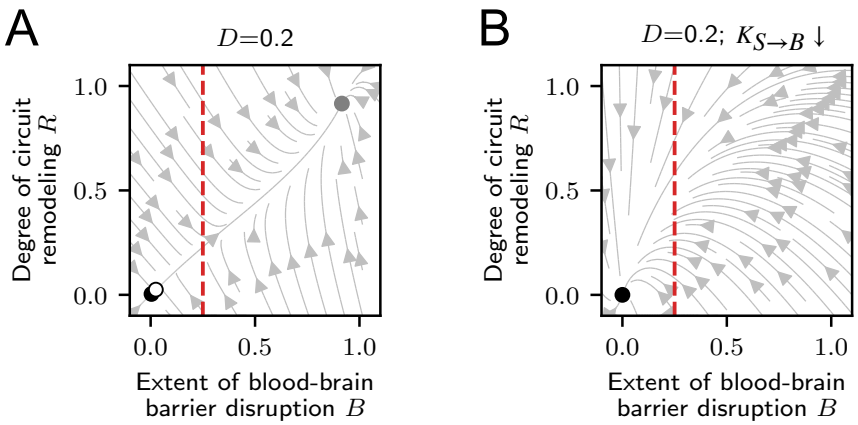

FIGURE 5.9: State-space plots illustrating the state of the system after the injury offset (D=0.2) without (A) and under (B) the effect of the intervention. The filled circles correspond to 'healthy' and 'epileptic' steady states. The empty circle corresponds to the saddle point. The red dashed lines indicate the neurotoxicity threshold Θ. Without suppression, the system has two attractor states, while under the effect of the intervention, only a single 'healthy' attractor remains. The figure was imported from Batulin et al., 2022.

Similarly to permanent intervention (type I in Fig. 5.8), transient suppression of the BBB disruption is also capable of epileptogenesis prevention. For instance, a simulation of 10 week long rapamycin application (intervention II in Fig. 5.8A) also shows epileptogenesis prevention (Figs. 5.8B, 5.10). On the other hand, a shorter 2-week long intervention (type III in Fig. 5.8A) is not sufficient for the prevention of epilepsy development (Figs. 5.8B, 5.10). Interestingly, not only the duration of the intervention time window but also the precise timing of the intervention onset relative to the injury is crucial for epileptogenesis prevention. This is illustrated

with the interventions of 5-week duration applied together with the on set of an injury (type IV in Fig. 5.8A), with 2 weeks delay (type V) and 5 weeks delay (type VI). Surprisingly, only the intervention applied with 2 weeks delay was sufficient to prevent the epileptogenesis (Figs. 5.8B, 5.10). This suggests that in SE-induced epileptogenesis a critical time window exists, in which intervention has to be applied to suppress the progression of the pathology.

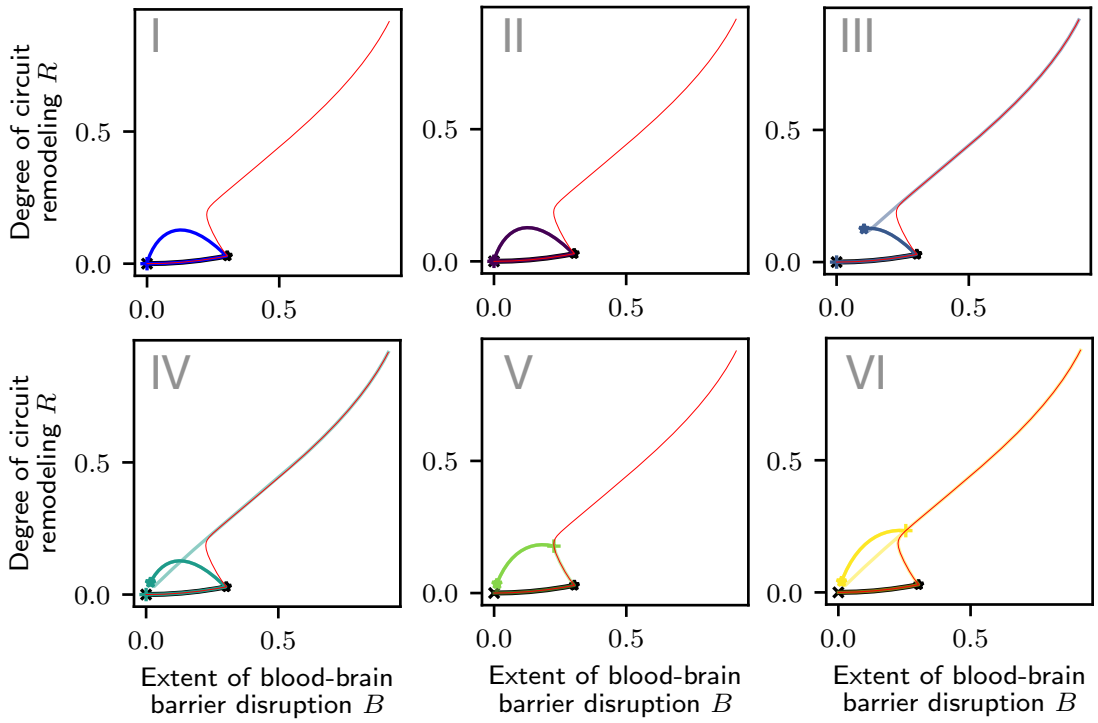

FIGURE 5.10: Response of the system to the injury in simulated animals exposed to various types of intervention illustrated in the B-R domain. For details of interventions I-VI, see Fig. 5.8A. The red lines correspond to the reference simulation without intervention. Solid black lines starting with the 'x'-symbol and ending with a star correspond to the time interval of injury induction. The solid color lines starting with the 'x'-symbol and ending with a star correspond to the time windows of the simulated interventions. The figure was imported from Batulin et al., 2022.

Another interesting aspect of therapeutic interventions in epilepsy is their injury-specificity in regard to the intervention targets and timings. In order to check whether the mathematical model accounts for the injury-specificity of therapeutic interventions, the simulations mimicking rapamycin effects on the infection-induced epileptogenesis (TMEV mouse model) are carried out. The permanent suppression of the effects of seizures on BBB integrity (intervention I in Fig. 5.11A) is sufficient to prevent epilepsy development (Fig. 5.11B). Interestingly, the 1-week long

intervention applied at the time of injury onset (type II) is also sufficient. However, interventions of the same duration that are applied with 1- and 2-week delays (types III and IV respectively) do not prevent epileptogenesis.

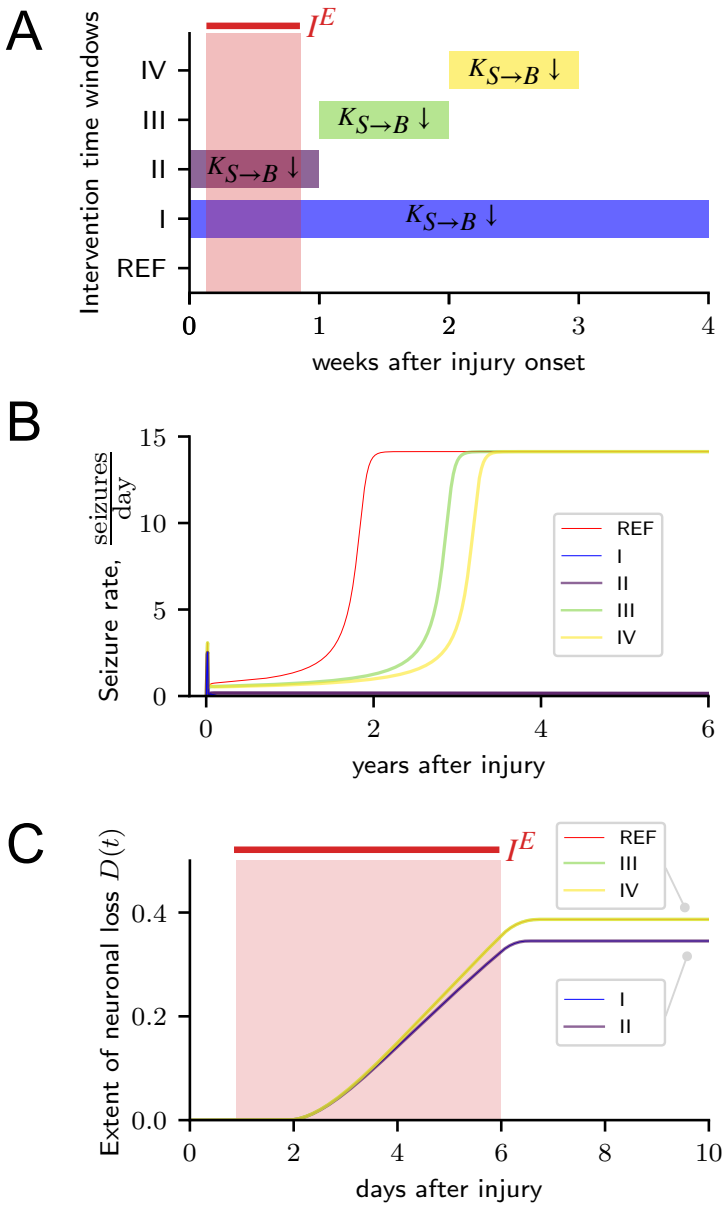

FIGURE 5.11: Simulation of the therapeutic intervention with suppression of the seizure effect on BBB integrity in the TMEV mouse model. A.) The time windows for 4 different interventions (I-IV) and a reference simulation without intervention (REF). The suppression of seizure effect on BBB integrity is simulated with a 100-fold decrease of respective model variable $K_{S\to B}\downarrow$. Simulations are performed using the rate model. B.) The seizure rate development in the simulated animals exposed to various types of intervention. C.) The neuronal loss progression in simulated animals exposed to various types of intervention. The red areas correspond to the time window of injury induction. The figure was imported from Batulin et al., 2022.

The difference in efficacy between interventions applied in different time windows likely originates from the fact that interventions applied not within the time window of injury induction fail to modulate the infection-induced neurotoxicity (Fig. 5.11C). Different extents of neuronal loss lead to the formation of different structures in the dynamical landscapes. For interventions that overlap with the injury induction time window (types I and II), a larger basin of attraction of the 'healthy' steady state is preserved due to a lower extent of neuronal loss (Fig. 5.12A). For the interventions that do not overlap with the injury induction time window, the state space composition remains identical to the reference simulation, in which a 'healthy' steady state is in the vicinity of a saddle point (Fig. 5.12B).

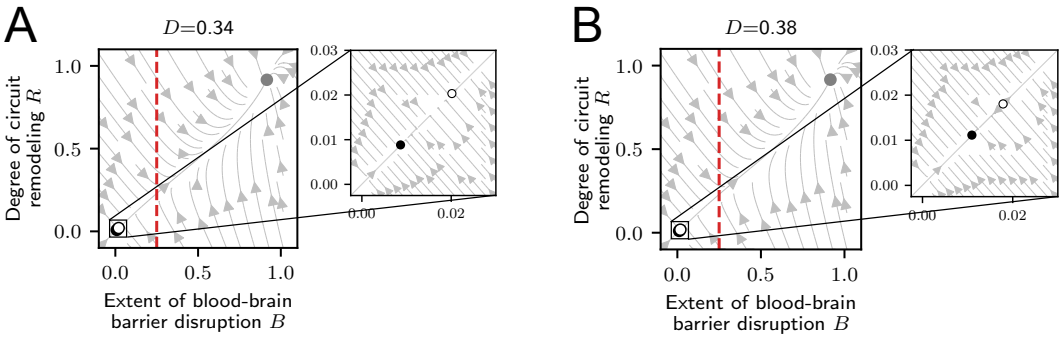

FIGURE 5.12: State-space plots illustrating the state of the system after the injury offset in simulations exposed to interventions I-II (A) and III-IV (B). The filled circles correspond to 'healthy' and 'epileptic' steady states. The empty circles correspond to the saddle point. The red dashed lines indicate the neurotoxicity threshold Θ. The figure was imported from Batulin et al., 2022.

Interestingly, when a different kind of intervention (suppression of neuroinflammatory reaction to the BBB leakage) is applied in the TMEV model simulation, the same effect is observed (Fig. 5.13). Thus, for the successful prevention of epileptogenesis in the TMEV model simulation, the time window of the intervention has to overlap with the time window of the injury induction, and this can be considered an injury-specific feature. On the other hand, in the pilocarpine SE model simulation, the transient simulation has to be applied with a certain delay in order to prevent epilepsy development (Figs. 5.8, 5.10). This highlights the injury-specific differences in interventions necessary for the successful prevention of epilepsy development. In sum, the developed mathematical model can be used as an *in silico* tool for the simulation of intervention strategies. It provides the means for studying the injury-specificity of prominent targets and timings of a successful therapeutic intervention.

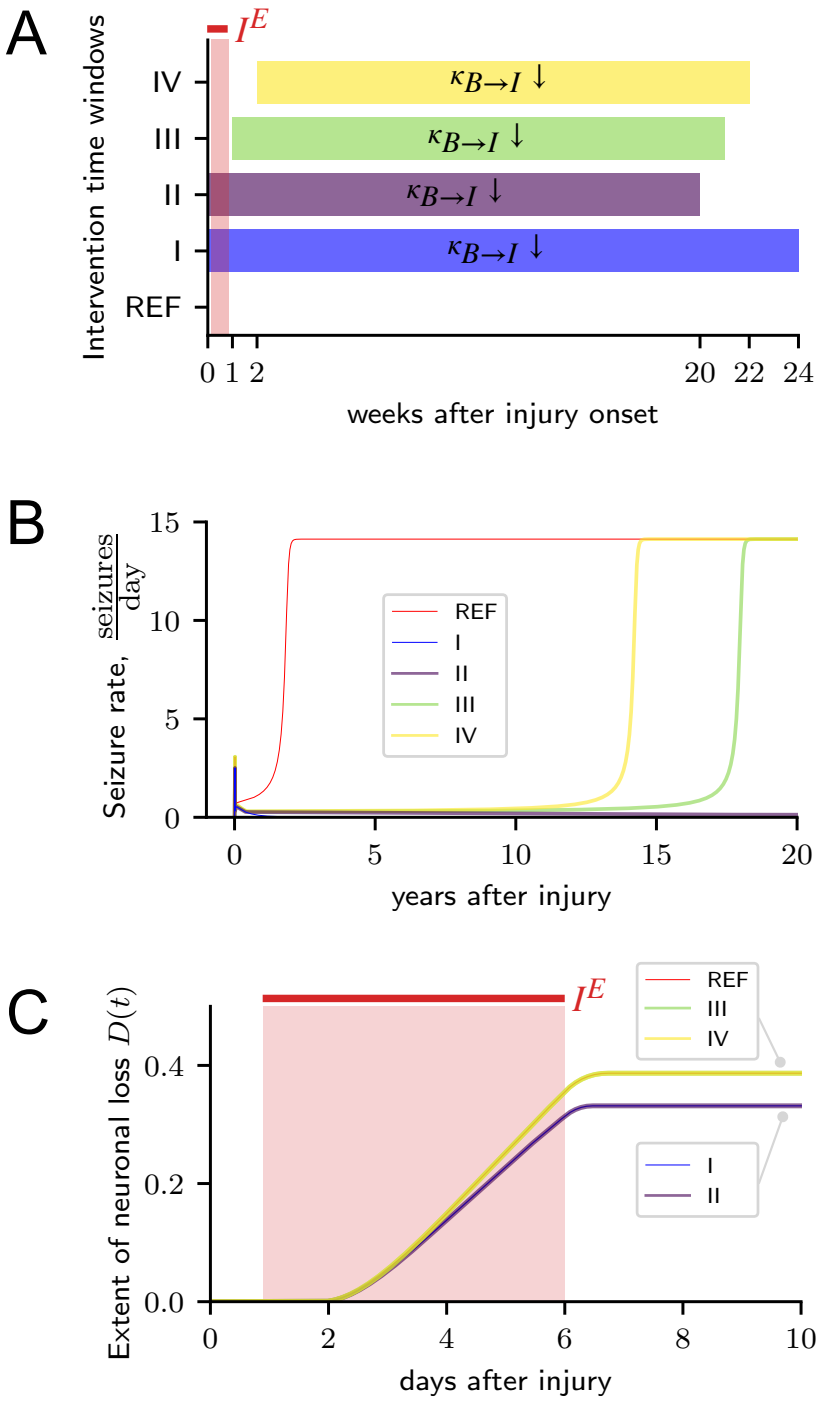

FIGURE 5.13: Simulation of the therapeutic intervention with suppression of neuroinflammatory reaction to the BBB leakage in the TMEV mouse model. A.) The time windows for 4 different interventions (I-IV) and a reference simulation without intervention (REF). The suppression of neuroinflammatory reaction to the BBB leakage is simulated with a 100-fold decrease of respective model variable $\kappa_{B\to I}\downarrow$. Simulations are performed using the rate model. B.) The seizure rate development in the simulated animals exposed to various types of intervention. C.) The neuronal loss progression in simulated animals exposed to various types of intervention. The red areas correspond to the time window of injury induction. The figure was imported from Batulin et al., 2022.

Chapter 6

Discussion

6.1 Conclusions

Epilepsy is a spectrum of diseases affecting around 70 million people worldwide. The key feature of this disease is the modification of the CNS to a pathological state, in which spontaneous recurrent seizures occur. Despite the extensive research on its development, the available pharmacological treatment options are not effective in approximately one-third of cases. One of the reasons for this is the fact that the complex interplay of physiological and pathological processes leading to epilepsy development remains poorly understood.

This thesis presents a mathematical model of epileptogenesis — a first-of-its-kind framework to describe the dynamics of the interaction between neural and immune systems in the context of epilepsy. This model enables the simulation of acquired epilepsy caused by a variety of neurological injuries. In addition, it can be used for the generation of testable predictions for pre-clinical research on new therapeutic strategies.

The structure of the model is designed taking into consideration the research findings from clinical and experimental studies that investigated the principles of epilepsy developments. The model accounts for the interplay of various processes upon neurological injury such as neuroinflammation, BBB disruption, neuronal death, circuit remodeling, and epileptic seizures. The developed framework, formulated as a system of stochastic nonlinear ordinary differential equations, captures the characteristic injury-specific time courses of pathology development. This is illustrated by a comparison of the simulation results with the data from three animal models of epileptogenesis mimicking epilepsy development after infection, chemically-triggered SE, and induced BBB leakage. The simulation of acquired epilepsy caused by different neurological injuries is carried out by the analysis of

the key effects of epileptogenic injuries and their translation into the input signal sequences that mimic injury effects in simulation. The simulations capture injury-specific temporal patterns of seizure occurrence, BBB disruption, the progression of neuronal loss, and neuroinflammation. In addition to reproducing the animal model data, the simulation results also generate insights into the principles of epileptogenesis.

The model provides a dynamical system's explanation for the dose-dependence of epileptogenesis on the severity of the neurological injury. Interestingly, the intensity of the epileptogenic injury not only can modulate the seizure burden and duration of epileptogenesis but it can even determine the clinical outcome of the epileptogenesis process. The neurological injury may result in a gradual recovery without progression of epileptogenesis if the injury is too weak to bring the state of the system across the separatrix into the basin of attraction of the epileptic steady state.

Similar to clinical and experimental observations, the simulations show that epileptogenesis course can develop over long time scales of years and decades. This is surprising considering the fact that the epileptogenic injury is transient in its nature and the 'slowest' processes of the mathematical model operate on the time scale of days and weeks. A mathematical analysis of the developed framework revealed that a paradoxically long epileptogenesis process can occur if the neurological injury pushes the state of the system in the vicinity of the saddle point, which is located on the separatrix between the basins of attraction for the 'healthy' and 'epileptic' steady states.

Another phenomenon that was found in experimental studies, but did not yet have a mechanistic explanation is the variability of the epileptogenesis outcomes in subjects exposed to a similar injury. The mathematical model captures this phenomenon and suggests that even in hypothetically identical subjects exposed to an identical injury the pathological outcomes are highly variable. This variability originates from the stochastic nature of spontaneous recurrent seizures.

The model also provides insights into the multicausality of epileptogenesis, suggesting that distinct processes may drive epilepsy development in isolation or combination with other pathological mechanisms. For example, neuronal death is not a necessary component for epileptogenesis, as was shown in human and animal model studies. However, the modeling results suggest that this pathological process by

itself may be sufficient to trigger epilepsy development.

Furthermore, the model can be utilized for the development of new efficient intervention strategies. The simulations of interventions that were carried out using the model suggest that therapeutic interventions applied during only a short but critical time period may be as effective as permanent treatments. The results highlight the injury-specificity of therapeutic targets and the time windows of interventions that allow for the successful suppression of epileptogenesis. For example, it is predicted that in the case of infection-induced epileptogenesis, the intervention has to be applied simultaneously with the injury onset, while in the case of SE-induced epileptogenesis, the critical time window does not necessarily overlap with the injury. In sum, the mathematical model can be used as an *in silico* tool for the generation of testable predictions for pre-clinical research on therapeutic interventions against epilepsy.

6.2 Limitations and outlook

The mathematical model of epileptogenesis has a list of limitations that originate from the modeling assumptions taken. Describing the processes with coarse-grained variables, the model does not account for the spatial organization of the CNS and inter-regional differences in the structure and function of the neural tissues. For instance, it is known that the cell type composition of neural tissue differs between areas of the CNS. This may, for example, affect the coupling strength between processes described in the model. Moreover, it is known that certain regions of the brain, such as the hippocampus, play a more prominent role in seizure generation and pathophysiology of epilepsy relative to others. Thus, in future work, the inclusion of the spatial component in the model design should be considered.

Additionally, the wide spectrum of neuro-immune reactions is summarized by the single neuroinflammation variable, which is assumed to only have pathological effects. Future versions of the model should account for the neuroprotective aspects of mild neuroinflammation, the diversity of microglial phenotypes, and phenotypic memory in glial cells.

Another limitation of the current model consists in not distinguishing between focal and generalized seizures, which are likely to have different effects on the state

of the CNS. Moreover, the modulation of seizure duration and severity, which is evident in the course of epileptogenesis, is also not captured by the model. Accounting for seizure diversity and the evolution of their features over time would allow for a more precise description of the epileptogenesis process, especially in the later stages of the disease.

Finally, due to the lack of available experimental data, the model does not account for inter-species and inter-individual variabilities. On one hand, this can be seen as a strength, as the model adequately describes epileptogenesis across species with only one set of parameters. On the other hand, it will be interesting to investigate how variation of these parameters defines susceptibility to epileptogenesis and its characteristic features.

Overall, the growing body of available animal model data, the unification of experimental protocols across laboratories, and the establishment of international collaborative initiatives aimed at understanding epileptogenesis provide fertile soil for future mathematical modeling work that can be based on the framework described in this thesis.

Appendix A

Detailed specifications of performed simulations

Modification	**Model type**	**Input type and intensity**	**Time of injury onset** T_{on}	**Time of injury offset** T_{off}	**Num. of simulations,** N	**Fig.**
Supracritical extent of neuronal loss	stochastic	Initial conditions $D_0 = 1$	-	-	5	5.5
Subcritical extent of neuronal loss	stochastic	Initial conditions $D_0 = 0.3$	-	-	5	5.5
Supracritical extent of neuronal loss	rate	Initial conditions $D_0 =$ [0.45; 0.5; 0.6 0.7; 0.8; 0.9; 1]	-	-	7	5.7

TABLE A.1: Detailed specifications of induced neuronal loss simulations.

Modification	**Model type**	**Input type and intensity**	**Time of injury onset** T_{on}	**Time of injury offset** T_{off}	**Num. of simulations,** N	**Fig.**
animal data fit	stochastic	$B^E = 0.25$	0 days	7 days	30	4.1-4.3, 4.11, 4.16, 4.18, 5.1
alternative $K_{S\to B} = 0.01$	stochastic	$B^E = 0.25$	0 days	7 days	30	4.11
alternative $K_{S\to B} = 1.5$	stochastic	$B^E = 0.25$	0 days	7 days	30	4.11
alternative $\tau_I : \tau_B = \tau_D = \tau_R$ ratio 1 : 1	stochastic	$B^E = 0.25$	0 days	7 days	30	4.16
alternative $\tau_I : \tau_B = \tau_D = \tau_R$ ratio 1 : 20	stochastic	$B^E = 0.25$	0 days	7 days	30	4.16
alternative $\kappa_{I\to S} = \kappa_{R\to S} = 1$	stochastic	$B^E = 0.25$	0 days	7 days	30	4.18
alternative $\kappa_{I\to S} = \kappa_{R\to S} = 5$	stochastic	$B^E = 0.25$	0 days	7 days	30	4.18
descreased injury intensity (50% concentration)	stochastic	$B^E = 0.125$	0 days	7 days	30	5.1
descreased injury intensity (50% time window duration)	stochastic	$B^E = 0.25$	0 days	3.5 days	30	5.1
increased injury intensity (150% time window duration)	stochastic	$B^E = 0.25$	0 days	10.5 days	30	5.1
animal data fit	rate	$B^E = 0.25$	0 days	7 days	1	5.2-5.3
increased injury intensity (150% time window duration)	rate	$B^E = 0.25$	0 days	10.5 days	1	5.2-5.3
descreased injury intensity (50% time window duration)	rate	$B^E = 0.25$	0 days	3.5 days	1	5.2-5.3
descreased injury intensity (25% time window duration)	rate	$B^E = 0.25$	0 days	1.75 days	1	5.2-5.3

TABLE A.2: Detailed specifications of BBB disruption rodent model simulations.

Modification	**Model type**	**Input type and intensity**	**Time of injury onset** T_{on}	**Time of injury offset** T_{off}	**Num. of simulations,** N	**Fig.**
animal data fit	stochastic	$I^E = 0.4$	0.9 day	6 days	30	4.4-4.7, 4.13-4.14, 5.4
alternative $\Theta = 0.1$	stochastic	$I^E = 0.4$	0.9 day	6 days	30	4.13
alternative $\Theta = 0.3$	stochastic	$I^E = 0.4$	0.9 day	6 days	30	4.13
alternative $\kappa_{I\to D} = 5$	stochastic	$I^E = 0.4$	0.9 day	6 days	30	4.14
alternative $\kappa_{I\to D} = 15$	stochastic	$I^E = 0.4$	0.9 day	6 days	30	4.14
testing intervention with suppression of seizure effect on BBB integrity $K_{S\to B} \downarrow= \frac{K_{S\to B}}{100}$ applied in different time intervals	rate	$I^E = 0.4$	0.9 day	6 days	5 (4 + 1 reference)	5.11
testing intervention with suppression of activation of glia by factors infiltrating the parenchyma $\kappa_{B\to I} \downarrow= \frac{\kappa_{B\to I}}{100}$ applied in different time intervals	rate	$I^E = 0.4$	0.9 day	6 days	5 (4 + 1 reference)	5.13

TABLE A.3: Detailed specifications of TMEV mouse model simulations.

Modification	**Model type**	**Input type and intensity**	**Time of injury onset** T_{on}	**Time of injury offset** T_{off}	**Num. of simulations,** N	**Fig.**
animal data fit	stochastic	D^E=1; B^E=1.65	0 days	2 days	30	4.8-4.10
animal data fit	rate	D^E=1; B^E=1.65	0 days	2 days	1	4.9-4.10
testing intervention with suppression of seizure effect on BBB integrity $K_{S\to B} \downarrow= \frac{K_{S\to B}}{100}$ applied in different time intervals	rate	D^E=1; B^E=1.65	0 days	2 days	7 (6 + 1 reference)	5.8, 5.10

TABLE A.4: Detailed specifications of pilocarpine SE rodent model simulations.

Appendix B

Neuronal loss score computation with masking procedure

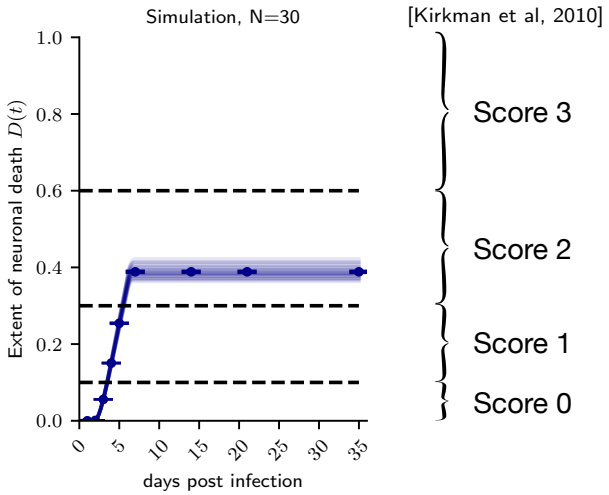

FIGURE B.1: Masking procedure for computation of neuronal loss score proposed in Kirkman et al., 2010: the raw data on the extent of neuronal loss from TMEV model simulation (left), and the neuronal loss score computation scheme (right). Horizontal dashed lines on the left correspond to 10%, 30%, and 60% extent of neuronal loss, which are the border values separating score values in the scheme from Kirkman et al., 2010. In Kirkman et al., 2010, neuronal loss score data are presented as a sum of scores for 2 hippocampi (maximum score: $3 \times 2 = 6$). Thus, the neuronal loss score computed for simulated TMEV animals was multiplied by a factor of 2 for comparability with experimental data. The absence of variability (0 SEM) in the neuronal loss score (Fig. 4.5C) is explained by the 'masking out' of the variability in neuronal loss score computation (left).

Bibliography

Abbott, N Joan et al. (2010). "Structure and function of the blood–brain barrier". In: *Neurobiology of disease* 37.1, pp. 13–25.

Adler, Miri et al. (2020). "Principles of cell circuits for tissue repair and fibrosis". In: *Iscience* 23.2, p. 100841.

Alberti, Andrea et al. (2008). "Early seizures in patients with acute stroke: frequency, predictive factors, and effect on clinical outcome". In: *Vascular health and risk management* 4.3, p. 715.

Alexopoulos, Andreas V (2013). "Pharmacoresistant epilepsy: Definition and explanation". In: *Epileptology* 1.1, pp. 38–42.

Altmann, Andre et al. (2022). "A systems-level analysis highlights microglial activation as a modifying factor in common epilepsies". In: *Neuropathology and applied neurobiology* 48.1, e12758.

Annegers, John F et al. (1998). "A population-based study of seizures after traumatic brain injuries". In: *New England Journal of Medicine* 338.1, pp. 20–24.

Badimon, Ana et al. (2020). "Negative feedback control of neuronal activity by microglia". In: *Nature* 586.7829, pp. 417–423.

Bandopadhyay, Ritam et al. (2021). "Recent developments in diagnosis of epilepsy: scope of microRNA and technological advancements". In: *Biology* 10.11, p. 1097.

Bankstahl, Marion et al. (2018). "Blood–brain barrier leakage during early epileptogenesis is associated with rapid remodeling of the neurovascular unit". In: *Eneuro* 5.3.

Bar-Klein, Guy et al. (2014). "Losartan prevents acquired epilepsy via TGF-β signaling suppression". In: *Annals of neurology* 75.6, pp. 864–875.

Batulin, Danylo et al. (2022). "A mathematical model of neuroimmune interactions in epileptogenesis for discovering treatment strategies". In: *Iscience* 25.6, p. 104343.

Becher, Burkhard, Sabine Spath, and Joan Goverman (2017). "Cytokine networks in neuroinflammation". In: *Nature Reviews Immunology* 17.1, pp. 49–59.

Berkovic, Samuel F et al. (2006). "Human epilepsies: interaction of genetic and acquired factors". In: *Trends in neurosciences* 29.7, pp. 391–397.

Betjemann, John P and Daniel H Lowenstein (2015). "Status epilepticus in adults". In: *The Lancet Neurology* 14.6, pp. 615–624.

Bladin, Christopher F et al. (2000). "Seizures after stroke: a prospective multicenter study". In: *Archives of neurology* 57.11, pp. 1617–1622.

Brackhan, Mirjam et al. (2016). "Serial quantitative TSPO-targeted PET reveals peak microglial activation up to 2 weeks after an epileptogenic brain insult". In: *Journal of Nuclear Medicine* 57.8, pp. 1302–1308.

Breemen, Melanie SM van, Erik B Wilms, and Charles J Vecht (2007). "Epilepsy in patients with brain tumours: epidemiology, mechanisms, and management". In: *The Lancet Neurology* 6.5, pp. 421–430.

Brown, Guy C and Jonas J Neher (2012). "Eaten alive! Cell death by primary phagocytosis:'phagoptosis'". In: *Trends in biochemical sciences* 37.8, pp. 325–332.

Buckmaster, Paul S (2014). "Does mossy fiber sprouting give rise to the epileptic state?" In: *Issues in clinical epileptology: a view from the bench*, pp. 161–168.

Chaney, Aisling M et al. (2021). "PET Imaging of Neuroinflammation". In: *Molecular Imaging*. Elsevier, pp. 1335–1371.

Chang, Wei-Chih et al. (2018). "Loss of neuronal network resilience precedes seizures and determines the ictogenic nature of interictal synaptic perturbations". In: *Nature neuroscience* 21.12, pp. 1742–1752.

Dam, Agnete Mouritzen (1980). "Epilepsy and neuron loss in the hippocampus". In: *Epilepsia* 21.6, pp. 617–629.

DeLorenzo, Robert J, David A Sun, and Laxmikant S Deshpande (2006). "Erratum to "Cellular mechanisms underlying acquired epilepsy: the calcium hypothesis of the induction and maintenance of epilepsy"[Pharmacol. Ther. 105 (3)(2005) 229–266]". In: *Pharmacology & therapeutics* 111.1, pp. 288–325.

Depannemaecker, Damien et al. (2021). "Modeling seizures: From single neurons to networks". In: *Seizure* 90, pp. 4–8.

DePaula-Silva, Ana Beatriz et al. (2017). "Theiler's murine encephalomyelitis virus infection of SJL/J and C57BL/6J mice: Models for multiple sclerosis and epilepsy". In: *Journal of neuroimmunology* 308, pp. 30–42.

Devinsky, Orrin et al. (2013). "Glia and epilepsy: excitability and inflammation". In: *Trends in neurosciences* 36.3, pp. 174–184.

Dingledine, Ray, Nicholas H Varvel, and F Edward Dudek (2014). "When and how do seizures kill neurons, and is cell death relevant to epileptogenesis?" In: *Issues in clinical epileptology: a view from the bench*, pp. 109–122.

Dinkelacker, Vera et al. (2015). "Hippocampal-thalamic wiring in medial temporal lobe epilepsy: enhanced connectivity per hippocampal voxel". In: *Epilepsia* 56.8, pp. 1217–1226.

DiSabato, Damon J, Ning Quan, and Jonathan P Godbout (2016). "Neuroinflammation: the devil is in the details". In: *Journal of neurochemistry* 139, pp. 136–153.

Dubbelaar, Marissa L et al. (2018). "The kaleidoscope of microglial phenotypes". In: *Frontiers in immunology* 9, p. 1753.

Duncan, John S (2019). "Brain imaging in epilepsy". In: *Practical Neurology* 19.5, pp. 438–443.

Duncan, John S et al. (2006). "Adult epilepsy". In: *The Lancet* 367.9516, pp. 1087–1100.

El Houssaini, Kenza, Christophe Bernard, and Viktor K Jirsa (2020). "The epileptor model: a systematic mathematical analysis linked to the dynamics of seizures, refractory status epilepticus, and depolarization block". In: *Eneuro* 7.2.

Engel Jr, Jerome (2018). "The current place of epilepsy surgery". In: *Current opinion in neurology* 31.2, p. 192.

Epi4K Consortium, Epilepsy Phenome/Genome Project (2013). "De novo mutations in epileptic encephalopathies". In: *Nature* 501.7466, pp. 217–221.

European Medicines Agency (2022). *Clinical Trials Regulation*. URL: `https://www.ema.europa.eu/en/human-regulatory/research-development/clinical-trials/clinical-trials-regulation.html` (visited on 01/31/2022).

Falco-Walter, Jessica J, Ingrid E Scheffer, and Robert S Fisher (2018). "The new definition and classification of seizures and epilepsy". In: *Epilepsy research* 139, pp. 73–79.

Fattorusso, Antonella et al. (2021). "The Pharmacoresistant Epilepsy: an overview on existant and new emerging therapies". In: *Frontiers in Neurology* 12, p. 1030.

Feeney, Dennis M and A Earl Walker (1979). "The prediction of posttraumatic epilepsy: a mathematical approach". In: *Archives of Neurology* 36.1, pp. 8–12.

Ferlazzo, Edoardo et al. (2017). "Methodological issues associated with clinical trials in epilepsy". In: *Expert Review of Clinical Pharmacology* 10.10, pp. 1103–1108.

Fisher, Robert S et al. (2005). "Epileptic seizures and epilepsy: definitions proposed by the International League Against Epilepsy (ILAE) and the International Bureau for Epilepsy (IBE)". In: *Epilepsia* 46.4, pp. 470–472.

Fisher, Robert S et al. (2012). "Seizure diaries for clinical research and practice: limitations and future prospects". In: *Epilepsy & Behavior* 24.3, pp. 304–310.

Fisher, Robert S et al. (2017). "Instruction manual for the ILAE 2017 operational classification of seizure types". In: *Epilepsia* 58.4, pp. 531–542.

Fuzzati-Armentero, Marie Therese, Silvia Cerri, and Fabio Blandini (2019). "Peripheral-Central neuroimmune crosstalk in Parkinson's disease: what do patients and animal models tell us?" In: *Frontiers in neurology* 10, p. 232.

Gaitatzis, Athanasios et al. (2004). "Life expectancy in people with newly diagnosed epilepsy". In: *Brain* 127.11, pp. 2427–2432.

Galluzzi, Lorenzo et al. (2018). "Molecular mechanisms of cell death: recommendations of the Nomenclature Committee on Cell Death 2018". In: *Cell Death & Differentiation* 25.3, pp. 486–541.

Goldenberg, Marvin M (2010). "Overview of drugs used for epilepsy and seizures: etiology, diagnosis, and treatment". In: *Pharmacy and Therapeutics* 35.7, p. 392.

González-Ramírez, Laura R et al. (2015). "A biologically constrained, mathematical model of cortical wave propagation preceding seizure termination". In: *PLoS computational biology* 11.2, e1004065.

Greenberg, David A and Ryan Subaran (2011). "Blinders, phenotype, and fashionable genetic analysis: a critical examination of the current state of epilepsy genetic studies". In: *Epilepsia* 52.1, pp. 1–9.

Grone, Brian P and Scott C Baraban (2015). "Animal models in epilepsy research: legacies and new directions". In: *Nature neuroscience* 18.3, pp. 339–343.

Guerrini, Renzo (2006). "Epilepsy in children". In: *The Lancet* 367.9509, pp. 499–524.

Gupta, Kunal and Eric Schnell (2019). "Neuronal network remodeling and Wnt pathway dysregulation in the intra-hippocampal kainate mouse model of temporal lobe epilepsy". In: *PloS one* 14.10, e0215789.

Harris, Melissa G et al. (2014). "Immune privilege of the CNS is not the consequence of limited antigen sampling". In: *Scientific reports* 4.1, pp. 1–10.

Harte-Hargrove, Lauren C et al. (2017). "Common data elements for preclinical epilepsy research: Standards for data collection and reporting. A TASK 3 report of the AES/ILAE Translational Task Force of the ILAE". In: *Epilepsia* 58, pp. 78–86.

Hendricks, William D, Gary L Westbrook, and Eric Schnell (2019). "Early detonation by sprouted mossy fibers enables aberrant dentate network activity". In: *Proceedings of the National Academy of Sciences* 116.22, pp. 10994–10999.

Henshall, David C and Brian S Meldrum (2012). "Cell death and survival mechanisms after single and repeated brief seizures". In: *Jasper's basic mechanisms of the epilepsies*, pp. 262–276.

Henshall, DC (2007). "Apoptosis signalling pathways in seizure-induced neuronal death and epilepsy". In: *Biochemical society transactions* 35.2, pp. 421–423.

Hornik, Tamara C, Anna Vilalta, and Guy C Brown (2016). "Activated microglia cause reversible apoptosis of pheochromocytoma cells, inducing their cell death by phagocytosis". In: *Journal of Cell Science* 129.1, pp. 65–79.

Horváth, András et al. (2016). "Epileptic seizures in Alzheimer disease". In: *Alzheimer Disease & Associated Disorders* 30.2, pp. 186–192.

Hufthy, Yousif et al. (2022). "Statins as antiepileptogenic drugs: Analyzing the evidence and identifying the most promising statin". In: *Epilepsia* 63.8, pp. 1889–1898.

Hughes, John R (2009). "Absence seizures: a review of recent reports with new concepts". In: *Epilepsy & behavior* 15.4, pp. 404–412.

Hunt, Robert F, Jeffery A Boychuk, and Bret N Smith (2013). "Neural circuit mechanisms of post–traumatic epilepsy". In: *Frontiers in cellular neuroscience* 7, p. 89.

Isacson, O and MV Sofroniew (1992). "Neuronal loss or replacement in the injured adult cerebral neocortex induces extensive remodeling of intrinsic and afferent neural systems". In: *Experimental neurology* 117.2, pp. 151–175.

Jana, Ranjan and Imon Mukherjee (2021). "Deep learning based efficient epileptic seizure prediction with EEG channel optimization". In: *Biomedical Signal Processing and Control* 68, p. 102767.

Jirsa, Viktor K et al. (2014). "On the nature of seizure dynamics". In: *Brain* 137.8, pp. 2210–2230.

Jo, Hang Joon et al. (2019). "Relationship between seizure frequency and functional abnormalities in limbic network of medial temporal lobe epilepsy". In: *Frontiers in Neurology* 10, p. 488.

Junges, Leandro et al. (2019). "The role that choice of model plays in predictions for epilepsy surgery". In: *Scientific reports* 9.1, pp. 1–12.

Junges, Leandro et al. (2020). "Epilepsy surgery: Evaluating robustness using dynamic network models". In: *Chaos: An Interdisciplinary Journal of Nonlinear Science* 30.11, p. 113106.

Jurga, Agnieszka M, Martyna Paleczna, and Katarzyna Z Kuter (2020). "Overview of general and discriminating markers of differential microglia phenotypes". In: *Frontiers in cellular neuroscience* 14, p. 198.

Juvale, Iman Imtiyaz Ahmed and Ahmad Tarmizi Che Has (2021). "Possible interplay between the theories of pharmacoresistant epilepsy". In: *European Journal of Neuroscience* 53.6, pp. 1998–2026.

Kaplan, David I, Lori L Isom, and Steven Petrou (2016). "Role of sodium channels in epilepsy". In: *Cold Spring Harbor perspectives in medicine* 6.6, a022814.

Kapur, Jaideep (2003). "Role of neuronal loss in the pathogenesis of recurrent spontaneous seizures". In: *Epilepsy currents* 3.5, pp. 166–167.

Keaney, James and Matthew Campbell (2015). "The dynamic blood–brain barrier". In: *The FEBS journal* 282.21, pp. 4067–4079.

Keith, Kristin A and Jason H Huang (2019). "Animal models of post-traumatic epilepsy". In: *Diagnostics* 10.1, p. 4.

Kempuraj, Duraisamy et al. (2017). "Brain and peripheral atypical inflammatory mediators potentiate neuroinflammation and neurodegeneration". In: *Frontiers in cellular neuroscience* 11, p. 216.

Kim, Hani et al. (2017a). "Structural and functional alterations at pre-epileptic stage are closely associated with epileptogenesis in pilocarpine-induced epilepsy model". In: *Experimental Neurobiology* 26.5, pp. 287–294.

Kim, Soo Young et al. (2016). "A potential role for glia-derived extracellular matrix remodeling in postinjury epilepsy". In: *Journal of Neuroscience Research* 94.9, pp. 794–803.

Kim, Soo Young et al. (2017b). "TGFβ signaling is associated with changes in inflammatory gene expression and perineuronal net degradation around inhibitory neurons following various neurological insults". In: *Scientific reports* 7.1, pp. 1–14.

Kirkman, Nikki J et al. (2010). "Innate but not adaptive immune responses contribute to behavioral seizures following viral infection". In: *Epilepsia* 51.3, pp. 454–464.

Klassen, Tara et al. (2011). "Exome sequencing of ion channel genes reveals complex profiles confounding personal risk assessment in epilepsy". In: *Cell* 145.7, pp. 1036–1048.

Klein, Pavel et al. (2018). "Commonalities in epileptogenic processes from different acute brain insults: Do they translate?" In: *Epilepsia* 59.1, pp. 37–66.

Knopp, Andreas et al. (2008). "Loss of GABAergic neurons in the subiculum and its functional implications in temporal lobe epilepsy". In: *Brain* 131.6, pp. 1516–1527.

Kuhlmann, Levin et al. (2018). "Seizure prediction—ready for a new era". In: *Nature Reviews Neurology* 14.10, pp. 618–630.

Kwan, Patrick et al. (2010). *Definition of drug resistant epilepsy: consensus proposal by the ad hoc Task Force of the ILAE Commission on Therapeutic Strategies.*

Lalwani, Ashna M et al. (2020). "The biochemical profile of post-mortem brain from people who suffered from epilepsy reveals novel insights into the etiopathogenesis of the disease". In: *Metabolites* 10.6, p. 261.

Langen, Urs H, Swathi Ayloo, and Chenghua Gu (2019). "Development and cell biology of the blood-brain barrier". In: *Annual review of cell and developmental biology* 35, p. 591.

Lennox, William Gordon and Margaret A Lennox-Buchthal (1960). *Epilepsy and related disorders*. Vol. 2. Little, Brown.

Lerche, Holger et al. (2013). "Ion channels in genetic and acquired forms of epilepsy". In: *The Journal of physiology* 591.4, pp. 753–764.

Lhatoo, Samden D et al. (2020). "Big data in epilepsy: clinical and research considerations. Report from the Epilepsy Big Data Task Force of the International League Against Epilepsy". In: *Epilepsia* 61.9, pp. 1869–1883.

Li, Jun-Wei et al. (2018). "Microglial priming in Alzheimer's disease". In: *Annals of translational medicine* 6.10.

Libbey, Jane E et al. (2008). "Seizures following picornavirus infection". In: *Epilepsia* 49.6, pp. 1066–1074.

Libbey, Jane E et al. (2011). "Lack of correlation of central nervous system inflammation and neuropathology with the development of seizures following acute virus infection". In: *Journal of virology* 85.16, pp. 8149–8157.

Loewen, Jaycie L et al. (2016). "Neuronal injury, gliosis, and glial proliferation in two models of temporal lobe epilepsy". In: *Journal of Neuropathology & Experimental Neurology* 75.4, pp. 366–378.

Lopim, Glauber Menezes et al. (2016). "Relationship between seizure frequency and number of neuronal and non-neuronal cells in the hippocampus throughout the life of rats with epilepsy". In: *Brain research* 1634, pp. 179–186.

Löscher, Wolfgang (2020). "The holy grail of epilepsy prevention: preclinical approaches to antiepileptogenic treatments". In: *Neuropharmacology* 167, p. 107605.

Löscher, Wolfgang and Alon Friedman (2020). "Structural, molecular, and functional alterations of the blood-brain barrier during epileptogenesis and epilepsy: a cause, consequence, or both?" In: *International journal of molecular sciences* 21.2, p. 591.

Lu, Diyuan et al. (2020). "Staging Epileptogenesis with Deep Neural Networks". In: *Proceedings of the 11th ACM International Conference on Bioinformatics, Computational Biology and Health Informatics*, pp. 1–10.

Lyman, Monty et al. (2014). "Neuroinflammation: the role and consequences". In: *Neuroscience research* 79, pp. 1–12.

Lynam, Laura M et al. (2007). "Frequency of seizures in patients with newly diagnosed brain tumors: a retrospective review". In: *Clinical neurology and neurosurgery* 109.7, pp. 634–638.

Meldrum, Brian S (1993). "Excitotoxicity and selective neuronal loss in epilepsy". In: *Brain pathology* 3.4, pp. 405–412.

Misra, Usha Kant, Chong Tin Tan, and Jayantee Kalita (2008). "Viral encephalitis and epilepsy". In: *Epilepsia* 49, pp. 13–18.

Mohan, Midhun et al. (2018). "The long-term outcomes of epilepsy surgery". In: *PLoS One* 13.5, e0196274.

More, Sandeep Vasant et al. (2013). "Cellular and molecular mediators of neuroinflammation in the pathogenesis of Parkinson's disease". In: *Mediators of inflammation* 2013.

Moshé, Solomon L et al. (2015). "Epilepsy: new advances". In: *The Lancet* 385.9971, pp. 884–898.

Mukhopadhyay, Swagoto et al. (2019). "The global neurosurgical workforce: a mixed-methods assessment of density and growth". In: *Journal of neurosurgery* 130.4, pp. 1142–1148.

Najm, Imad et al. (2013). "Temporal patterns and mechanisms of epilepsy surgery failure". In: *Epilepsia* 54.5, pp. 772–782.

Naze, Sebastien, Christophe Bernard, and Viktor Jirsa (2015). "Computational modeling of seizure dynamics using coupled neuronal networks: factors shaping epileptiform activity". In: *PLOS Computational Biology* 11.5, e1004209.

Nold, Andreas et al. (2020). "How repair-or-dispose decisions under stress can initiate disease progression". In: *Iscience* 23.11, p. 101701.

Olsen, Tom Skyhøj (2001). "Post-stroke epilepsy". In: *Current Atherosclerosis Reports* 3.4, pp. 340–344.

Patel, Dipan C et al. (2017). "Hippocampal TNFα signaling contributes to seizure generation in an infection-induced mouse model of limbic epilepsy". In: *Eneuro* 4.2.

Patel, Dipan C et al. (2019). "Neuron–glia interactions in the pathophysiology of epilepsy". In: *Nature Reviews Neuroscience* 20.5, pp. 282–297.

Pati, Sandipan and Andreas V Alexopoulos (2010). "Pharmacoresistant epilepsy: from pathogenesis to current and emerging therapies". In: *Cleve Clin J Med* 77.7, pp. 457–567.

Peletier, Lambertus A and Johan Gabrielsson (2018). "Impact of mathematical pharmacology on practice and theory: four case studies". In: *Journal of pharmacokinetics and pharmacodynamics* 45.1, pp. 3–21.

Peng, Peizhen, Yang Song, and Lu Yang (2021). "Seizure prediction in EEG signals using STFT and domain adaptation". In: *Frontiers in Neuroscience*, p. 1880.

Pennell, Page B (2020). "Unravelling the heterogeneity of epilepsy for optimal individualised treatment: advances in 2019". In: *The Lancet Neurology* 19.1, pp. 8–10.

Perry, V Hugh and Jessica Teeling (2013). "Microglia and macrophages of the central nervous system: the contribution of microglia priming and systemic inflammation

to chronic neurodegeneration". In: *Seminars in immunopathology*. Vol. 35. 5. Springer, pp. 601–612.

Perucca, Emilio (2015). "Introduction to the choice of antiepileptic drugs". In: *The treatment of epilepsy*, pp. 365–375.

Perucca, Emilio and Torbjörn Tomson (2011). "The pharmacological treatment of epilepsy in adults". In: *The Lancet Neurology* 10.5, pp. 446–456.

Perucca, Piero and Ingrid E Scheffer (2021). "Genetic Contributions to Acquired Epilepsies". In: *Epilepsy currents* 21.1, pp. 5–13.

Pillai, Jyoti and Michael R Sperling (2006). "Interictal EEG and the diagnosis of epilepsy". In: *Epilepsia* 47, pp. 14–22.

Pitkänen, Asla and Riikka Immonen (2014). "Epilepsy related to traumatic brain injury". In: *Neurotherapeutics* 11.2, pp. 286–296.

Pitkänen, Asla, Reina Roivainen, and Katarzyna Lukasiuk (2016). "Development of epilepsy after ischaemic stroke". In: *The Lancet Neurology* 15.2, pp. 185–197.

Pitkänen, Asla and Thomas P Sutula (2002). "Is epilepsy a progressive disorder? Prospects for new therapeutic approaches in temporal-lobe epilepsy". In: *The Lancet Neurology* 1.3, pp. 173–181.

Pitkänen, Asla et al. (2015). "Epileptogenesis". In: *Cold Spring Harbor perspectives in medicine* 5.10, a022822.

Polascheck, Nadine, Marion Bankstahl, and Wolfgang Löscher (2010). "The COX-2 inhibitor parecoxib is neuroprotective but not antiepileptogenic in the pilocarpine model of temporal lobe epilepsy". In: *Experimental neurology* 224.1, pp. 219–233.

Preux, Pierre-Marie and Michel Druet-Cabanac (2005). "Epidemiology and aetiology of epilepsy in sub-Saharan Africa". In: *The Lancet Neurology* 4.1, pp. 21–31.

Rüber, Theodor et al. (2018). "Evidence for peri-ictal blood–brain barrier dysfunction in patients with epilepsy". In: *Brain* 141.10, pp. 2952–2965.

Rubin, LL and JM Staddon (1999). "The cell biology of the blood-brain barrier". In: *Annual review of neuroscience* 22, p. 11.

Rubinos, Clio, Brandon Waters, and Lawrence J Hirsch (2022). "Predicting and Treating Post-traumatic Epilepsy". In: *Current Treatment Options in Neurology*, pp. 1–17.

Salucci, Sara et al. (2021). "How Inflammation Pathways Contribute to Cell Death in Neuro-Muscular Disorders". In: *Biomolecules* 11.8, p. 1109.

Santhakumar, Vijayalakshmi, Ildiko Aradi, and Ivan Soltesz (2005). "Role of mossy fiber sprouting and mossy cell loss in hyperexcitability: a network model of the dentate gyrus incorporating cell types and axonal topography". In: *Journal of neurophysiology* 93.1, pp. 437–453.

Savin, Cristina, Jochen Triesch, and Michael Meyer-Hermann (2009). "Epileptogenesis due to glia-mediated synaptic scaling". In: *Journal of The Royal Society Interface* 6.37, pp. 655–668.

Scaffidi, Paola, Tom Misteli, and Marco E Bianchi (2002). "Release of chromatin protein HMGB1 by necrotic cells triggers inflammation". In: *Nature* 418.6894, pp. 191–195.

Scheffer, Ingrid E et al. (2017). "ILAE classification of the epilepsies: position paper of the ILAE Commission for Classification and Terminology". In: *Epilepsia* 58.4, pp. 512–521.

Seiffert, Ernst et al. (2004). "Lasting blood-brain barrier disruption induces epileptic focus in the rat somatosensory cortex". In: *Journal of Neuroscience* 24.36, pp. 7829–7836.

Sendrowski, Krzysztof and Wojciech Sobaniec (2013). "Hippocampus, hippocampal sclerosis and epilepsy". In: *Pharmacological Reports* 65.3, pp. 555–565.

Shorvon, Simon D (2011). "The causes of epilepsy: changing concepts of etiology of epilepsy over the past 150 years". In: *Epilepsia* 52.6, pp. 1033–1044.

Singhi, Pratibha (2011). "Infectious causes of seizures and epilepsy in the developing world". In: *Developmental Medicine & Child Neurology* 53.7, pp. 600–609.

Sirven, Joseph I (2015). "Epilepsy: a spectrum disorder". In: *Cold Spring Harbor perspectives in medicine* 5.9, a022848.

Sliwa, Anna et al. (2012). "Post-treatment with rapamycin does not prevent epileptogenesis in the amygdala stimulation model of temporal lobe epilepsy". In: *Neuroscience letters* 509.2, pp. 105–109.

Sloviter, Robert S (1987). "Decreased hippocampal inhibition and a selective loss of interneurons in experimental epilepsy". In: *Science* 235.4784, pp. 73–76.

Smith, Quentin R (2003). "A review of blood-brain barrier transport techniques". In: *The Blood-Brain Barrier*, pp. 193–208.

Sochocka, Marta, Breno Satler Diniz, and Jerzy Leszek (2017). "Inflammatory response in the CNS: friend or foe?" In: *Molecular neurobiology* 54.10, pp. 8071–8089.

Steinlein, Ortrud K (2004). "Genetic mechanisms that underlie epilepsy". In: *Nature Reviews Neuroscience* 5.5, pp. 400–408.

Stephen, Linda J and Martin J Brodie (2011). "Pharmacotherapy of epilepsy". In: *CNS drugs* 25.2, pp. 89–107.

Stewart, Kerry-Ann A et al. (2010). "Development of postinfection epilepsy after Theiler's virus infection of C57BL/6 mice". In: *Journal of Neuropathology & Experimental Neurology* 69.12, pp. 1210–1219.

Tauck, David L and J Victor Nadler (1985). "Evidence of functional mossy fiber sprouting in hippocampal formation of kainic acid-treated rats". In: *Journal of Neuroscience* 5.4, pp. 1016–1022.

Téllez-Zenteno, Jose F and Lizbeth Hernández-Ronquillo (2012). "A review of the epidemiology of temporal lobe epilepsy". In: *Epilepsy research and treatment* 2012.

Theocharis, Achilleas D et al. (2016). "Extracellular matrix structure". In: *Advanced drug delivery reviews* 97, pp. 4–27.

Thijs, Roland D et al. (2019). "Epilepsy in adults". In: *The Lancet* 393.10172, pp. 689–701.

Thom, Maria (2014). "Hippocampal sclerosis in epilepsy: a neuropathology review". In: *Neuropathology and applied neurobiology* 40.5, pp. 520–543.

Tomlinson, Samuel B and Arun Venkataraman (2017). "Secondary generalization of focal-onset seizures: examining the relationship between seizure propagation and epilepsy surgery outcome". In: *Journal of Neurophysiology* 117.4, pp. 1426–1430.

Usman, Syed Muhammad, Shehzad Khalid, and Sadaf Bashir (2021). "A deep learning based ensemble learning method for epileptic seizure prediction". In: *Computers in Biology and Medicine* 136, p. 104710.

Van Vliet, EA, E Aronica, and JA Gorter (2015). "Blood–brain barrier dysfunction, seizures and epilepsy". In: *Seminars in cell & Developmental biology*. Vol. 38. Elsevier, pp. 26–34.

Van Vliet, EA et al. (2007). "Blood–brain barrier leakage may lead to progression of temporal lobe epilepsy". In: *Brain* 130.2, pp. 521–534.

Vezzani, Annamaria, Silvia Balosso, and Teresa Ravizza (2019). "Neuroinflammatory pathways as treatment targets and biomarkers in epilepsy". In: *Nature Reviews Neurology* 15.8, pp. 459–472.

Vezzani, Annamaria et al. (2016). "Infections, inflammation and epilepsy". In: *Acta neuropathologica* 131.2, pp. 211–234.

Vezzani, Annamaria et al. (2022). "Astrocytes in the initiation and progression of epilepsy". In: *Nature Reviews Neurology*, pp. 1–16.

Vliet, Erwin A van et al. (2012). "Inhibition of mammalian target of rapamycin reduces epileptogenesis and blood–brain barrier leakage but not microglia activation". In: *Epilepsia* 53.7, pp. 1254–1263.

Wagenaar, Joost B et al. (2015). "Collaborating and sharing data in epilepsy research". In: *Journal of clinical neurophysiology: official publication of the American Electroencephalographic Society* 32.3, p. 235.

Weissberg, Itai et al. (2015). "Albumin induces excitatory synaptogenesis through astrocytic TGF-β/ALK5 signaling in a model of acquired epilepsy following blood–brain barrier dysfunction". In: *Neurobiology of disease* 78, pp. 115–125.

World Health Organization (2022). *Epilepsy*. URL: `https://www.who.int/news-room/fact-sheets/detail/epilepsy.html` (visited on 02/09/2022).

Yang, Yanli et al. (2018). "Epileptic seizure prediction based on permutation entropy". In: *Frontiers in computational neuroscience* 12, p. 55.

Yu, Pen-Ning et al. (2021). "A sparse multiscale nonlinear autoregressive model for seizure prediction". In: *Journal of Neural Engineering* 18.2, p. 026012.

Zhang, Liang et al. (2015). "FDG-PET and NeuN-GFAP immunohistochemistry of hippocampus at different phases of the pilocarpine model of temporal lobe epilepsy". In: *International journal of medical sciences* 12.3, p. 288.

Zilberter, Yuri, Irina Popova, and Misha Zilberter (2021). "Unifying mechanism behind the onset of acquired epilepsy". In: *Trends in Pharmacological Sciences*.

Zou, Safeng et al. (2015). "The pooled incidence of post-stroke seizure in 102 008 patients". In: *Topics in stroke rehabilitation* 22.6, pp. 460–467.